AD-A165 305 A STUDY OF SEA ICE KINEMATICS AND THEIR RELATIONSHIP TO ARCTIC AMBIENT NO..(U) HONEYWELL INC DUARTE CA ORDNANCE DIV J K LEWIS ET AL. FEB 86 SAIC-85/1950-PT-3-SEC-3 1/2

UNCLASSIFIED N00014-85-C-0531 F/G 8/12 NL

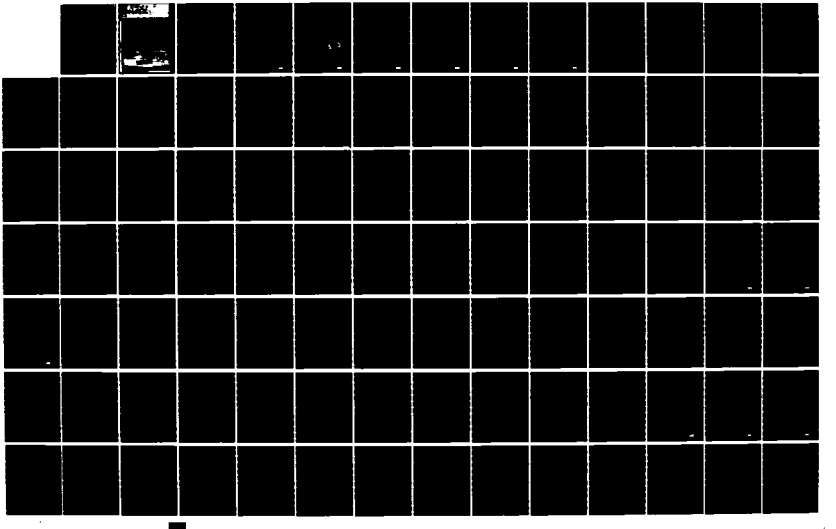

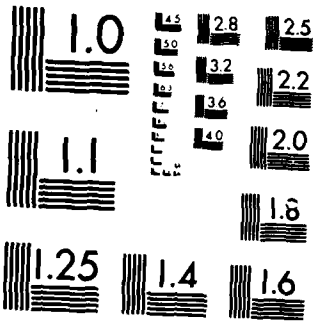

MICROCOPY RESOLUTION TEST CHART
NATIONAL BUREAU OF STANDARDS-1963-A

AD-A165 305

A Study of Sea Ice Kinematics and Their Relationships to Arctic Ambient Noise

DTIC FILE COPY

Part 3
Section 3 - Ambient Noise

Science Applications International Corp.

SAIC

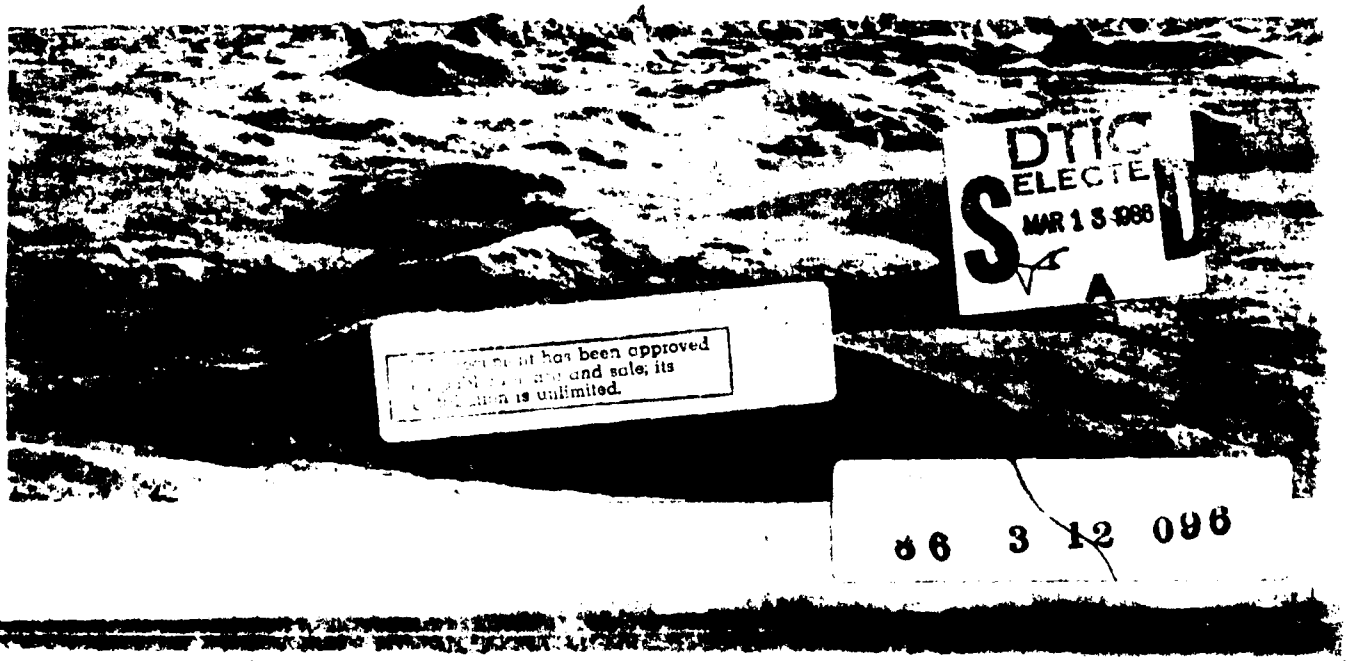

...it has been approved
... and sale; its
...tion is unlimited.

86 3 12 096

Unclassified

SECURITY CLASSIFICATION OF THIS PAGE (When Data Entered)

REPORT DOCUMENTATION PAGE	READ INSTRUCTIONS BEFORE COMPLETING FORM
1. REPORT NUMBER: SAIC - 85/1950	2. GOVT ACCESSION NO.: AD-A165305
3. RECIPIENT'S CATALOG NUMBER:	
4. TITLE (and Subtitle): A Study of Sea Ice Kinematics and Their Relationships to Arctic Ambient Noise	5. TYPE OF REPORT & PERIOD COVERED: Final Report March 1985-February 1986
	6. PERFORMING ORG. REPORT NUMBER: SAIC 1-425-07-356-10
7. AUTHOR(s): James K. Lewis, Warren W. Denner	8. CONTRACT OR GRANT NUMBER(s): N00014-85-C-0531
9. PERFORMING ORGANIZATION NAME AND ADDRESS: Science Applications International Corporation, 1304 Deacon, College Station, Texas 77840	10. PROGRAM ELEMENT, PROJECT, TASK AREA & WORK UNIT NUMBERS:
11. CONTROLLING OFFICE NAME AND ADDRESS: Office of Naval Research, Department of the Navy, Arlington, Virginia 22217	12. REPORT DATE: February 1986
	13. NUMBER OF PAGES: ~~770~~
14. MONITORING AGENCY NAME & ADDRESS(if different from Controlling Office)	15. SECURITY CLASS. (of this report): Unclassified
	15a. DECLASSIFICATION/DOWNGRADING SCHEDULE:

16. DISTRIBUTION STATEMENT (of this Report)

Approved for public release; distribution unlimited.

17. DISTRIBUTION STATEMENT (of the abstract entered in Block 20, if different from Report)

18. SUPPLEMENTARY NOTES

19. KEY WORDS (Continue on reverse side if necessary and identify by block number)

sea ice processes
arctic ambient noise
Lagrangian data
ice kinematics
thermal cracking

20. ABSTRACT (Continue on reverse side if necessary and identify by block number)

This report details the kinematic analysis of sea ice motion data collected during the Arctic Ice Dynamics Joint Experiment (AIDJEX) in the Beaufort Sea. In addition, relationships between the ice kinematic parameters and associated ambient noise are presented. These relationships were determined by an extensive correlation process between the noise and ice motion time histories. Time scales of the various modes of ice motion were calculated by season. Also, seasonal time and space scales were calculated for ambient noise at 10 Hz, 32 Hz, and 1000 Hz. Contents of the section [illegible] (UNCL)

DD FORM 1 JAN 73 1473 EDITION OF 1 NOV 65 IS OBSOLETE

S/N 0102-LF-014-6601

Unclassified

SECURITY CLASSIFICATION OF THIS PAGE (When Data Entered)

Table of Contents

	Page
Appendix G - Seasonal Arctic Ambient Noise Temporal Autocorrelations, Beaufort Sea, 1975-1976	3.3-1
Appendix H - Seasonal Arctic Ambient Noise Spatial Autocorrelations, Beaufort Sea, 1975-1976	3.3-49
Appendix I - Seasonal Arctic Ambient Noise Power Spectra, Beaufort Sea, 1975-1976	3.3-76

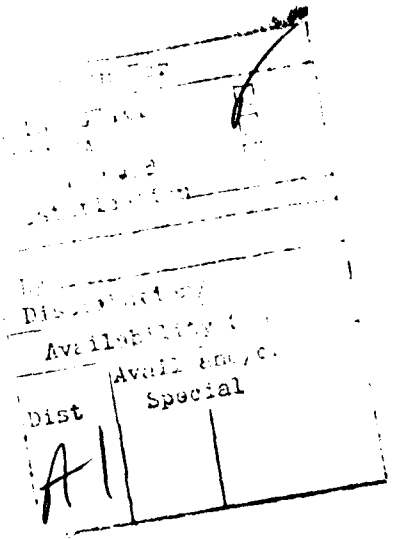

QUALITY INSPECTED 3

2

A STUDY OF SEA ICE KINEMATICS AND THEIR RELATIONSHIPS TO ARCTIC AMBIENT NOISE

PART 3, SECTION 3 - AMBIENT NOISE

DTIC
ELECTE
MAR 1 3 1986
S D
A

SAIC
Science Applications
International Corporation

Appendix G

Seasonal Arctic Ambient Noise Temporal Autocorrelations, Beaufort Sea, 1975-1976

This appendix shows graphically the autocorrelations of the AIDJEX 10 Hz, 32 Hz, and 1000 Hz ambient noise signals for phase lags up to three days (at 3 hr intervals). These autocorrelations were calculated for each station at which noise data were available. One month of data was used, and each season is represented:

Summer - noise data from August 1975,
Fall - noise data from November 1975,
Winter - noise data from February 1976, and
Spring - noise data from May 1976.

Although the use of decibell units gives results that are important for the Navy operationally, these units do not always give a true indication of the physics involved in generating the noise. Thus, this appendix also gives the autocorrelations for the ambient noise in terms of pressure amplitude (relative to 1 μPa) using

$$\text{Pressure Amplitude} = 10^{(dB/20)}.$$

List of Figures

Appendix G

Summer (dB) — Page

Fig. G.1. Ambient noise autocorrelations, Station 5 . . . 3.3-5
Fig. G.2. Ambient noise autocorrelations, Station 8 . . . 3.3-6
Fig. G.3. Ambient noise autocorrelations, Station 10 . . 3.3-7
Fig. G.4. Ambient noise autocorrelations, Station 13 . . 3.3-8
Fig. G.5. Ambient noise autocorrelations, Station 66 . . 3.3-9

Summer (Pressure Amplitude)

Fig. G.6. Ambient noise autocorrelations, Station 5 . . . 3.3-10
Fig. G.7. Ambient noise autocorrelations, Station 8 . . . 3.3-11
Fig. G.8. Ambient noise autocorrelations, Station 10 . . 3.3-12
Fig. G.9. Ambient noise autocorrelations, Station 13 . . 3.3-13
Fig. G.10. Ambient noise autocorrelations, Station 66 . . 3.3-14

Fall (dB)

Fig. G.11. Ambient noise autocorrelations, Station 5 . . . 3.3-15
Fig. G.12. Ambient noise autocorrelations, Station 8 . . . 3.3-16
Fig. G.13. Ambient noise autocorrelations, Station 10 . . 3.3-17
Fig. G.14. Ambient noise autocorrelations, Station 12 . . 3.3-18
Fig. G.15. Ambient noise autocorrelations, Station 13 . . 3.3-19
Fig. G.16. Ambient noise autocorrelations, Station 66 . . 3.3-20

Fall (Pressure Amplitude)

Fig. G.17. Ambient noise autocorrelations, Station 5 . . . 3.3-21
Fig. G.18. Ambient noise autocorrelations, Station 8 . . . 3.3-22
Fig. G.19. Ambient noise autocorrelations, Station 10 . . 3.3-23

Fall (Pressure Amplitude) cont'd — Page

Fig. G.20. Ambient noise autocorrelations, Station 12 . . 3.3-24
Fig. G.21. Ambient noise autocorrelations, Station 13 . . 3.3-25
Fig. G.22. Ambient noise autocorrelations, Station 66 . . 3.3-26

Winter (dB)

Fig. G.23. Ambient noise autocorrelations, Station 5 . . . 3.3-27
Fig. G.24. Ambient noise autocorrelations, Station 8 . . . 3.3-28
Fig. G.25. Ambient noise autocorrelations, Station 10 . . 3.3-29
Fig. G.26. Ambient noise autocorrelations, Station 13 . . 3.3-30
Fig. G.27. Ambient noise autocorrelations, Station 44 . . 3.3-31
Fig. G.28. Ambient noise autocorrelations, Station 66 . . 3.3-32

Winter (Pressure Amplitude)

Fig. G.29. Ambient noise autocorrelations, Station 5 . . . . 3.3-33
Fig. G.30. Ambient noise autocorrelations, Station 8 . . . . 3.3-34
Fig. G.31. Ambient noise autocorrelations, Station 10 . . 3.3-35
Fig. G.32. Ambient noise autocorrelations, Station 13 . . 3.3-36
Fig. G.33. Ambient noise autocorrelations, Station 44 . . 3.3-37
Fig. G.34. Ambient noise autocorrelations, Station 66 . . 3.3-38

Spring (dB)

Fig. G.35. Ambient noise autocorrelations, Station 5 . . . 3.3-39
Fig. G.36. Ambient noise autocorrelations, Station 10 . . 3.3-40
Fig. G.37. Ambient noise autocorrelations, Station 13 . . 3.3-41
Fig. G.38. Ambient noise autocorrelations, Station 44 . . 3.3-42
Fig. G.39. Ambient noise autocorrelations, Station 66 . . 3.3-43

Spring (Pressure Amplitude) Page

Fig. G.40. Ambient noise autocorrelations, Station 5 . . . 3.3-44

Fig. G.41. Ambient noise autocorrelations, Station 10 . . 3.3-45

Fig. G.42. Ambient noise autocorrelations, Station 13 . . 3.3-46

Fig. G.43. Ambient noise autocorrelations, Station 44 . . 3.3-47

Fig. G.44. Ambient noise autocorrelations, Station 66 . . 3.3-48

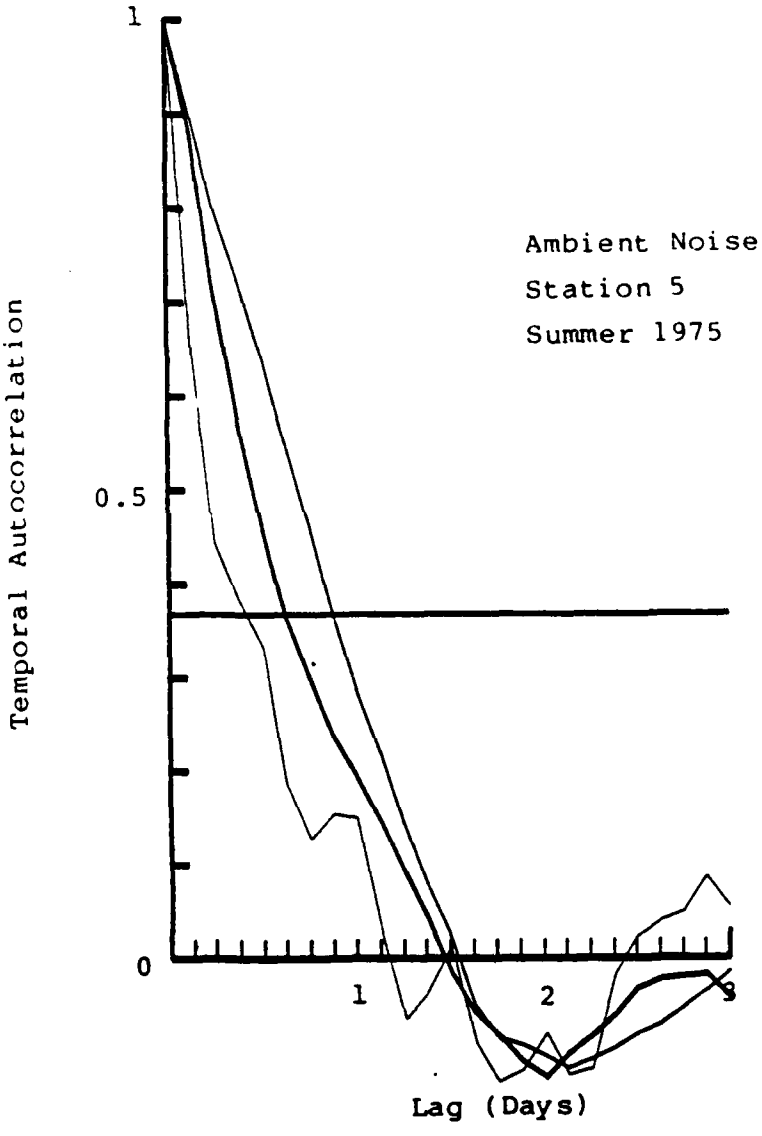

Fig. G.1. Ambient noise autocorrelations, Station 5, based on summer AIDJEX noise data (dB): 10 Hz (lightest line), 32 Hz (darker line), and 1000 Hz (darkest line).

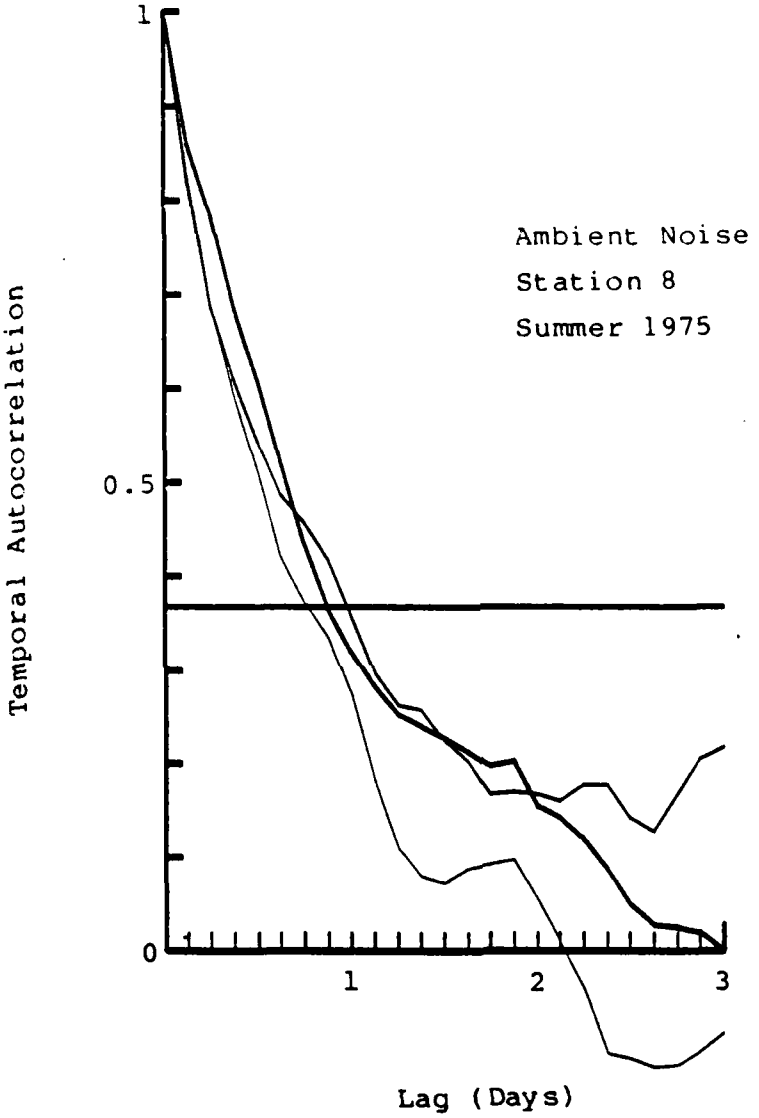

Fig. G.2. Ambient noise autocorrelations, Station 8, based on summer AIDJEX noise data (dB): 10 Hz (lightest line), 32 Hz (darker line), and 1000 Hz (darkest line).

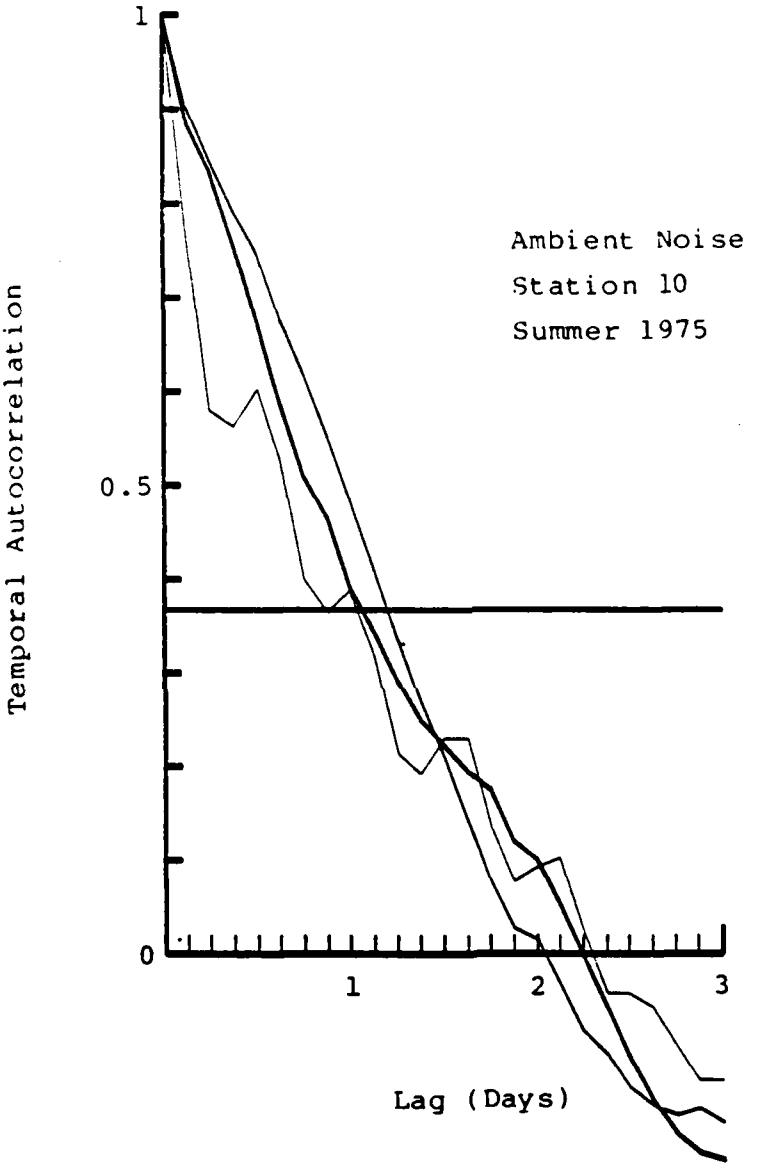

Fig. G.3. Ambient noise autocorrelations, Station 10, based on summer AIDJEX noise data (dB): 10 Hz (lightest line), 32 Hz (darker line), and 1000 Hz (darkest line).

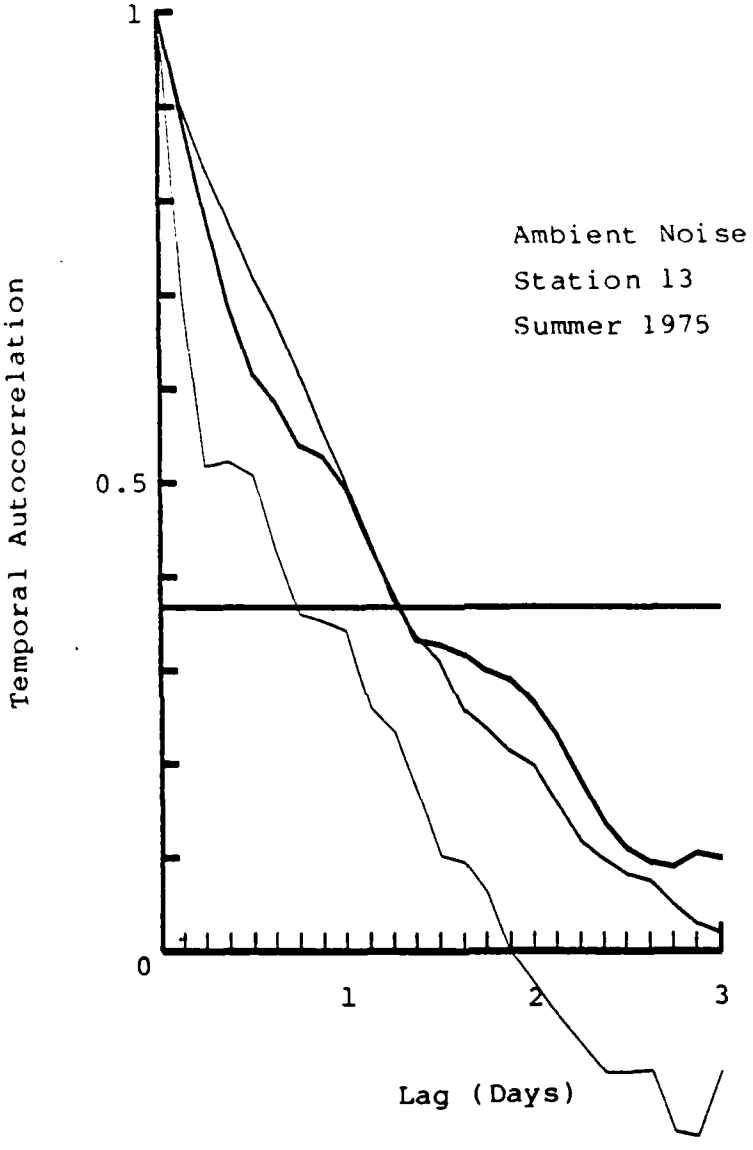

Fig. G.4. Ambient noise autocorrelations, Station 13, based on summer AIDJEX noise data (dB): 10 Hz (lightest line), 32 Hz (darker line), and 1000 Hz (darkest line).

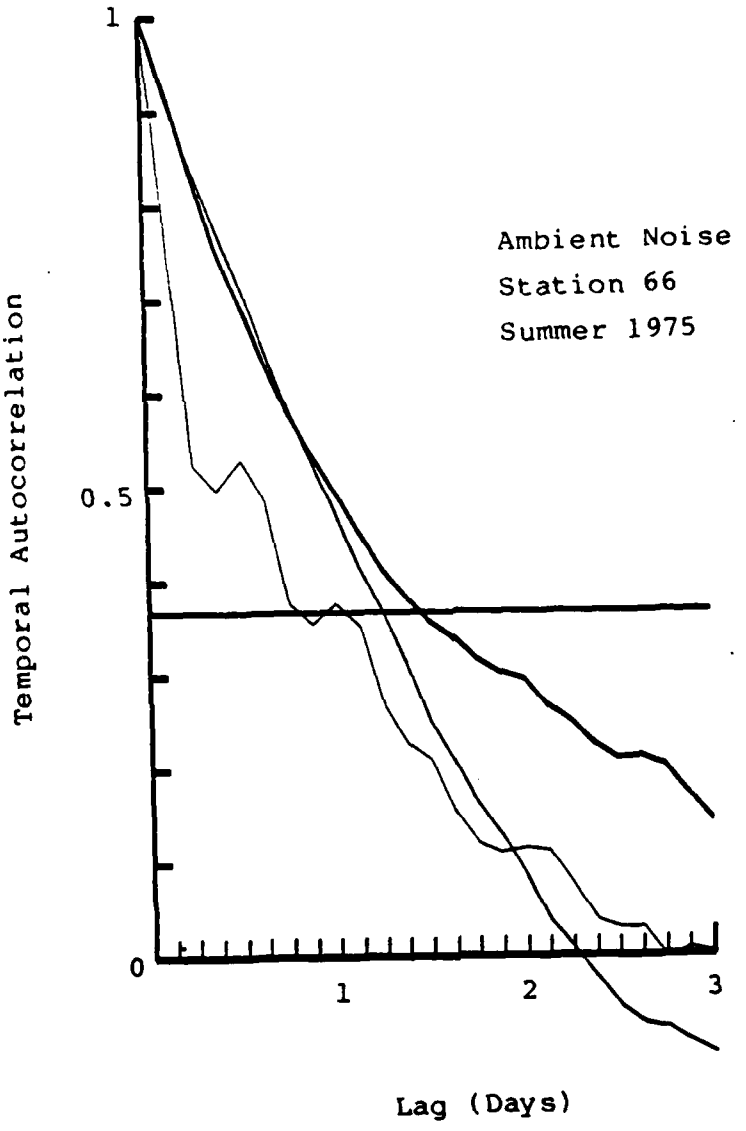

Fig. G.5. Ambient noise autocorrelations, Station 66, based on summer AIDJEX noise data (dB): 10 Hz (lightest line), 32 Hz (darker line), and 1000 Hz (darkest line).

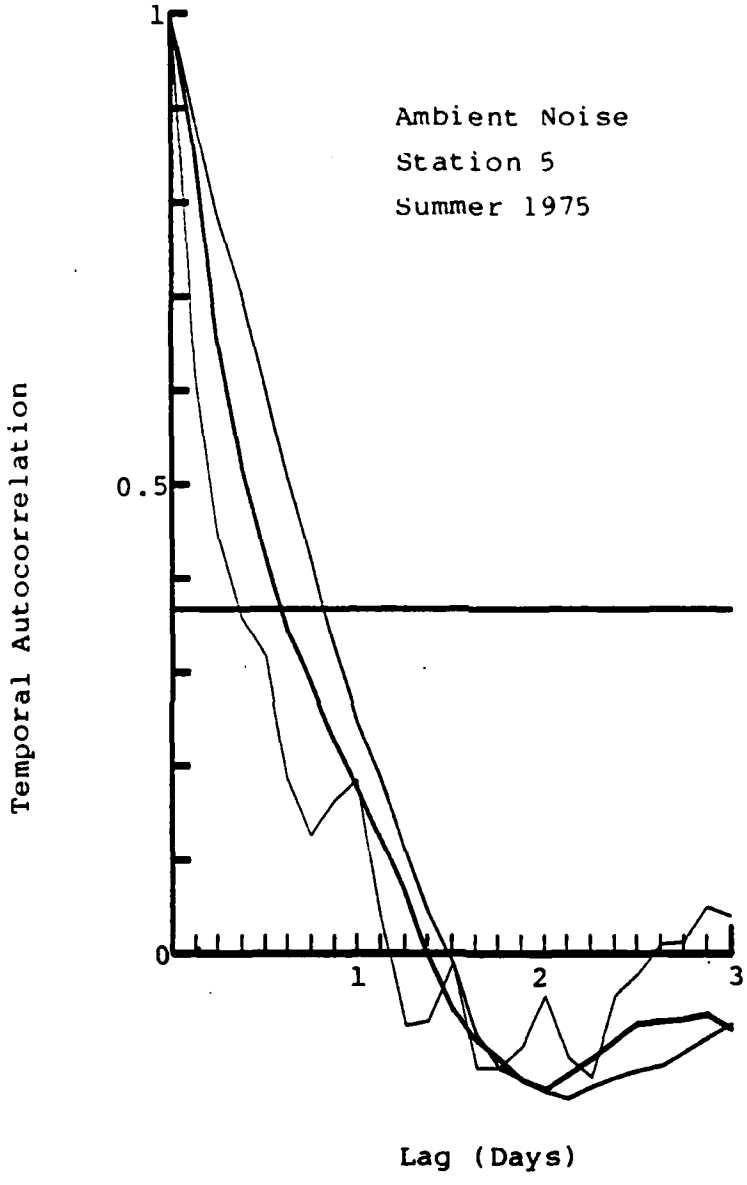

Fig. G.6. Ambient noise autocorrelations, Station 5, based on summer AIDJEX noise data (pressure amplitude): 10 Hz (lightest line), 32 Hz (darker line), and 1000 Hz (darkest line).

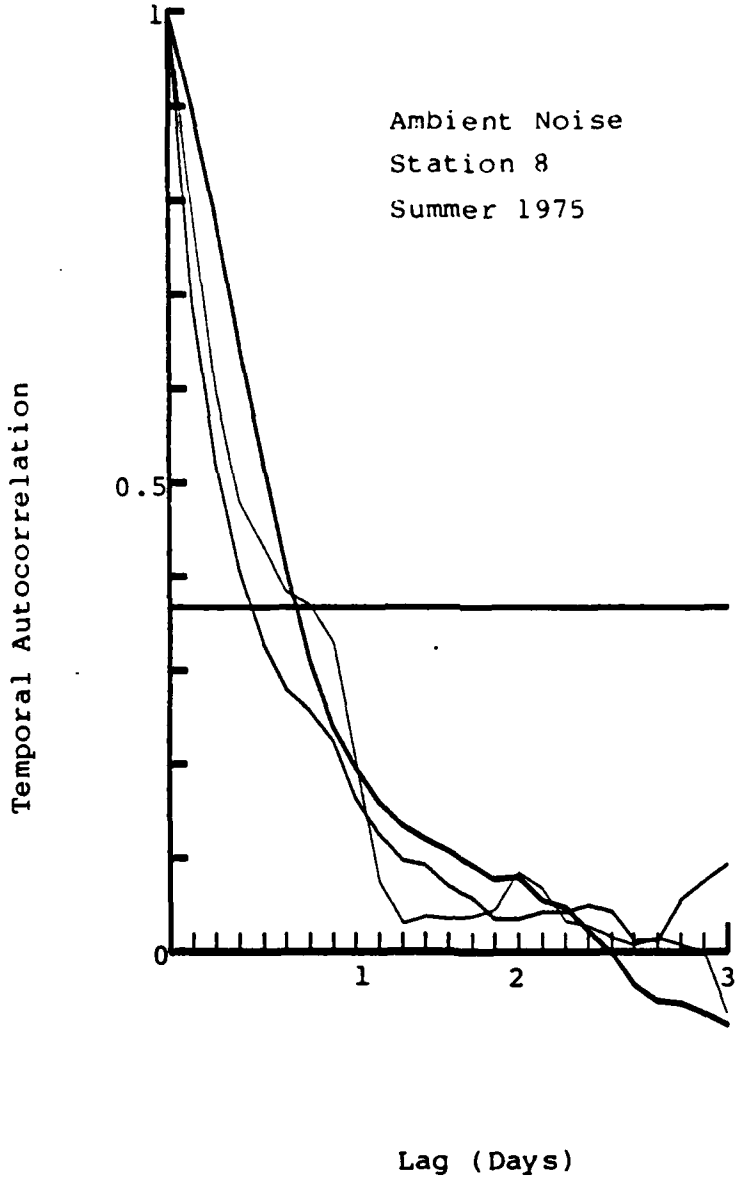

Fig. G.7. Ambient noise autocorrelations, Station 8, based on summer AIDJEX noise data (pressure amplitude): 10 Hz (lightest line), 32 Hz (darker line), and 1000 Hz (darkest line).

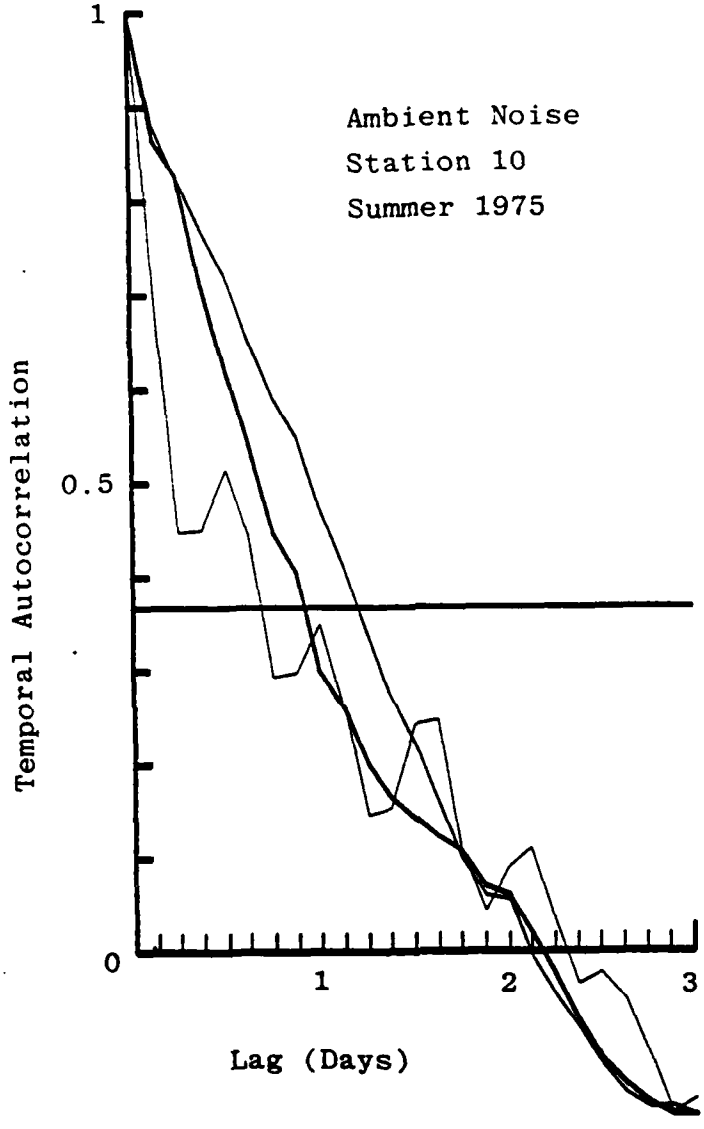

Fig. G.8. Ambient noise autocorrelations, Station 10, based on summer AIDJEX noise data (pressure amplitude): 10 Hz (lightest line), 32 Hz (darker line), and 1000 Hz (darkest line).

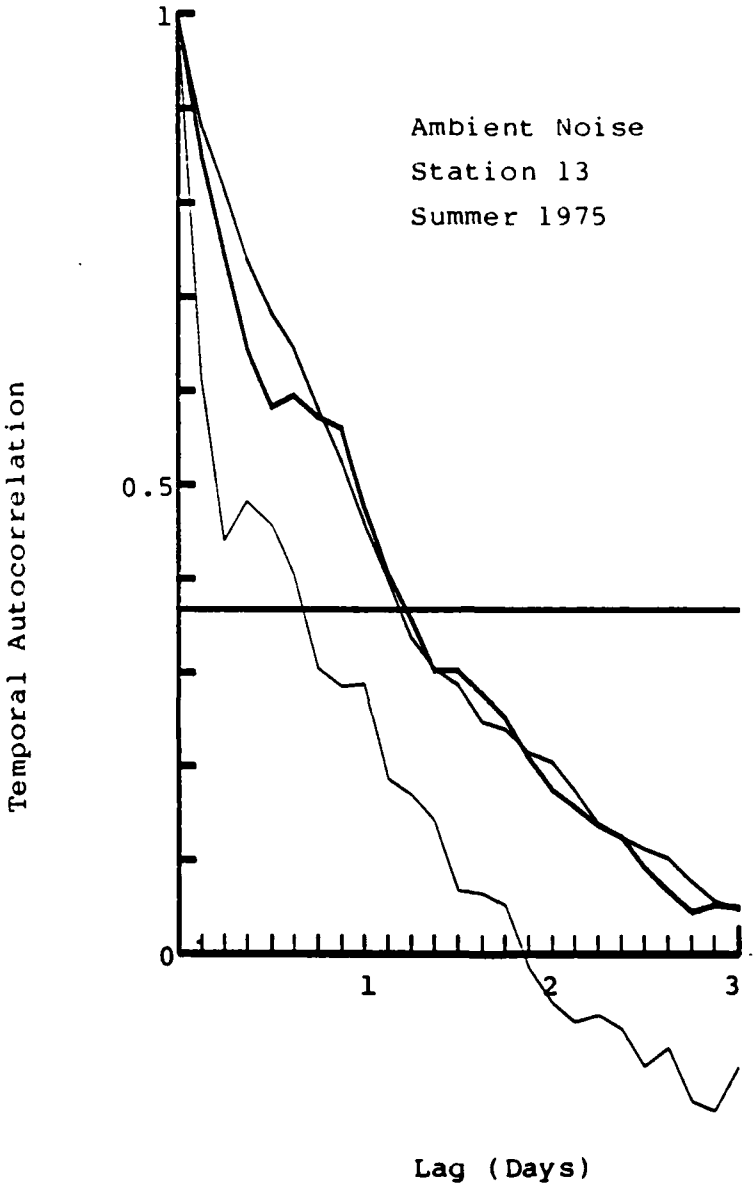

Fig. G.9. Ambient noise autocorrelations, Station 13, based on summer AIDJEX noise data (pressure amplitude): 10 Hz (lightest line), 32 Hz (darker line), and 1000 Hz (darkest line).

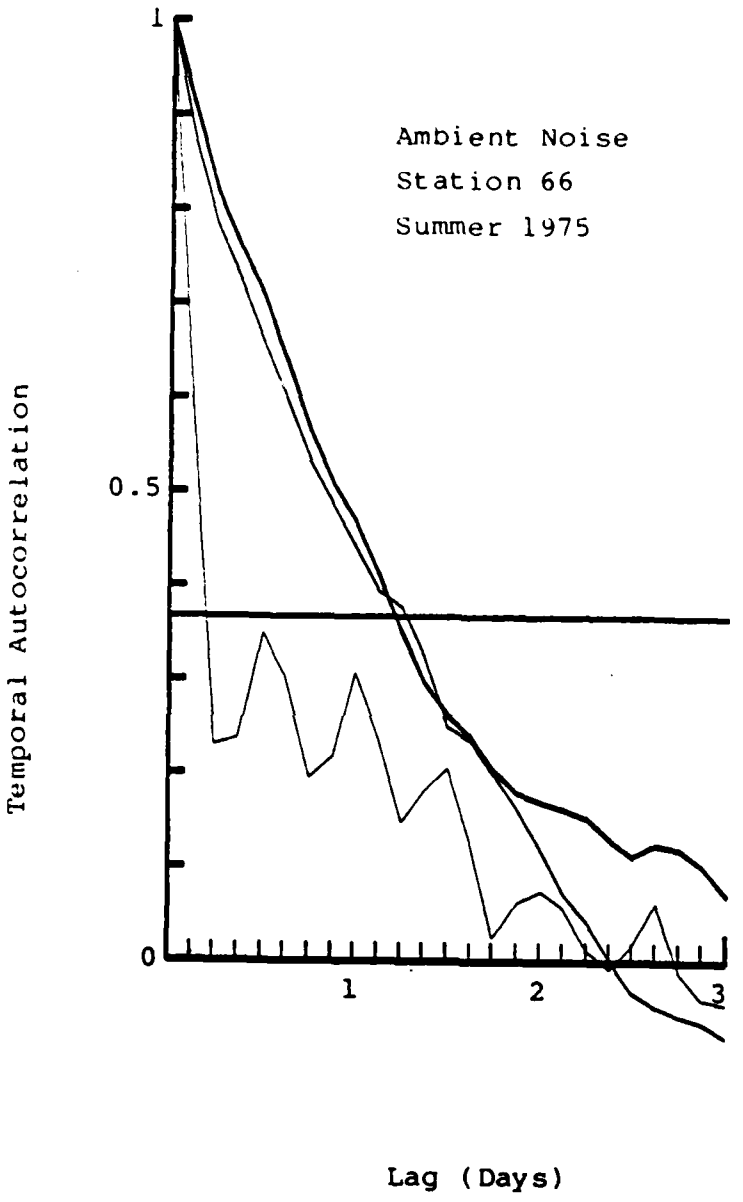

Fig. G.10. Ambient noise autocorrelations, Station 66, based on summer AIDJEX noise data (pressure amplitude): 10 Hz (lightest line), 32 Hz (darker line), and 1000 Hz (darkest line).

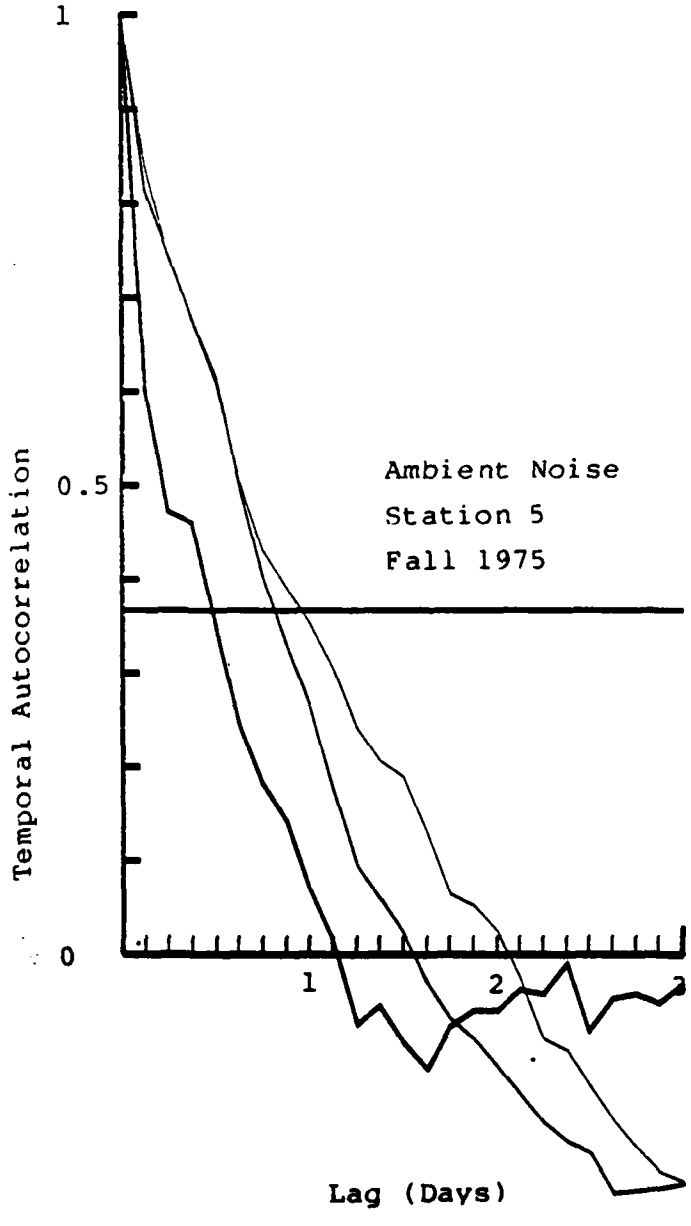

Fig. G.11. Ambient noise autocorrelations, Station 5, based on fall AIDJEX noise data (dB): 10 Hz (lightest line), 32 Hz (darker line), and 1000 Hz (darkest line).

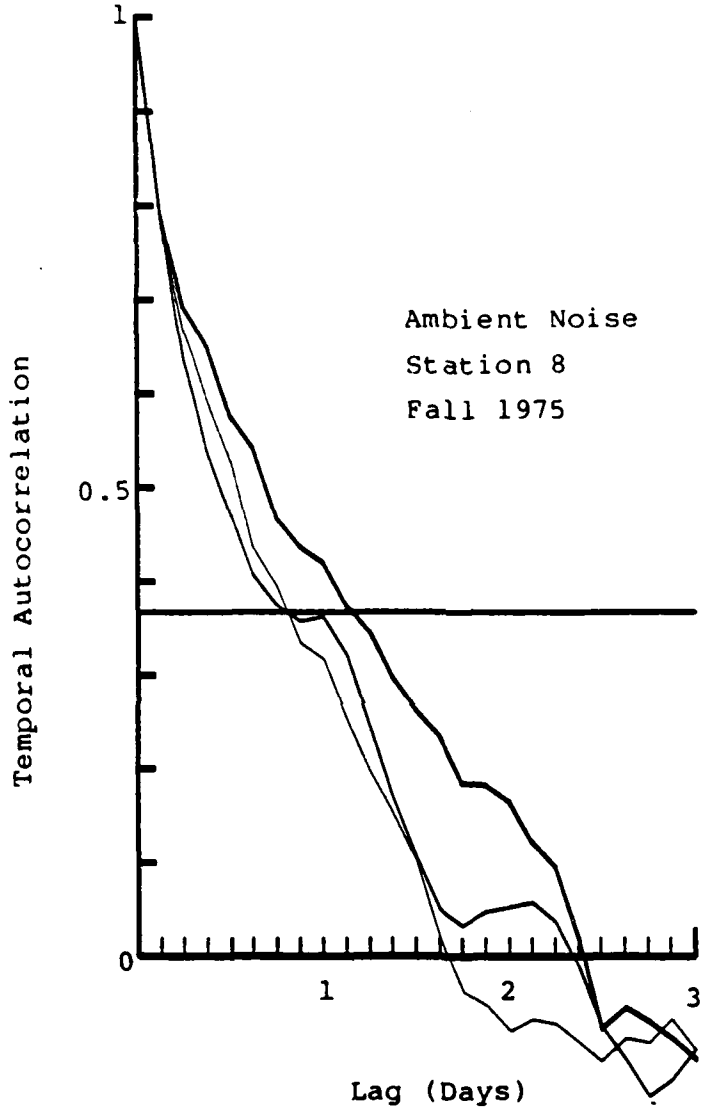

Fig. G.12. Ambient noise autocorrelations, Station 8, based on fall AIDJEX noise data (dB): 10 Hz (lightest line), 32 Hz (darker line), and 1000 Hz (darkest line).

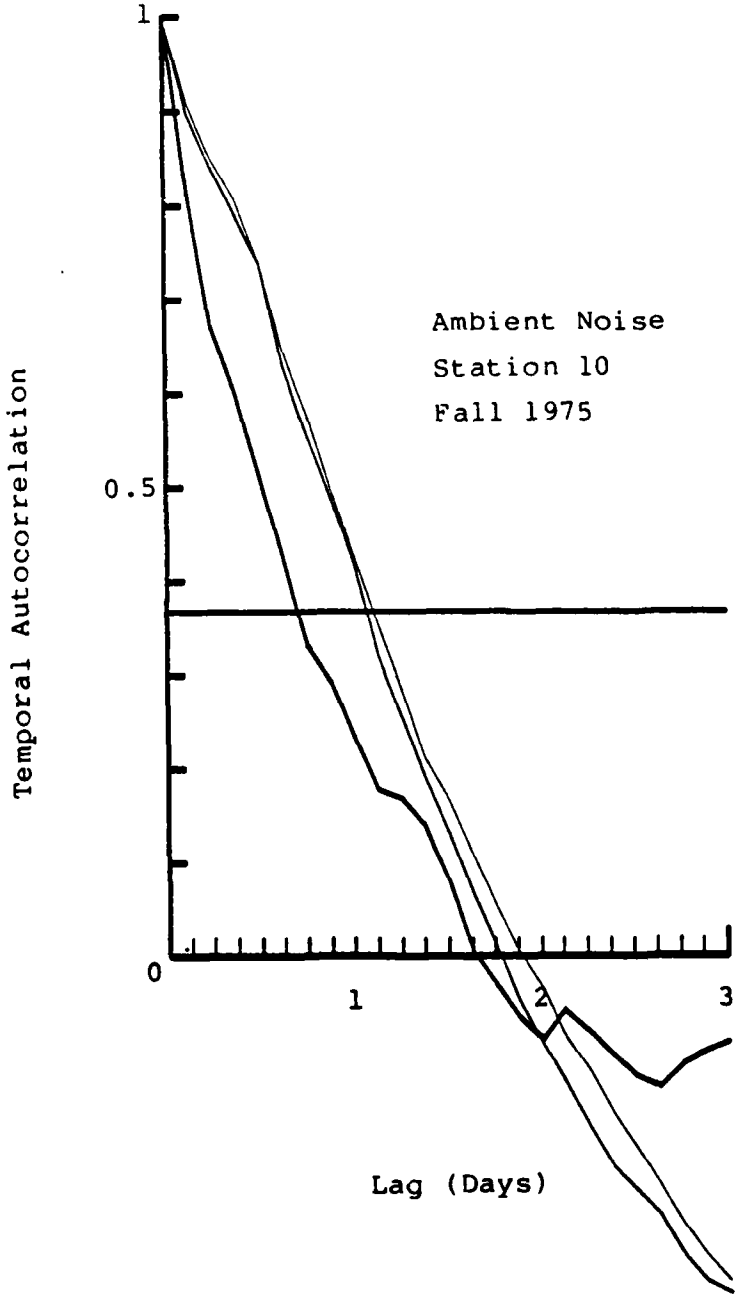

Fig. G.13. Ambient noise autocorrelations, Station 10, based on fall AIDJEX noise data (dB): 10 Hz (lightest line), 32 Hz (darker line), and 1000 Hz (darkest line).

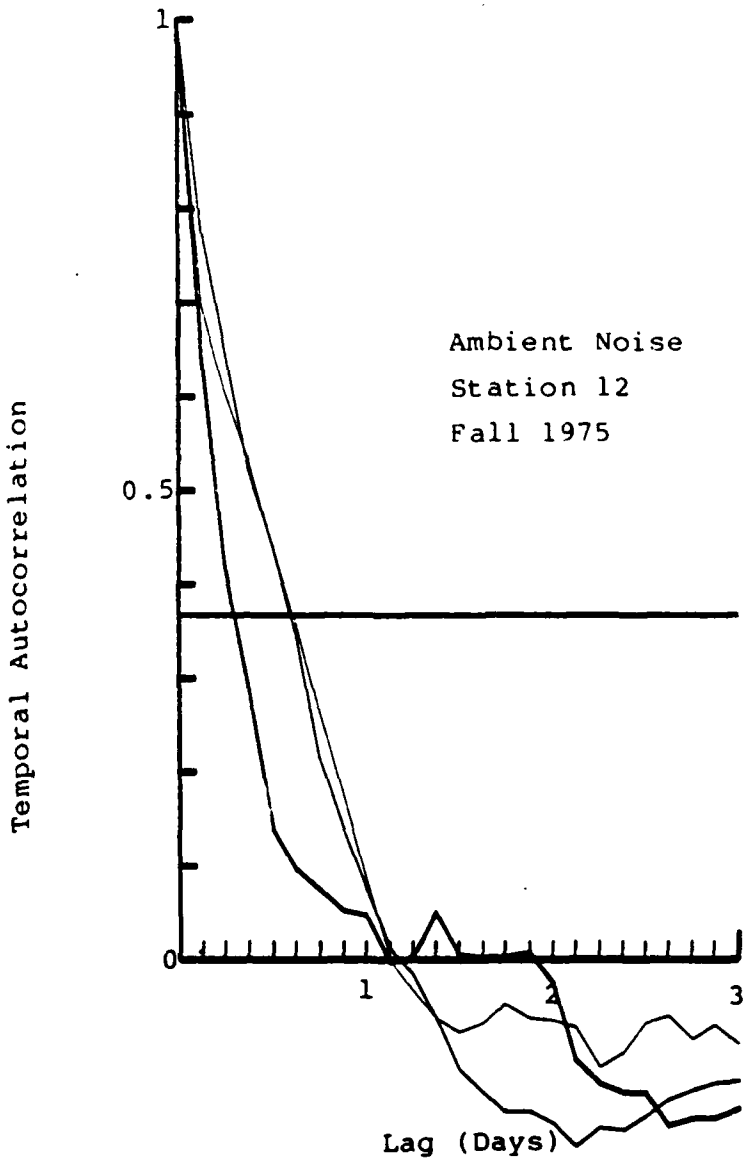

Fig. G.14. Ambient noise autocorrelations, Station 12, based on fall AIDJEX noise data (dB): 10 Hz (lightest line), 32 Hz (darker line), and 1000 Hz (darkest line).

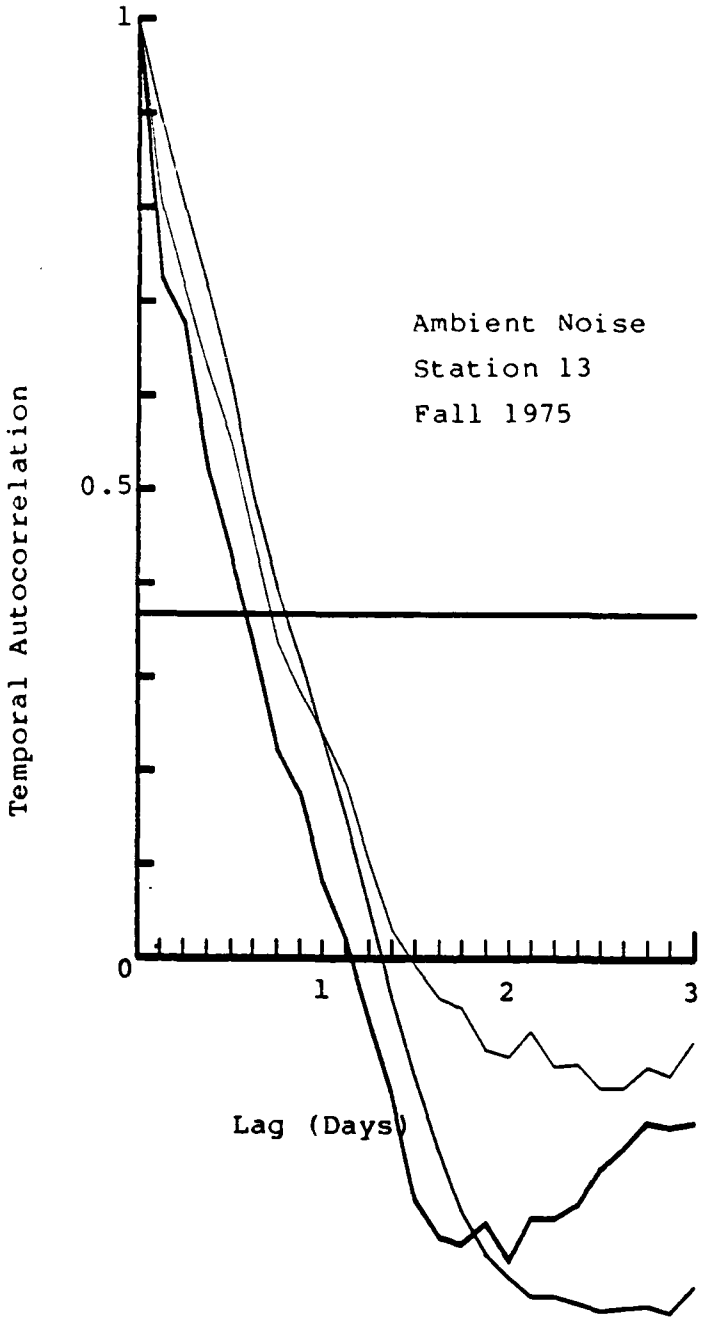

Fig. G.15. Ambient noise autocorrelations, Station 13, based on fall AIDJEX noise data (dB): 10 Hz (lightest line), 32 Hz (darker line), and 1000 Hz (darkest line).

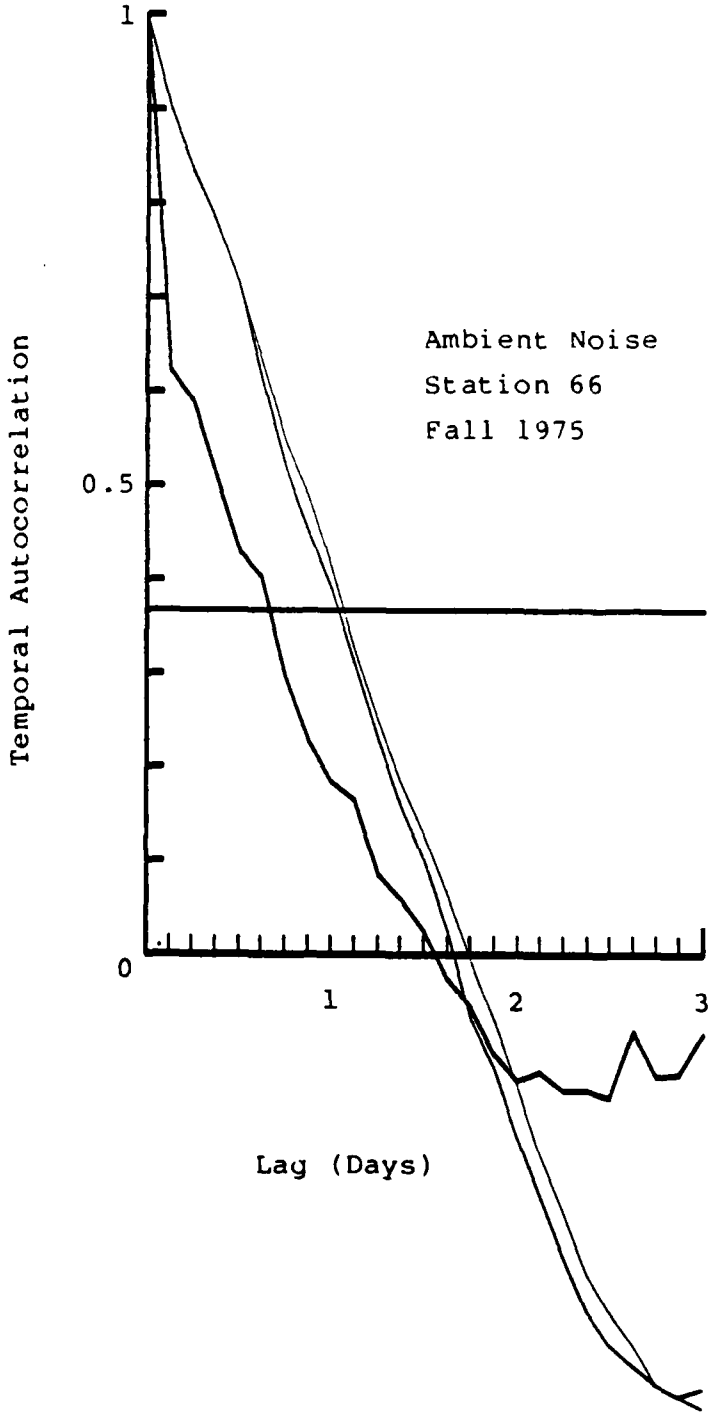

Fig. G.16. Ambient noise autocorrelations, Station 66, based on fall AIDJEX noise data (dB): 10 Hz (lightest line), 32 Hz (darker line), and 1000 Hz (darkest line).

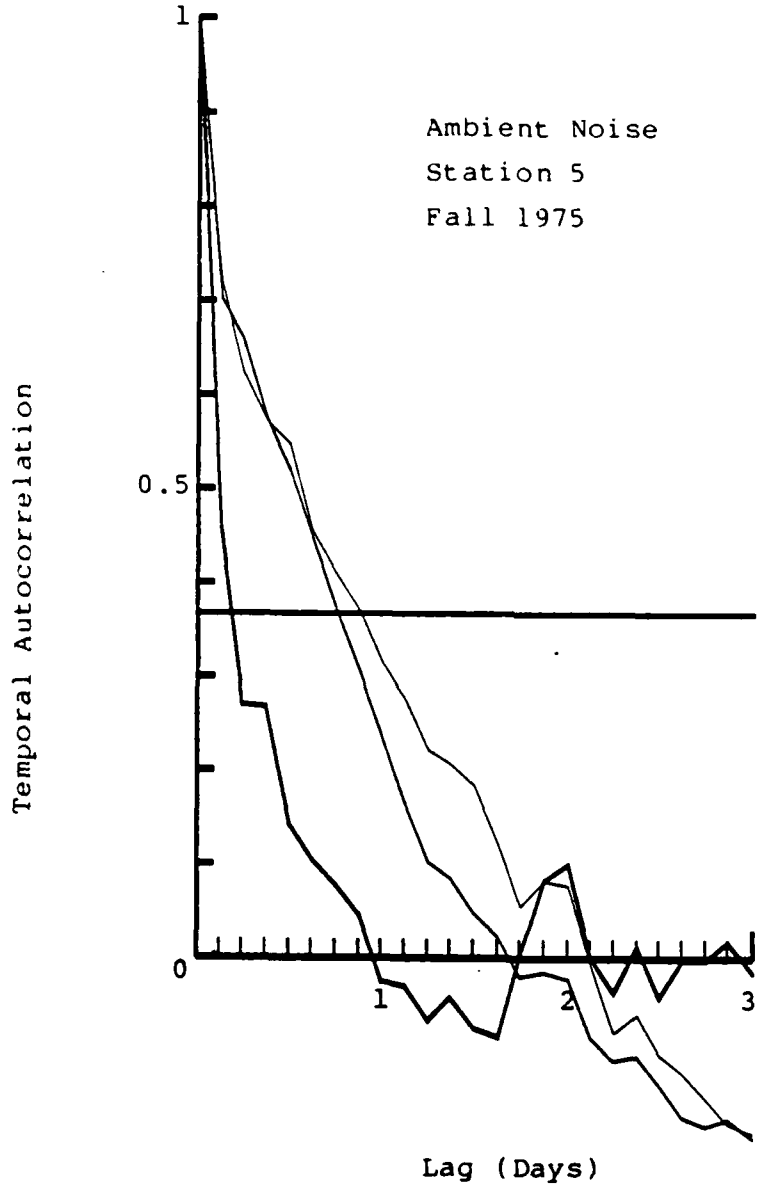

Fig. G.17. Ambient noise autocorrelations, Station 5, based on fall AIDJEX noise data (pressure amplitude): 10 Hz (lightest line), 32 Hz (darker line), and 1000 Hz (darkest line).

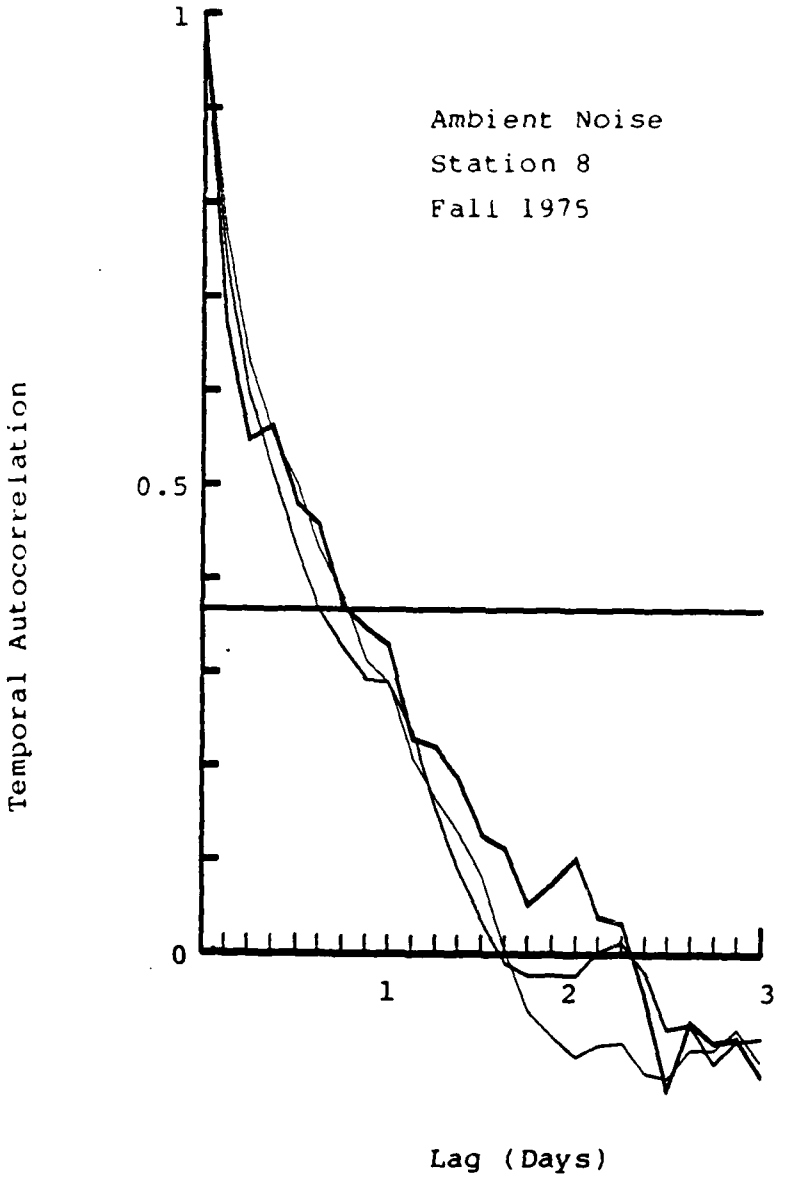

Fig. G.18. Ambient noise autocorrelations, Station 8, based on fall AIDJEX noise data (pressure amplitude): 10 Hz (lightest line), 32 Hz (darker line), and 1000 Hz (darkest line).

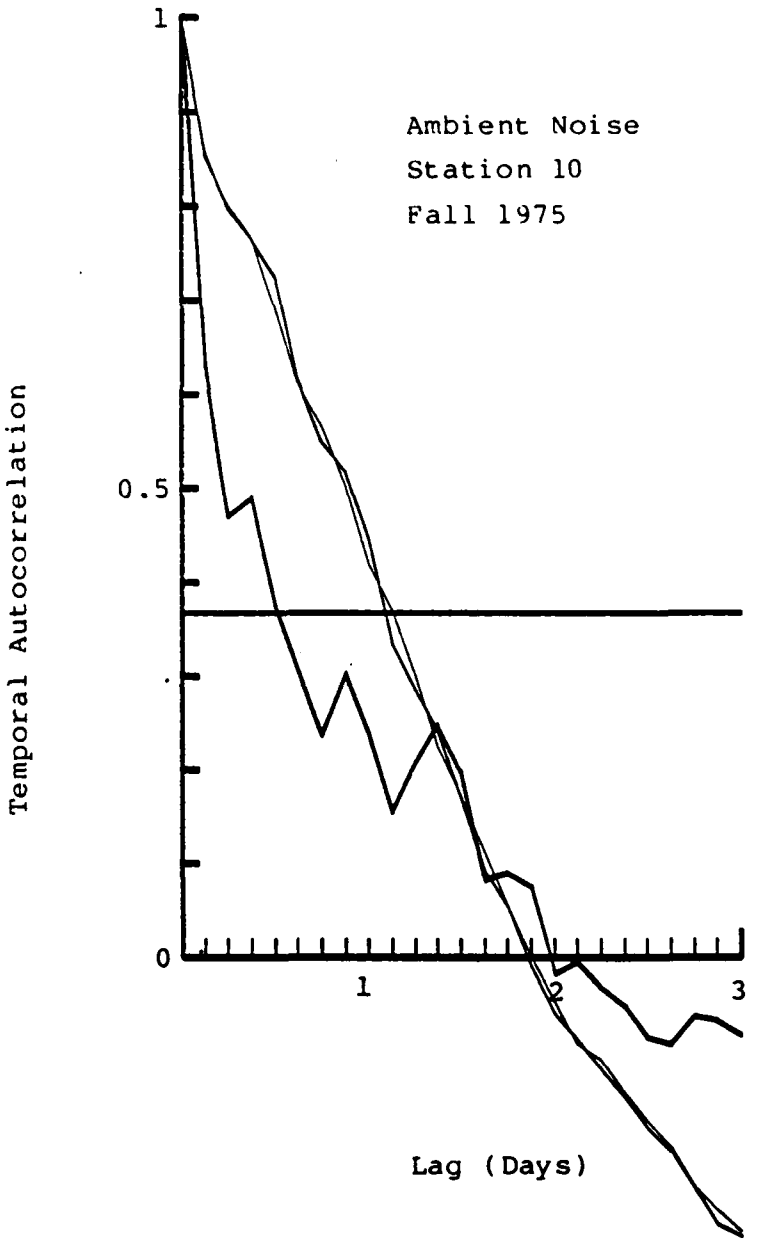

Fig. G.19. Ambient noise autocorrelations, Station 10, based on fall AIDJEX noise data (pressure amplitude): 10 Hz (lightest line), 32 Hz (darker line), and 1000 Hz (darkest line).

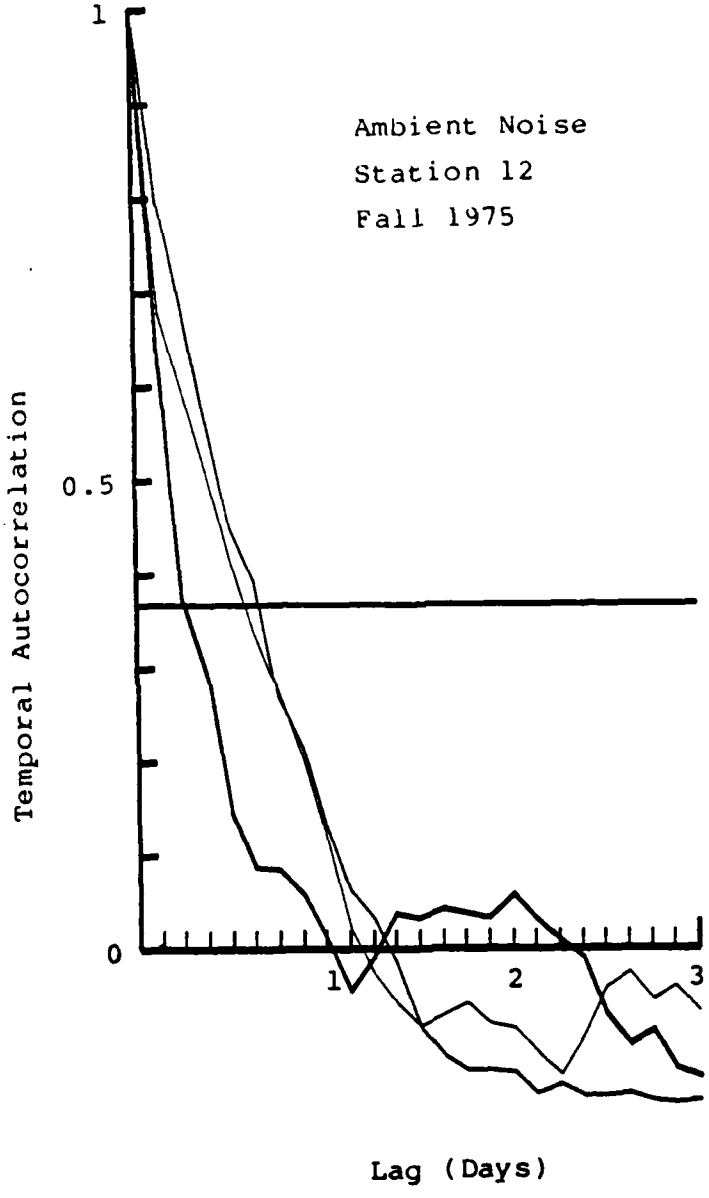

Fig. G.20. Ambient noise autocorrelations, Station 12, based on fall AIDJEX noise data (pressure amplitude): 10 Hz (lightest line), 32 Hz (darker line), and 1000 Hz (darkest line).

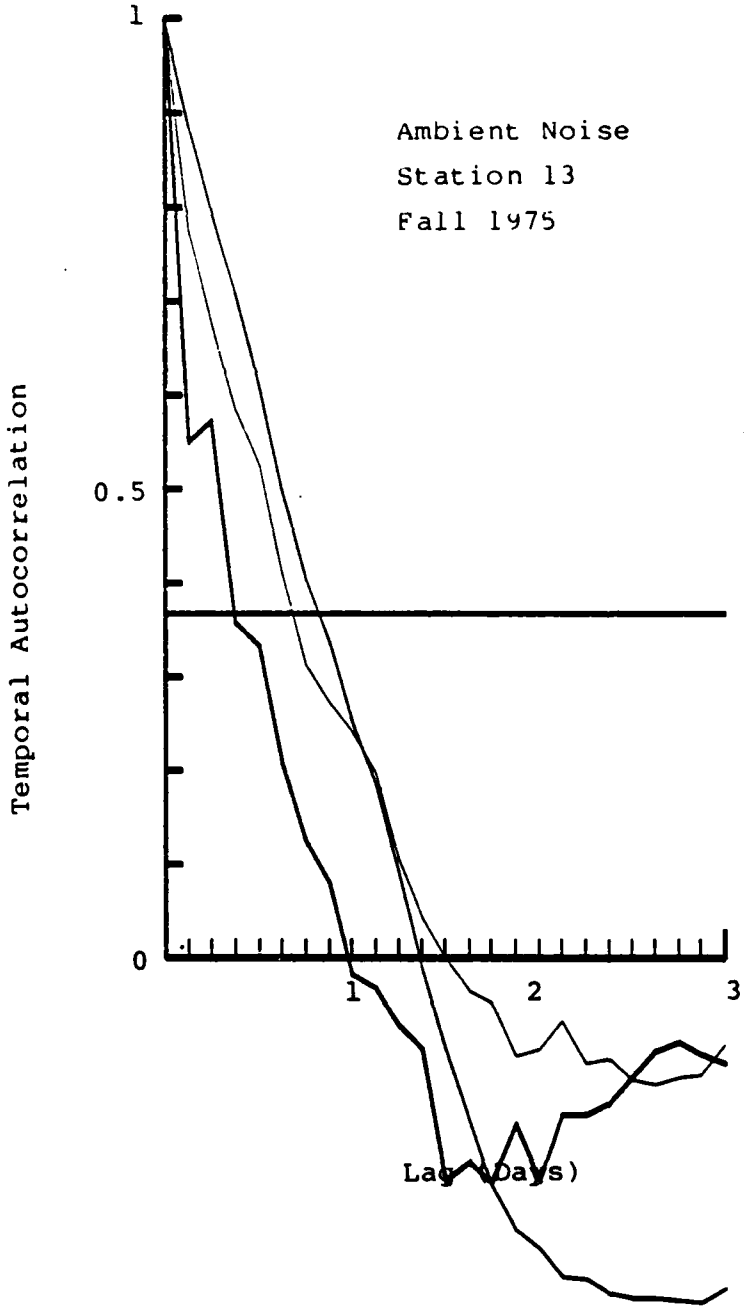

Fig. G.21. Ambient noise autocorrelations, Station 13, based on fall AIDJEX noise data (pressure amplitude): 10 Hz (lightest line), 32 Hz (darker line), and 1000 Hz (darkest line).

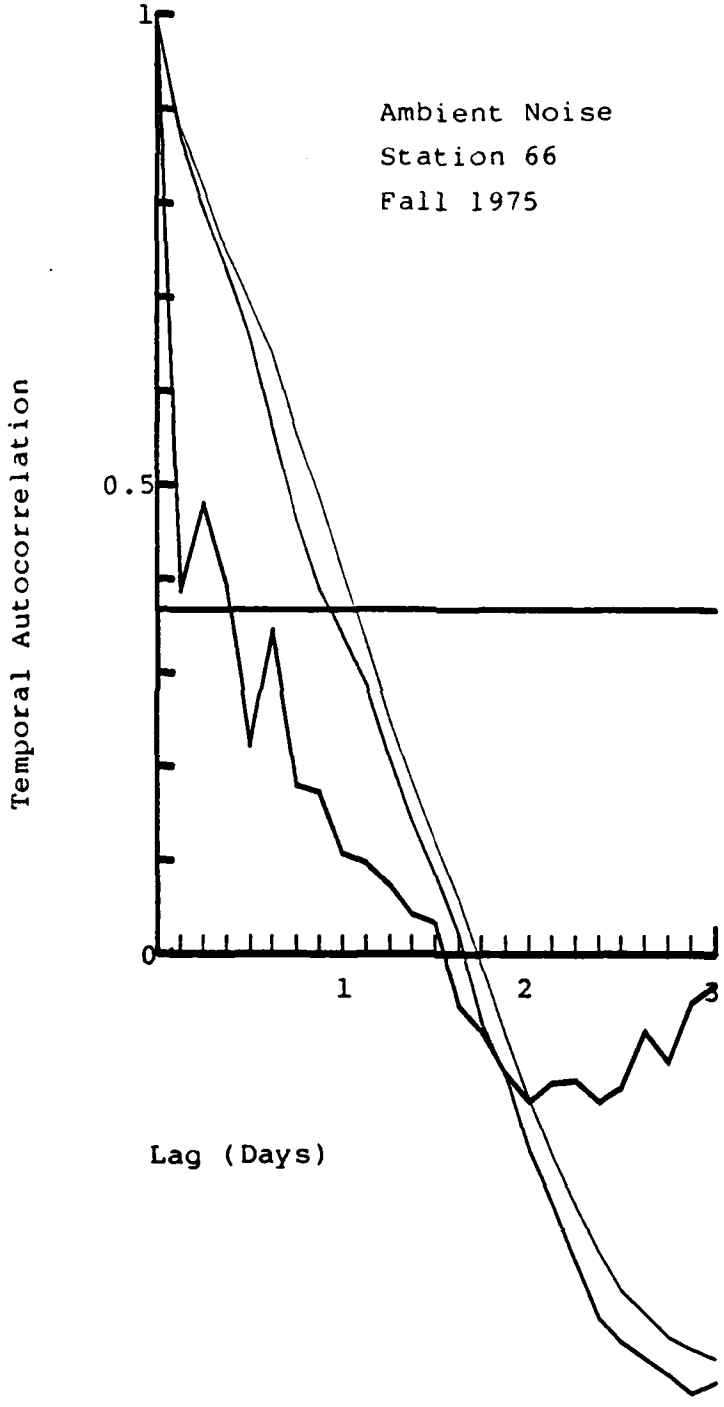

Fig. G.22. Ambient noise autocorrelations, Station 66, based on fall AIDJEX noise data (pressure amplitude): 10 Hz (lightest line), 32 Hz (darker line), and 1000 Hz (darkest line).

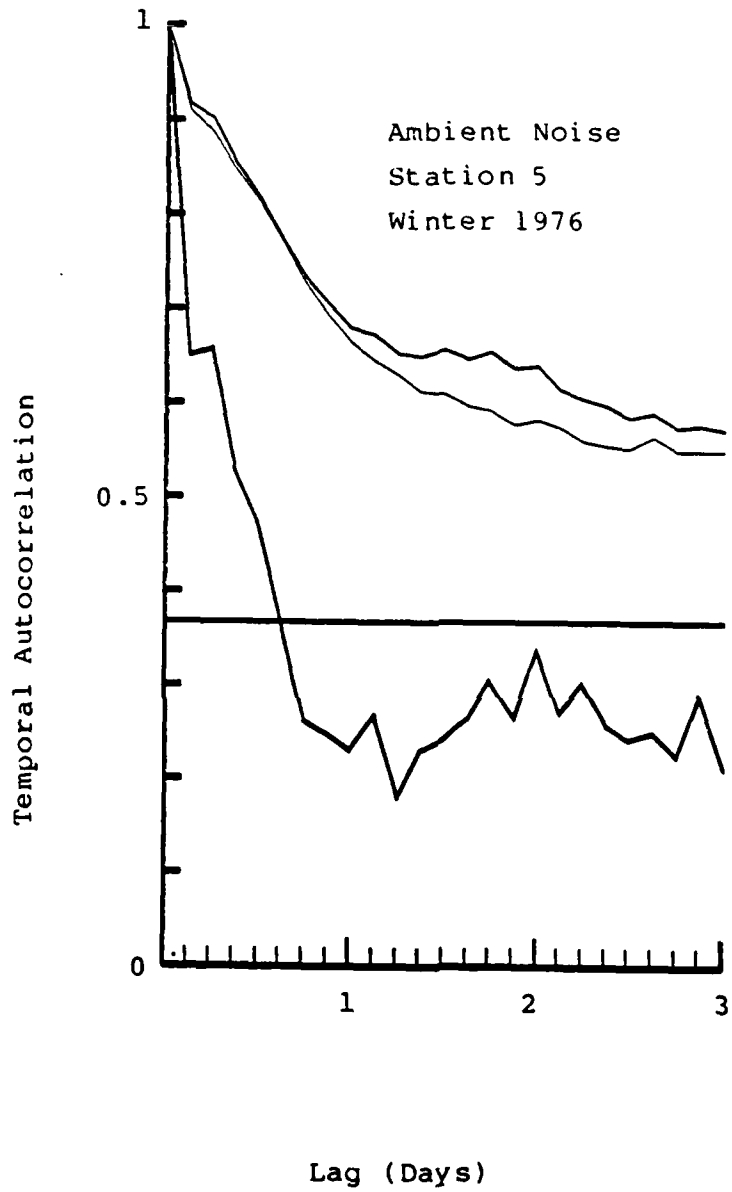

Fig. G.23. Ambient noise autocorrelations, Station 5, based on winter AIDJEX noise data (dB): 10 Hz (lightest line), 32 Hz (darker line), and 1000 Hz (darkest line).

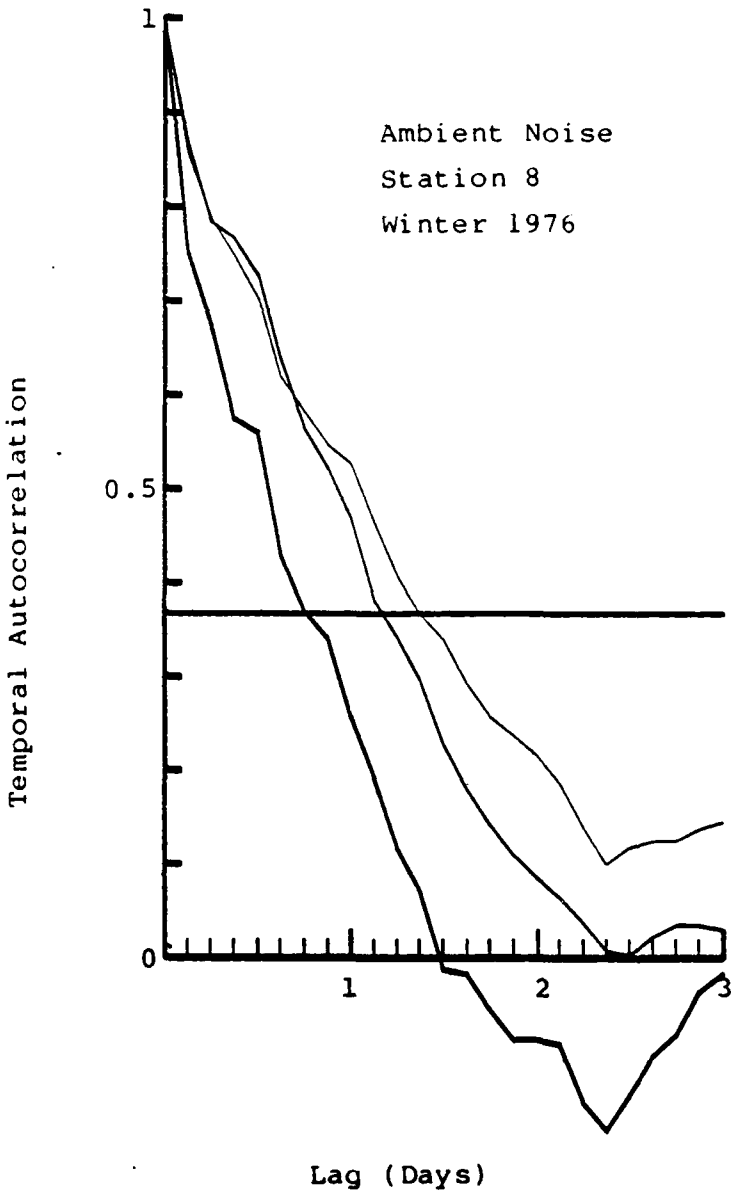

Fig. G.24. Ambient noise autocorrelations, Station 8, based on winter AIDJEX noise data (dB): 10 Hz (lightest line), 32 Hz (darker line), and 1000 Hz (darkest line).

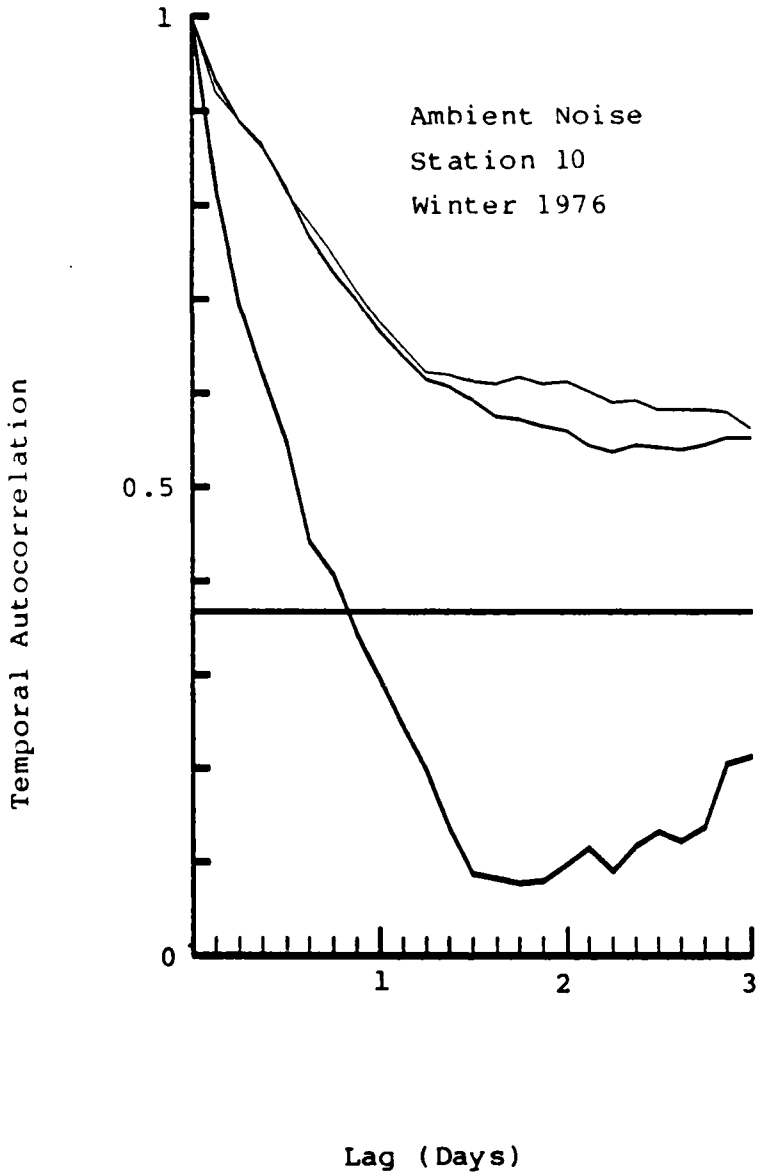

Fig. G.25. Ambient noise autocorrelations, Station 10, based on winter AIDJEX noise data (dB): 10 Hz (lightest line), 32 Hz (darker line), and 1000 Hz (darkest line).

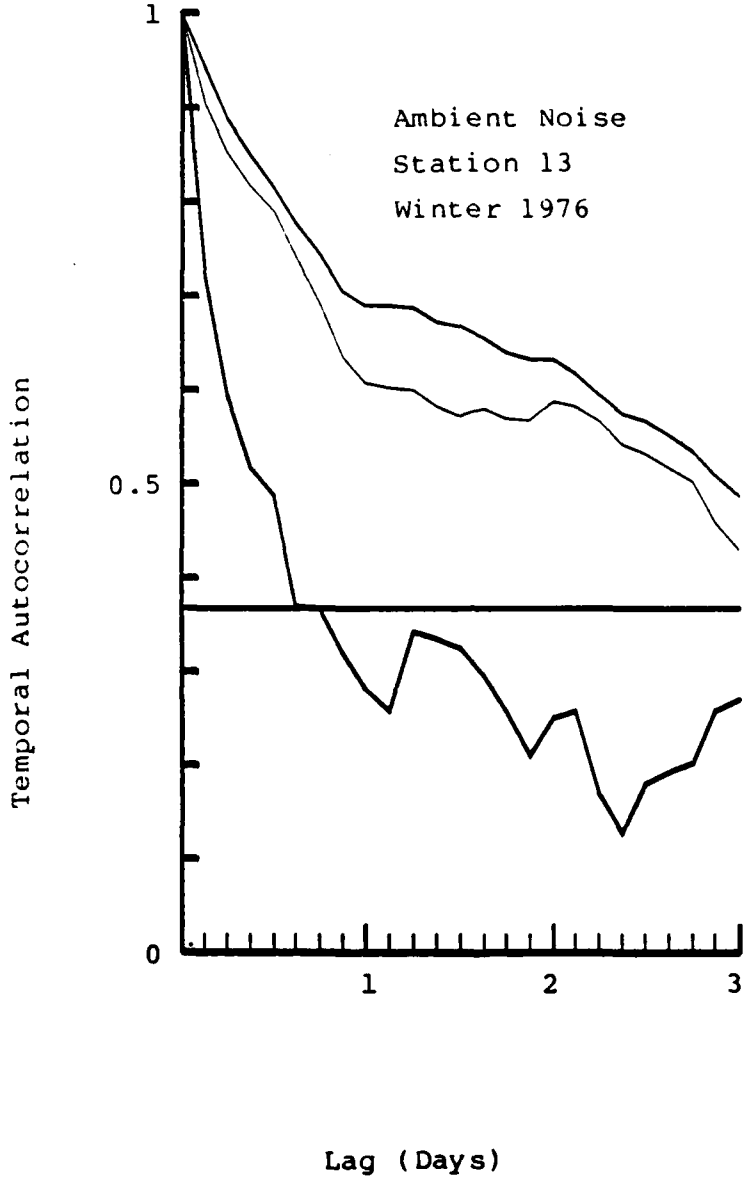

Fig. G.26. Ambient noise autocorrelations, Station 13, based on winter AIDJEX noise data (dB): 10 Hz (lightest line), 32 Hz (darker line), and 1000 Hz (darkest line).

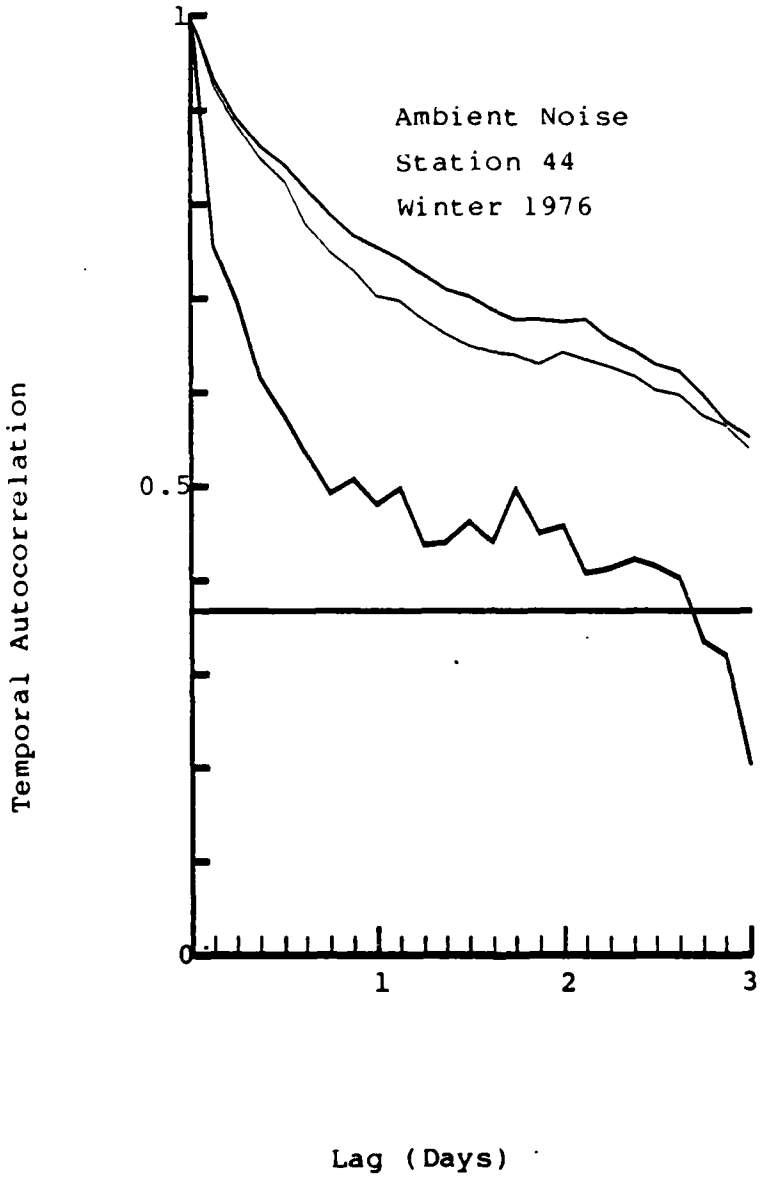

Fig. G.27. Ambient noise autocorrelations, Station 44, based on winter AIDJEX noise data (dB): 10 Hz (lightest line), 32 Hz (darker line), and 1000 Hz (darkest line).

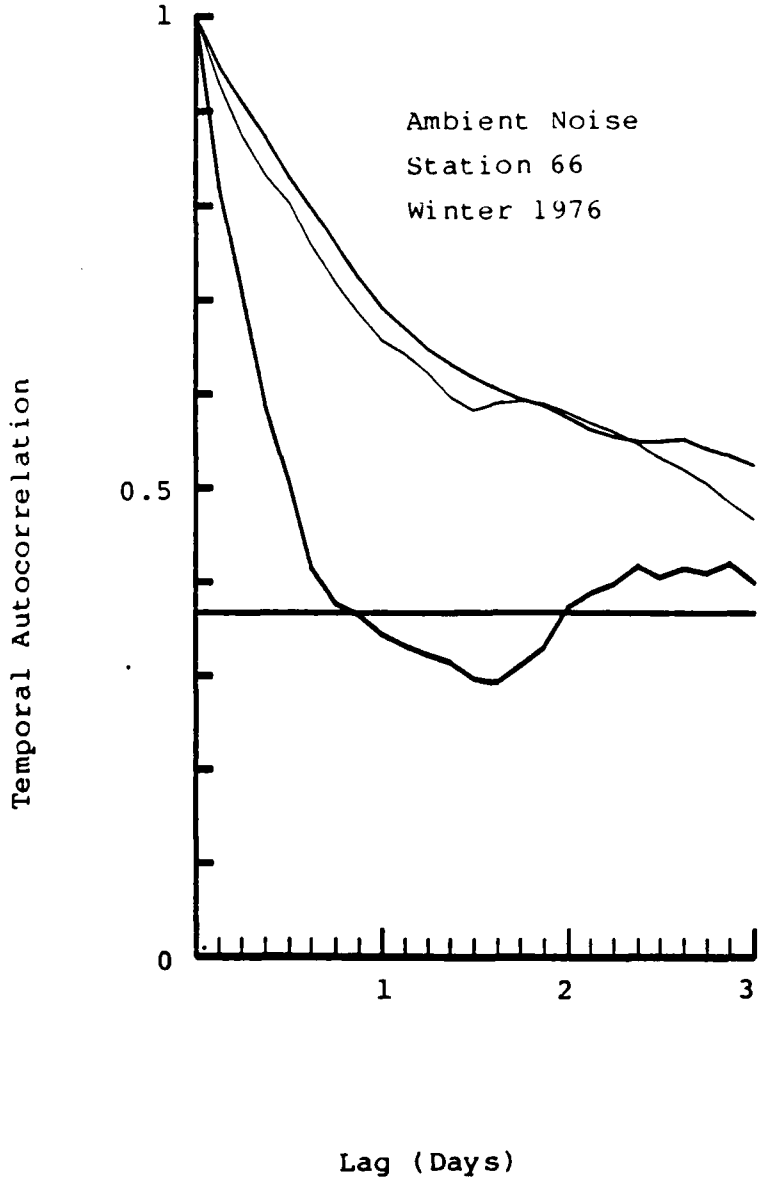

Fig. G.28. Ambient noise autocorrelations, Station 66, based on winter AIDJEX noise data (dB): 10 Hz (lightest line), 32 Hz (darker line), and 1000 Hz (darkest line).

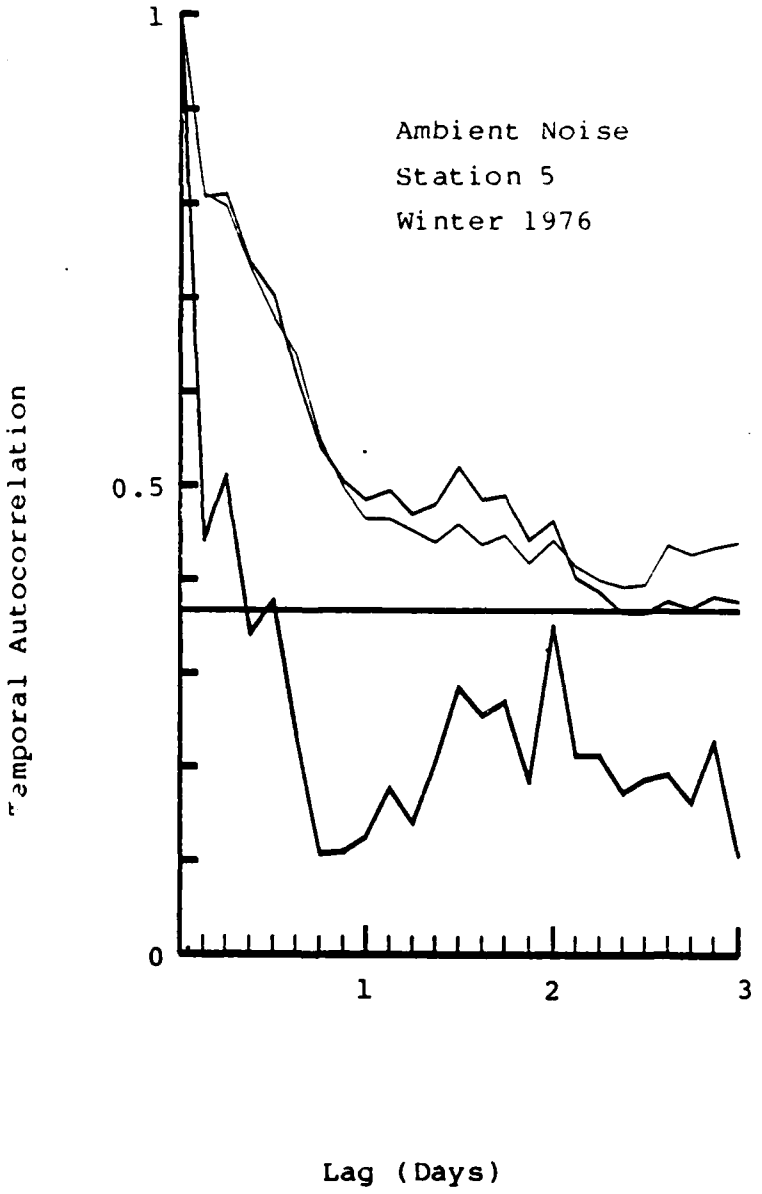

Fig. G.29. Ambient noise autocorrelations, Station 5, based on winter AIDJEX noise data (pressure amplitude): 10 Hz (lightest line), 32 Hz (darker line), and 1000 Hz (darkest line).

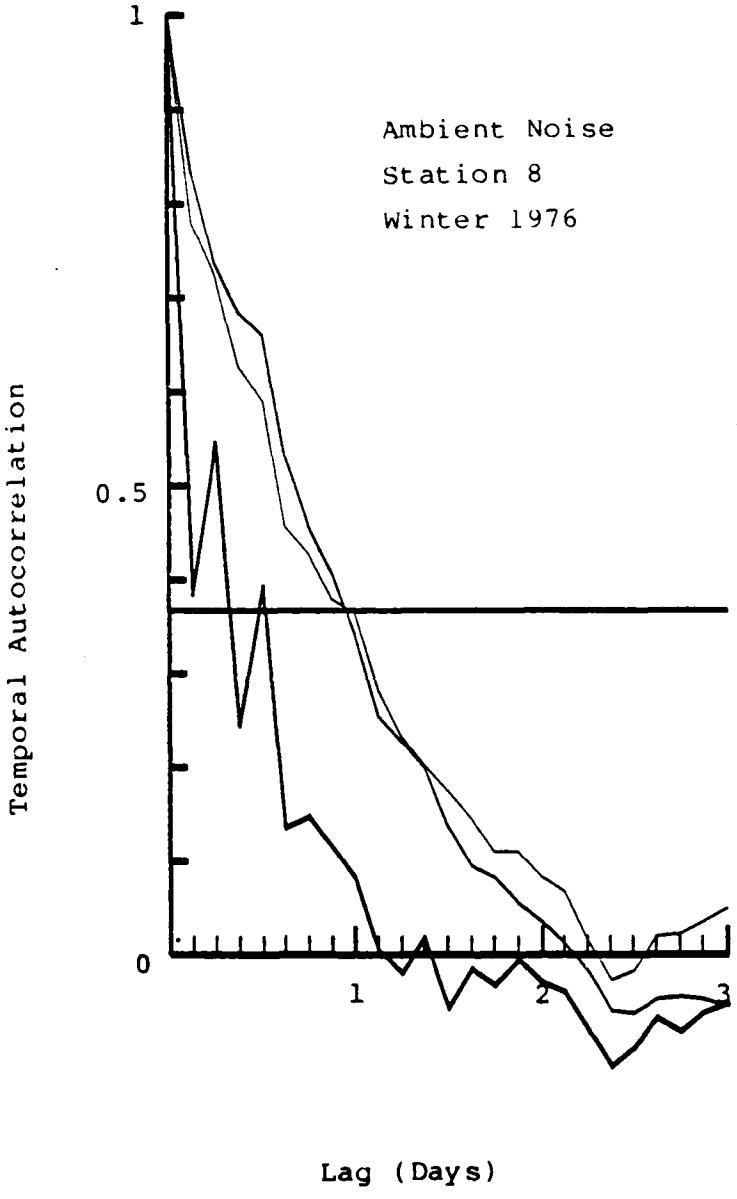

Fig. G.30. Ambient noise autocorrelations, Station 8, based on winter AIDJEX noise data (pressure amplitude): 10 Hz (lightest line), 32 Hz (darker line), and 1000 Hz (darkest line).

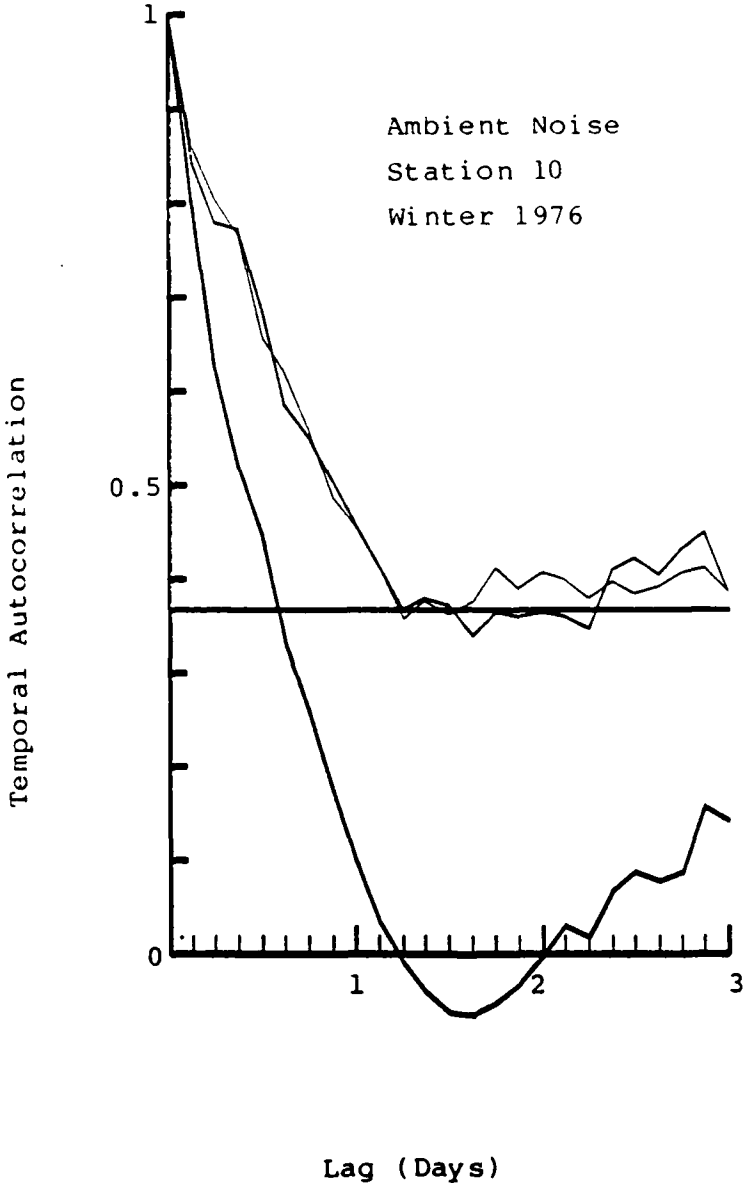

Fig. G.31. Ambient noise autocorrelations, Station 10, based on winter AIDJEX noise data (pressure amplitude): 10 Hz (lightest line), 32 Hz (darker line), and 1000 Hz (darkest line).

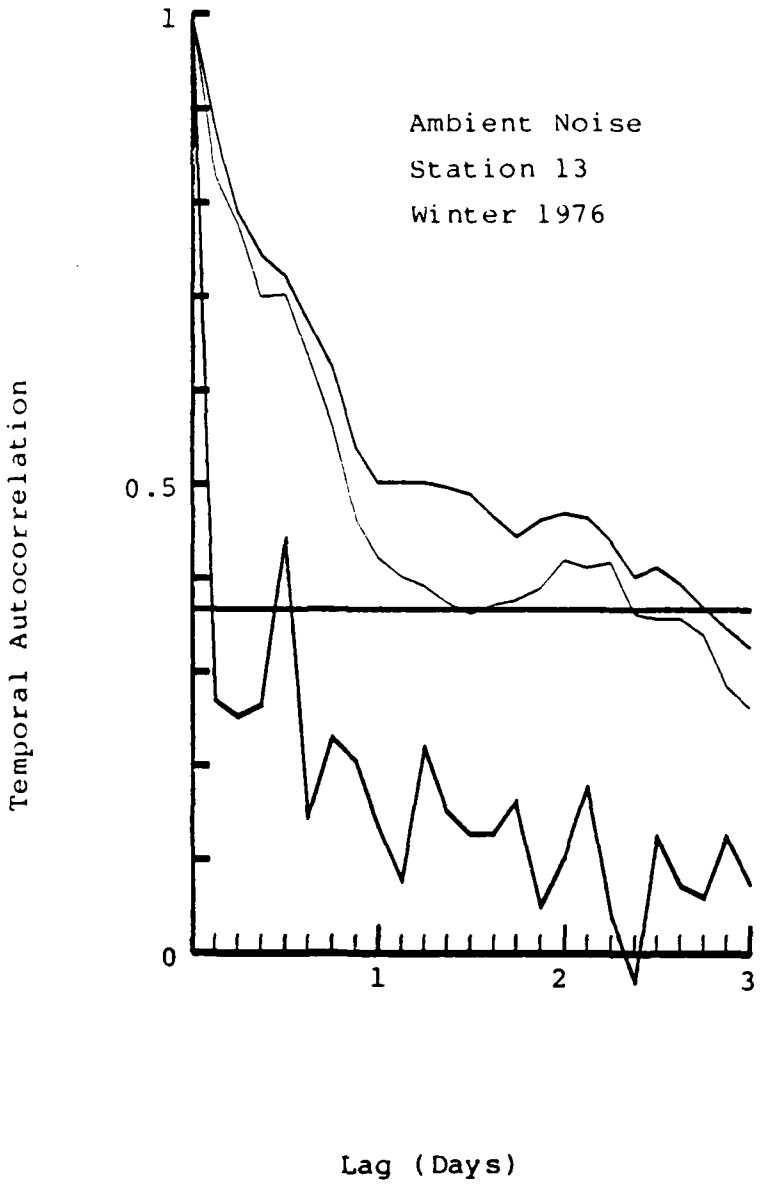

Fig. G.32. Ambient noise autocorrelations, Station 13, based on winter AIDJEX noise data (pressure amplitude): 10 Hz (lightest line), 32 Hz (darker line), and 1000 Hz (darkest line).

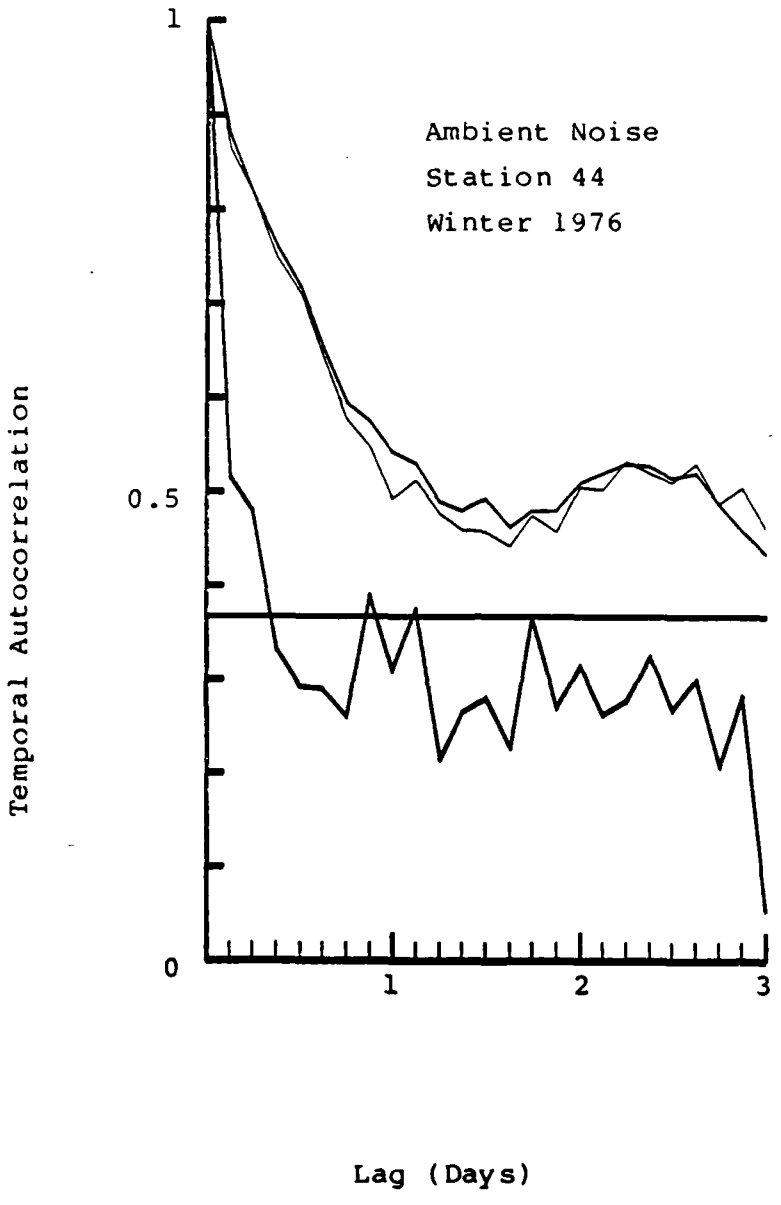

Fig. G.33. Ambient noise autocorrelations, Station 44, based on winter AIDJEX noise data (pressure amplitude): 10 Hz (lightest line), 32 Hz (darker line), and 1000 Hz (darkest line).

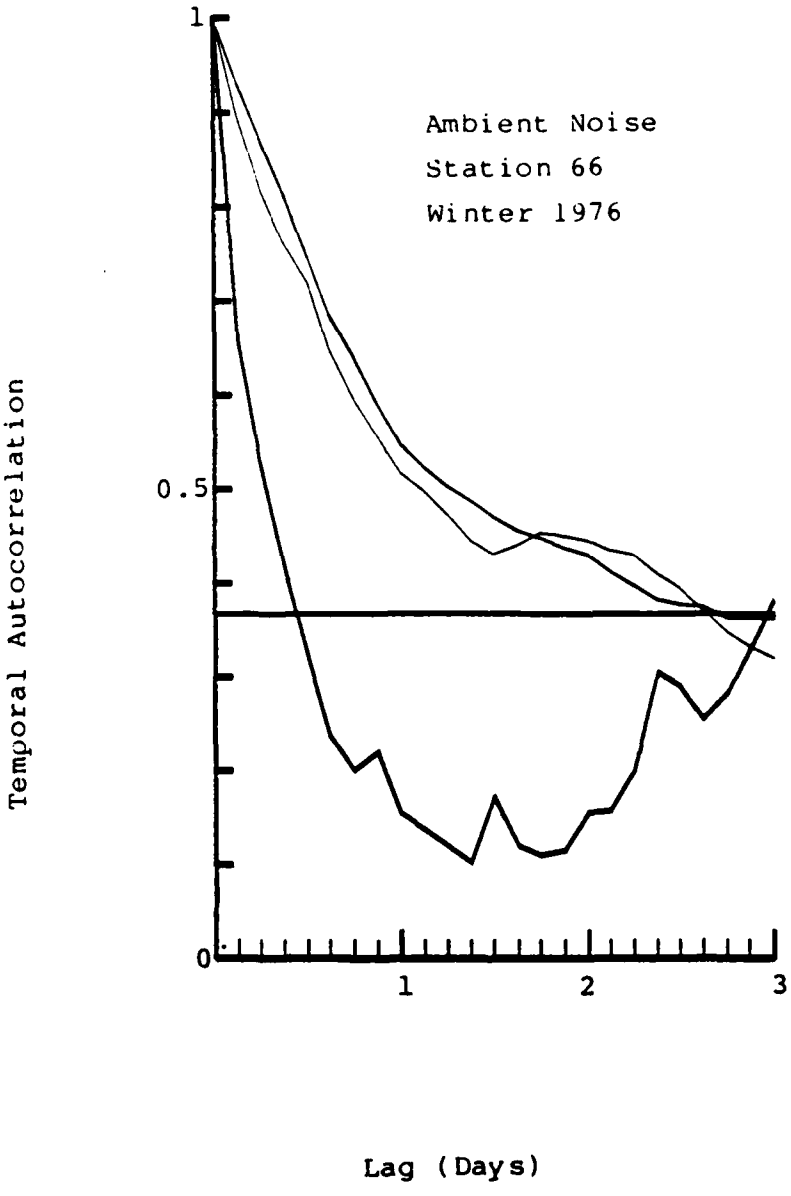

Fig. G.34. Ambient noise autocorrelations, Station 66, based on winter AIDJEX noise data (pressure amplitude): 10 Hz (lightest line), 32 Hz (darker line), and 1000 Hz (darkest line).

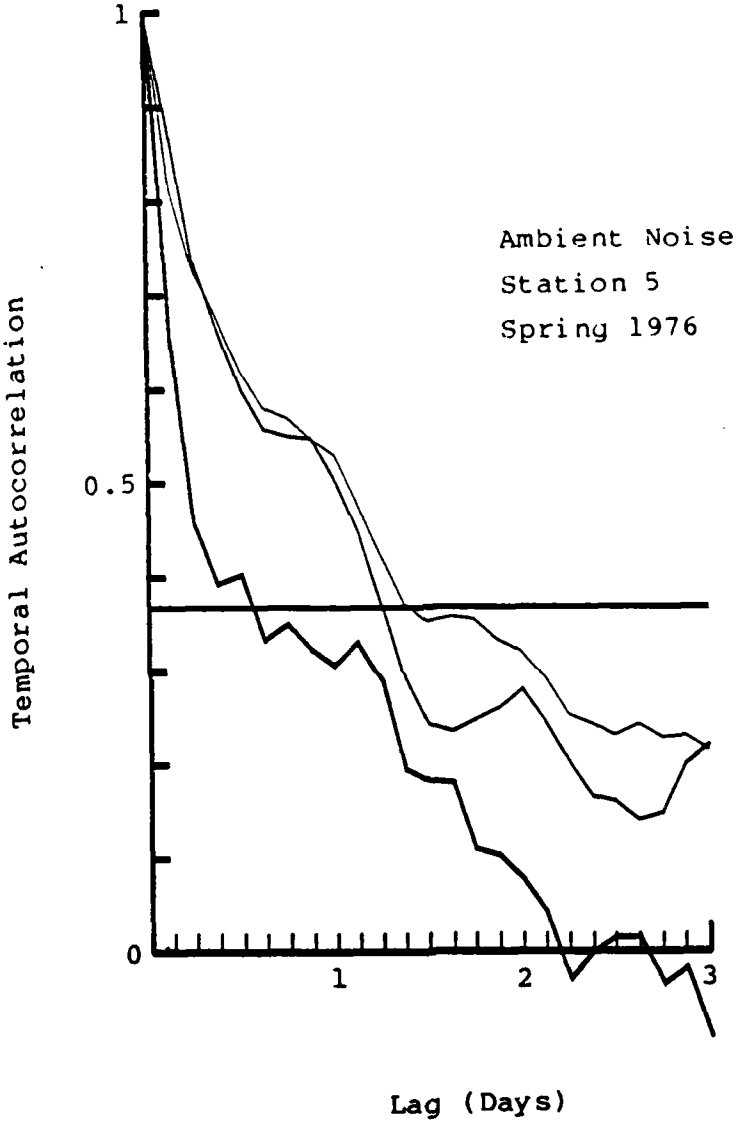

Fig. G.35. Ambient noise autocorrelations, Station 5, based on spring AIDJEX noise data (dB): 10 Hz (lightest line), 32 Hz (darker line), and 1000 Hz (darkest line).

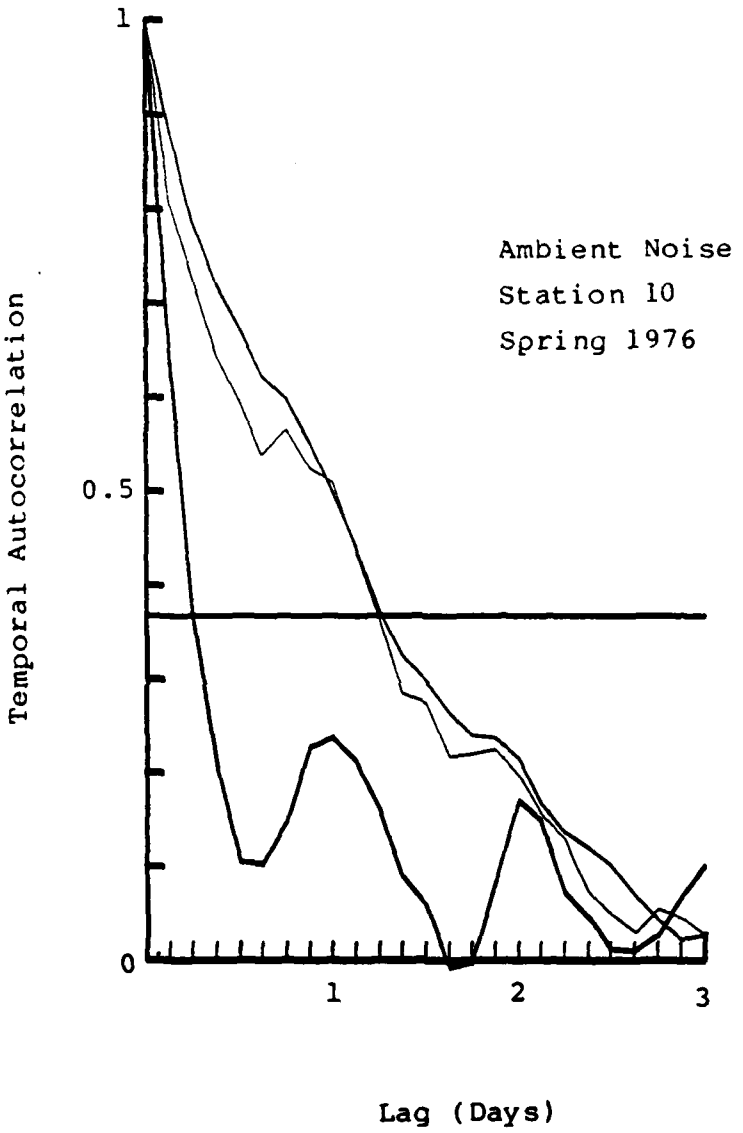

Fig. G.36. Ambient noise autocorrelations, Station 10, based on spring AIDJEX noise data (dB): 10 Hz (lightest line), 32 Hz (darker line), and 1000 Hz (darkest line).

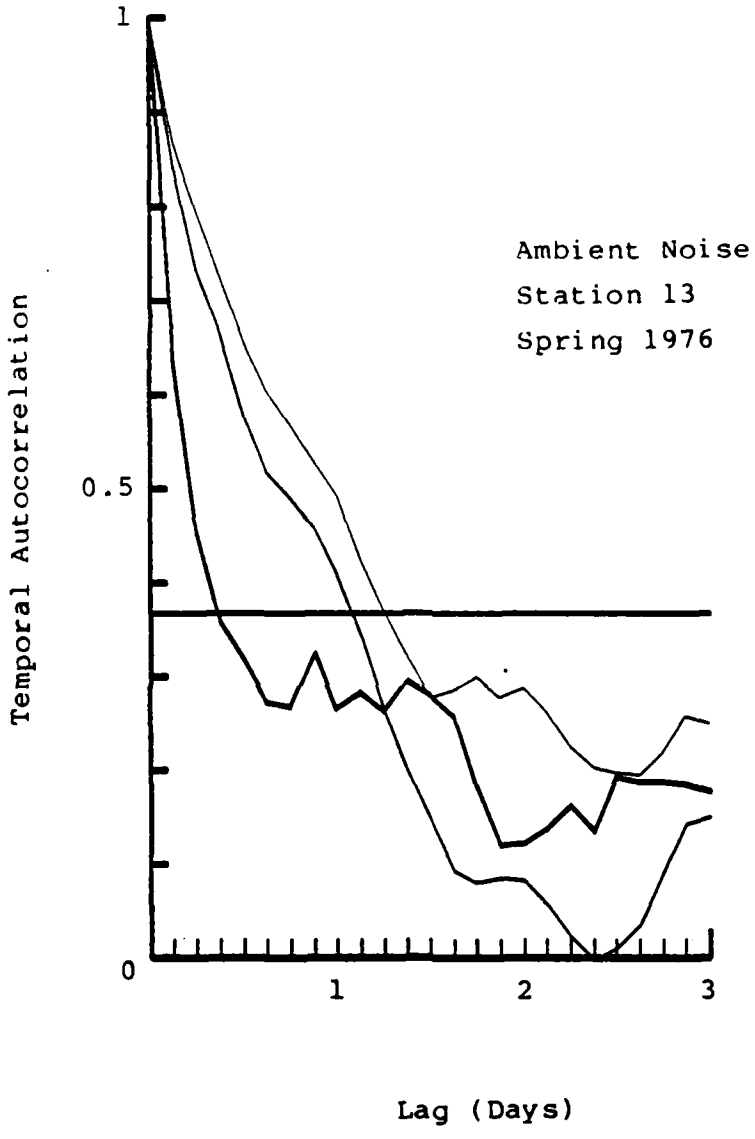

Fig. G.37. Ambient noise autocorrelations, Station 13, based on spring AIDJEX noise data (dB): 10 Hz (lightest line), 32 Hz (darker line), and 1000 Hz (darkest line).

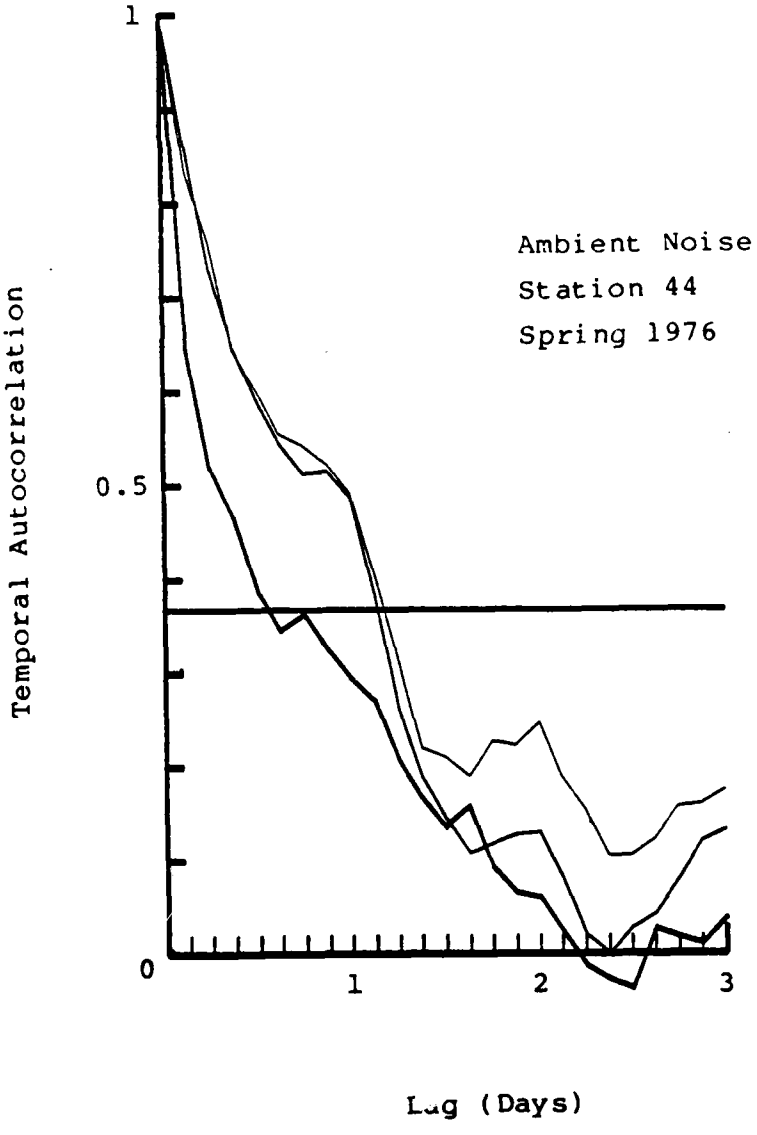

Fig. G.38. Ambient noise autocorrelations, Station 44, based on spring AIDJEX noise data (dB): 10 Hz (lightest line), 32 Hz (darker line), and 1000 Hz (darkest line).

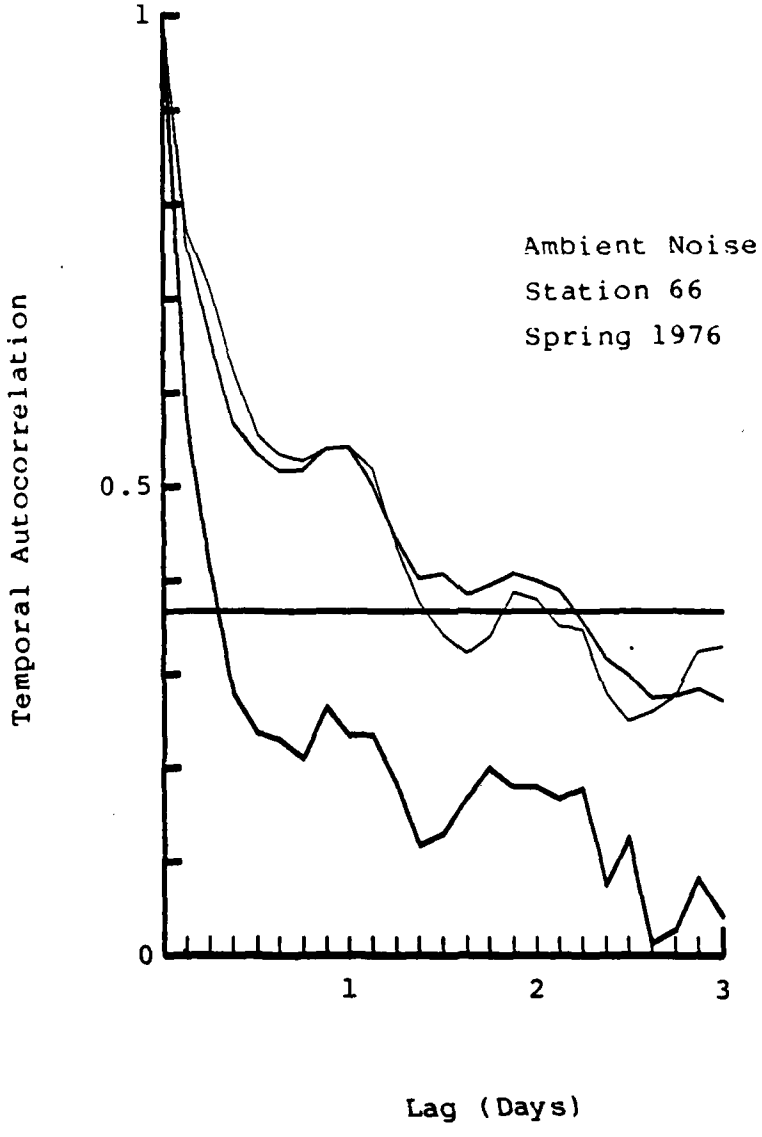

Fig. G.39. Ambient noise autocorrelations, Station 66, based on spring AIDJEX noise data (dB): 10 Hz (lightest line), 32 Hz (darker line), and 1000 Hz (darkest line).

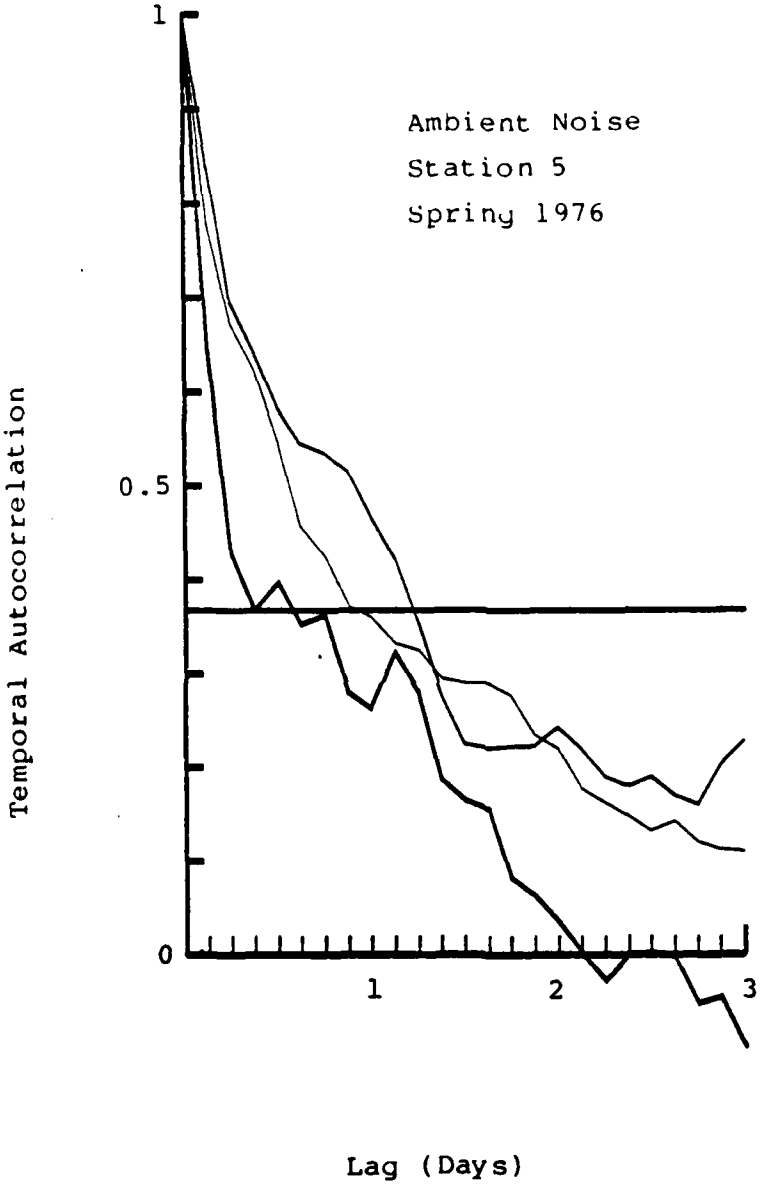

Fig. G.40. Ambient noise autocorrelations, Station 5, based on spring AIDJEX noise data (pressure amplitude): 10 Hz (lightest line), 32 Hz (darker line), and 1000 Hz (darkest line).

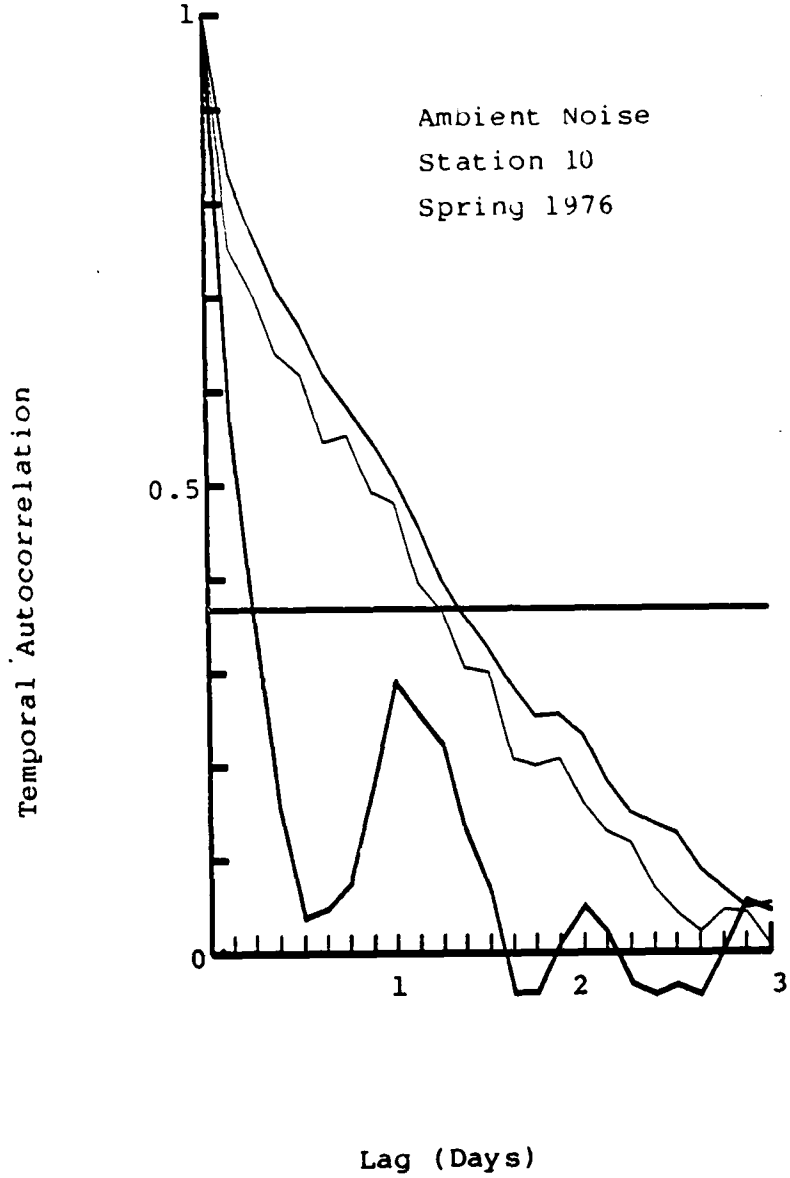

Fig. G.41. Ambient noise autocorrelations, Station 10, based on spring AIDJEX noise data (pressure amplitude): 10 Hz (lightest line), 32 Hz (darker line), and 1000 Hz (darkest line).

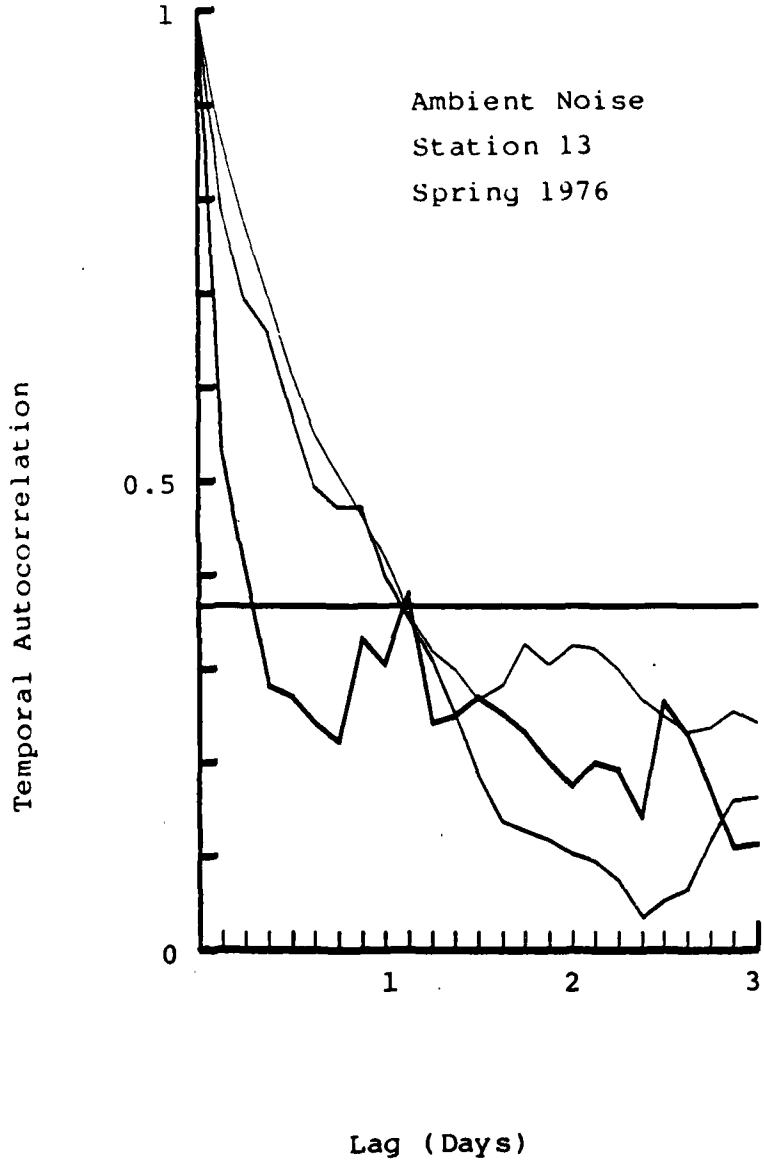

Fig. G.42. Ambient noise autocorrelations, Station 13, based on spring AIDJEX noise data (pressure amplitude): 10 Hz (lightest line), 32 Hz (darker line), and 1000 Hz (darkest line).

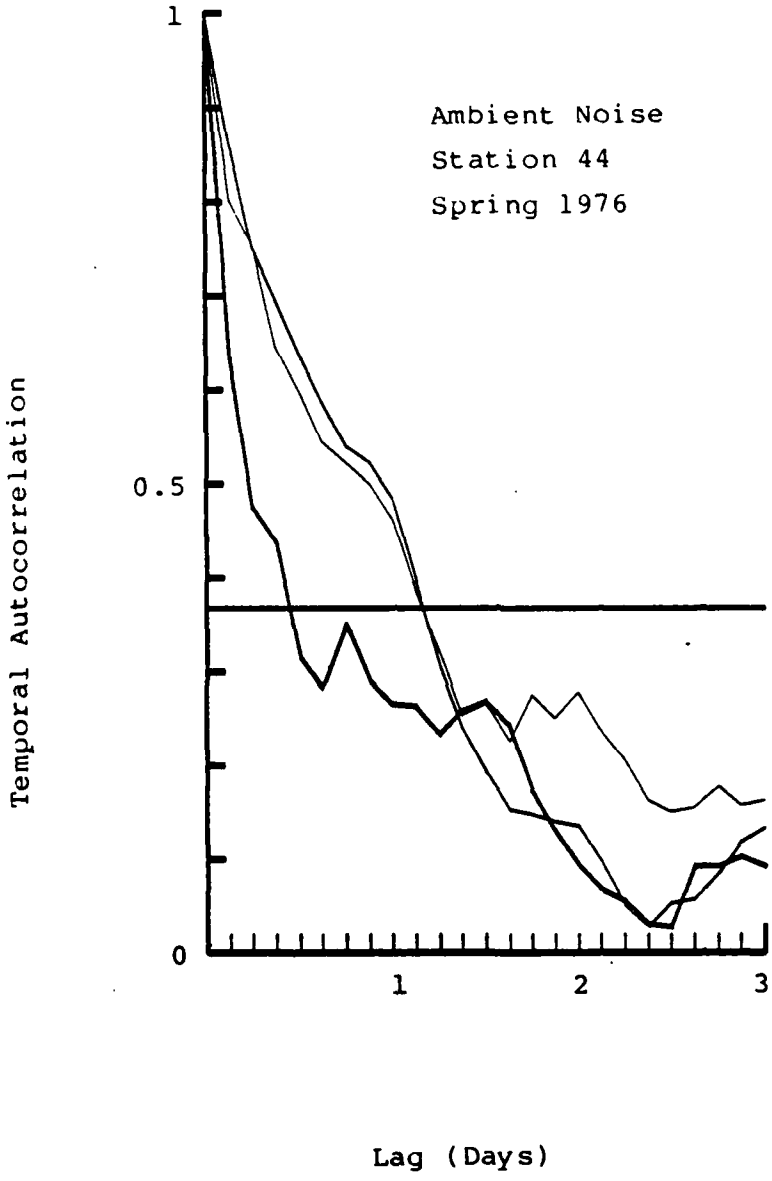

Fig. G.43. Ambient noise autocorrelations, Station 44, based on spring AIDJEX noise data (pressure amplitude): 10 Hz (lightest line), 32 Hz (darker line), and 1000 Hz (darkest line).

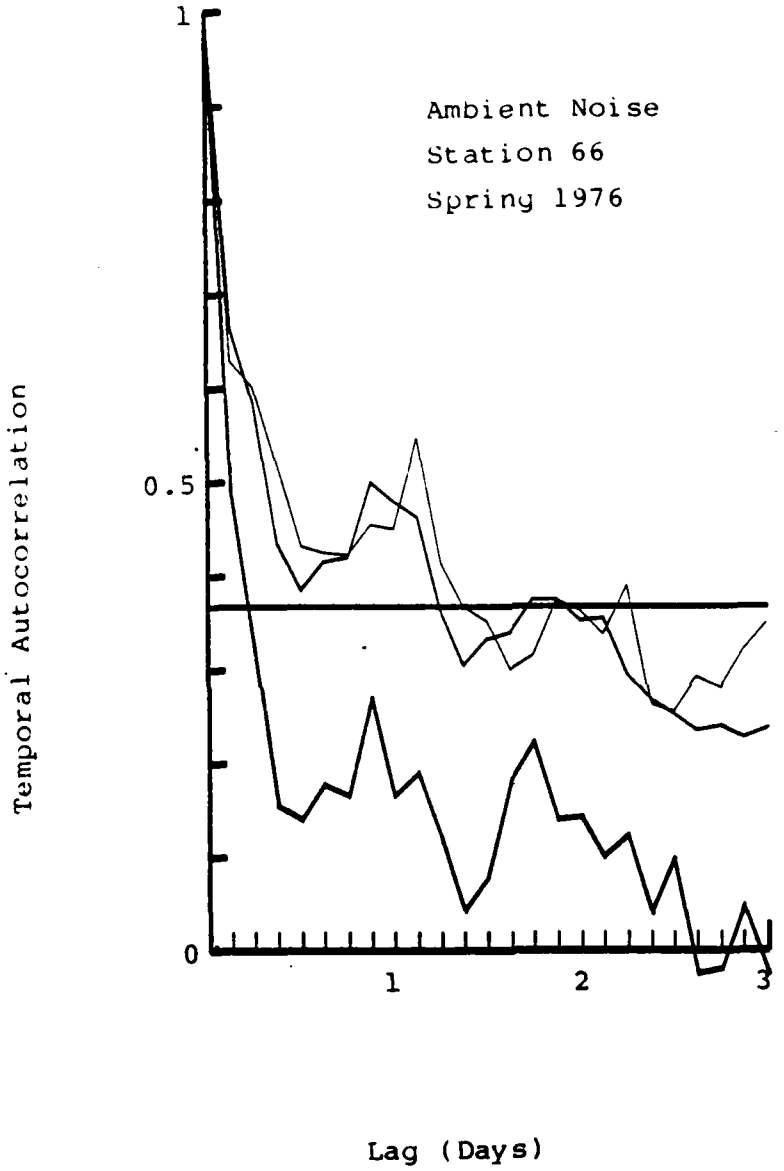

Fig. G.44. Ambient noise autocorrelations, Station 66, based on spring AIDJEX noise data (pressure amplitude): 10 Hz (lightest line), 32 Hz (darker line), and 1000 Hz (darkest line).

Appendix H

Seasonal Arctic Ambient Noise Spatial Autocorrelations, Beaufort Sea, 1975-1976

This appendix depicts graphically Arctic ambient noise spatial correlations using the AIDJEX 10 Hz, 32 Hz, and 1000 Hz noise data. One month of noise data from all stations were used in the calculations, each station correlated with all the others. Spatial autocorrelations were calculated for each season:

Summer - noise data from August 1975,
Fall - noise data from November 1975,
Winter - noise data from February 1976, and
Spring - noise data from May 1976.

As in the temporal autocorrelations, the results in this appendix are given for the data in decibells and in pressure amplitudes.

Since the correlation between any two stations covers a monthly period, the distance between the two stations is not constant. This variation in distance is represented in the correlation plot by a horizontal line, the projection of which onto the x axis (distance) represents the maximum difference in the separations of the two stations during the month:

Maximum Variation in Station Separation =
Maximum Distance Between Stations -
Minimum Distance Between Stations.

List of Figures

Appendix H

Summer (dB) — Page

Fig. H.1. Spatial autocorrelations, 10 Hz 3.3-52

Fig. H.2. Spatial autocorrelations, 32 Hz 3.3-53

Fig. H.3. Spatial autocorrelations, 1000 Hz 3.3-54

Summer (Pressure Amplitude)

Fig. H.4. Spatial autocorrelations, 10 Hz 3.3-55

Fig. H.5. Spatial autocorrelations, 32 Hz 3.3-56

Fig. H.6. Spatial autocorrelations, 1000 Hz 3.3-57

Fall (dB)

Fig. H.7. Spatial autocorrelations, 10 Hz 3.3-58

Fig. H.8. Spatial autocorrelations, 32 Hz 3.3-59

Fig. H.9. Spatial autocorrelations, 1000 Hz 3.3-60

Fall (Pressure Amplitude)

Fig. H.10. Spatial autocorrelations, 10 Hz 3.3-61

Fig. H.11. Spatial autocorrelations, 32 Hz 3.3-62

Fig. H.12. Spatial autocorrelations, 1000 Hz 3.3-63

Winter (dB)

Fig. H.13. Spatial autocorrelations, 10 Hz 3.3-64

Fig. H.14. Spatial autocorrelations, 32 Hz 3.3-65

Fig. H.15. Spatial autocorrelations, 1000 Hz 3.3-66

Winter (Pressure Amplitude) Page

Fig. H.16. Spatial autocorrelations, 10 Hz 3.3-67

Fig. H.17. Spatial autocorrelations, 32 Hz 3.3-68

Fig. H.18. Spatial autocorrelations, 1000 Hz 3.3-69

Spring (dB)

Fig. H.19. Spatial autocorrelations, 10 Hz 3.3-70

Fig. H.20. Spatial autocorrelations, 32 Hz 3.3-71

Fig. H.21. Spatial autocorrelations, 1000 Hz 3.3-72

Spring (Pressure Amplitude)

Fig. H.22. Spatial autocorrelations, 10 Hz 3.3-73

Fig. H.23. Spatial autocorrelations, 32 Hz 3.3-74

Fig. H.24. Spatial autocorrelations, 1000 Hz 3.3-75

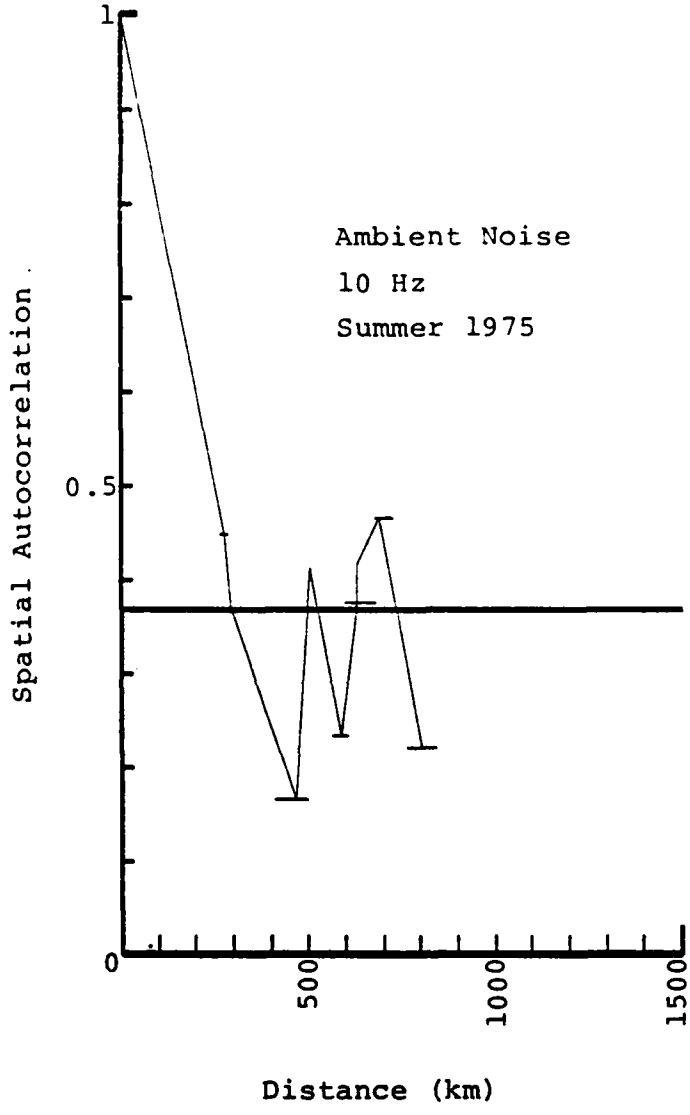

Fig. H.1. Spatial autocorrelations, 10 Hz (dB), based on the AIDJEX noise data.

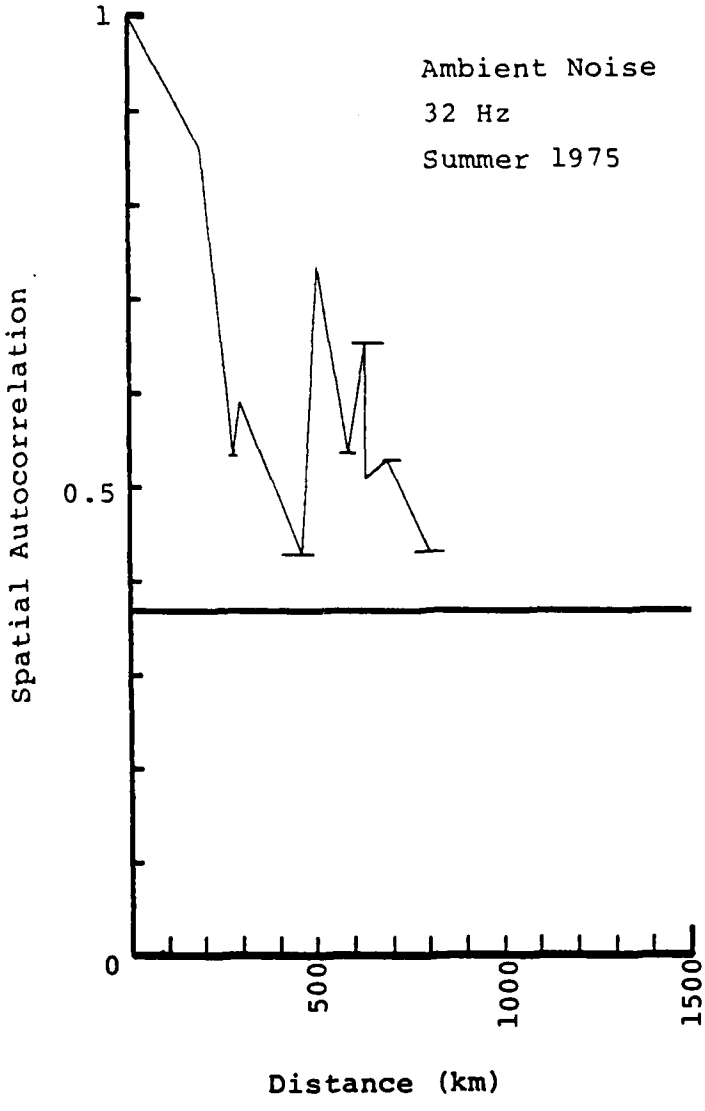

Fig. H.2. Spatial autocorrelations, 32 Hz (dB), based on the AIDJEX noise data.

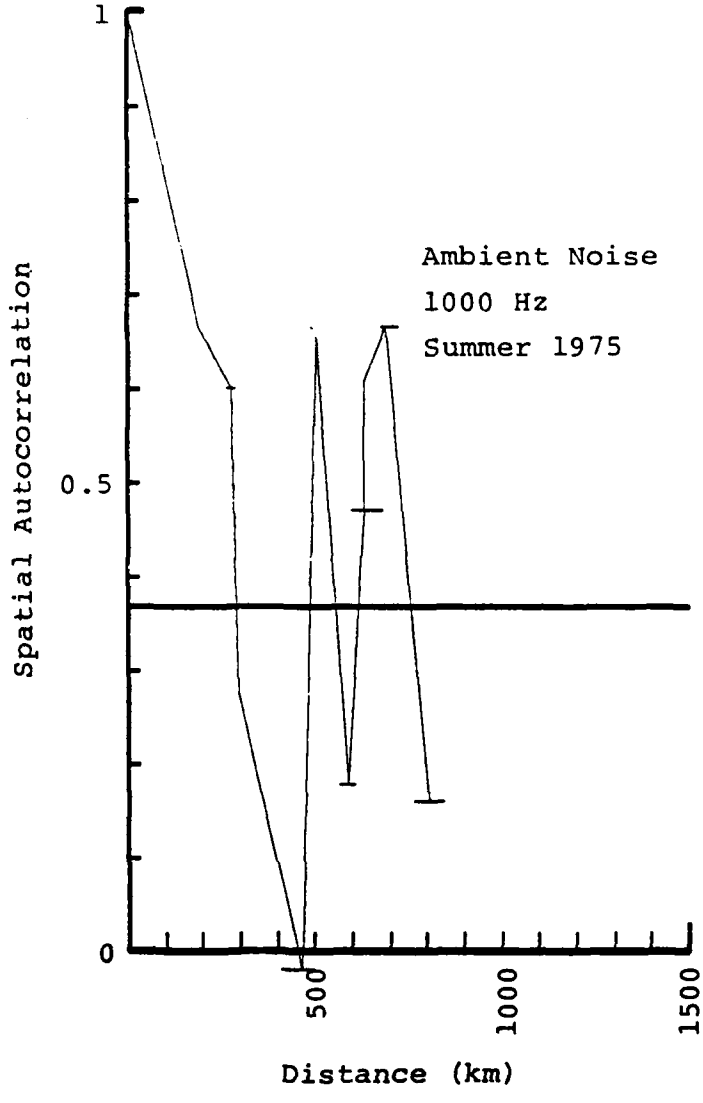

Fig. H.3. Spatial autocorrelations, 1000 Hz (dB), based on the AIDJEX noise data.

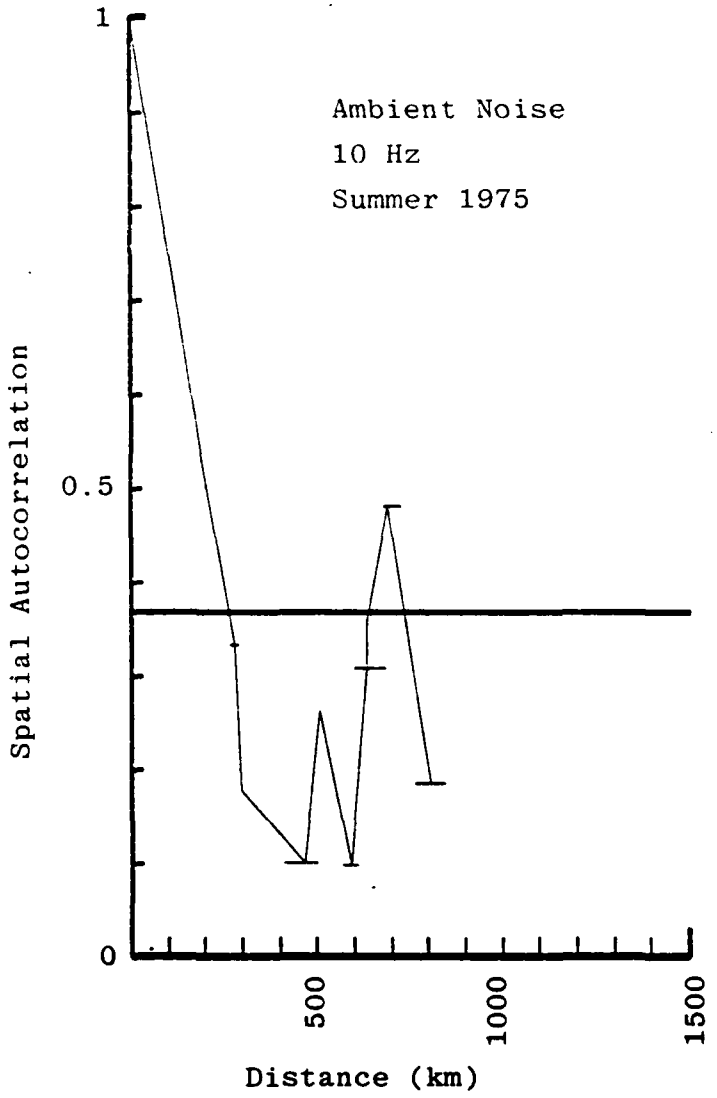

Fig. H.4. Spatial autocorrelations, 10 Hz (pressure amplitude), based on the AIDJEX noise data.

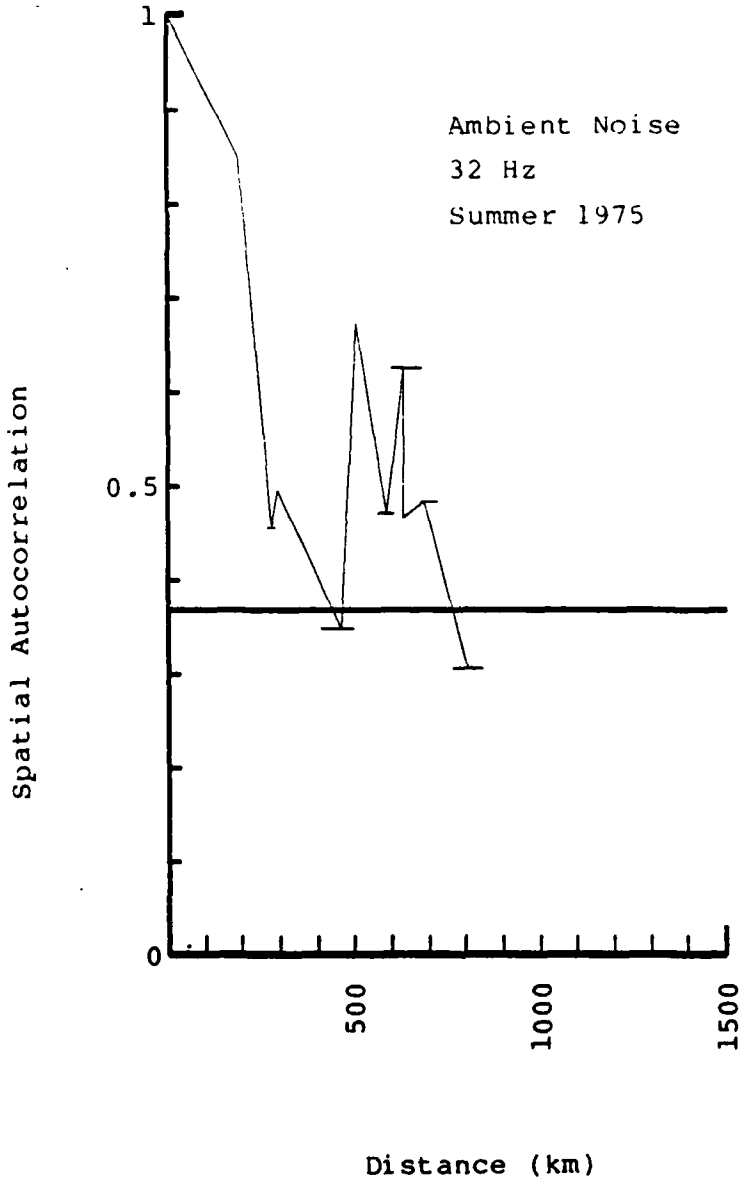

Fig. H.5. Spatial autocorrelations, 32 Hz (pressure amplitude), based on the AIDJEX noise data.

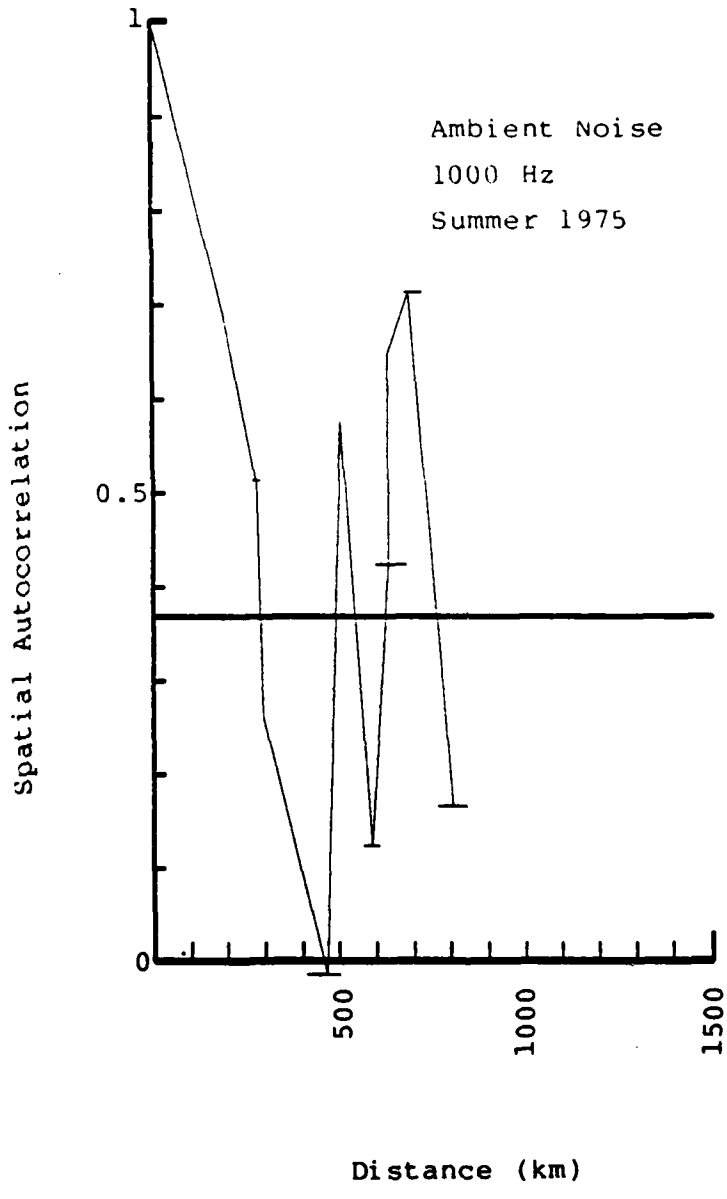

Fig. H.6. Spatial autocorrelations, 1000 Hz (pressure amplitude), based on the AIDJEX noise data.

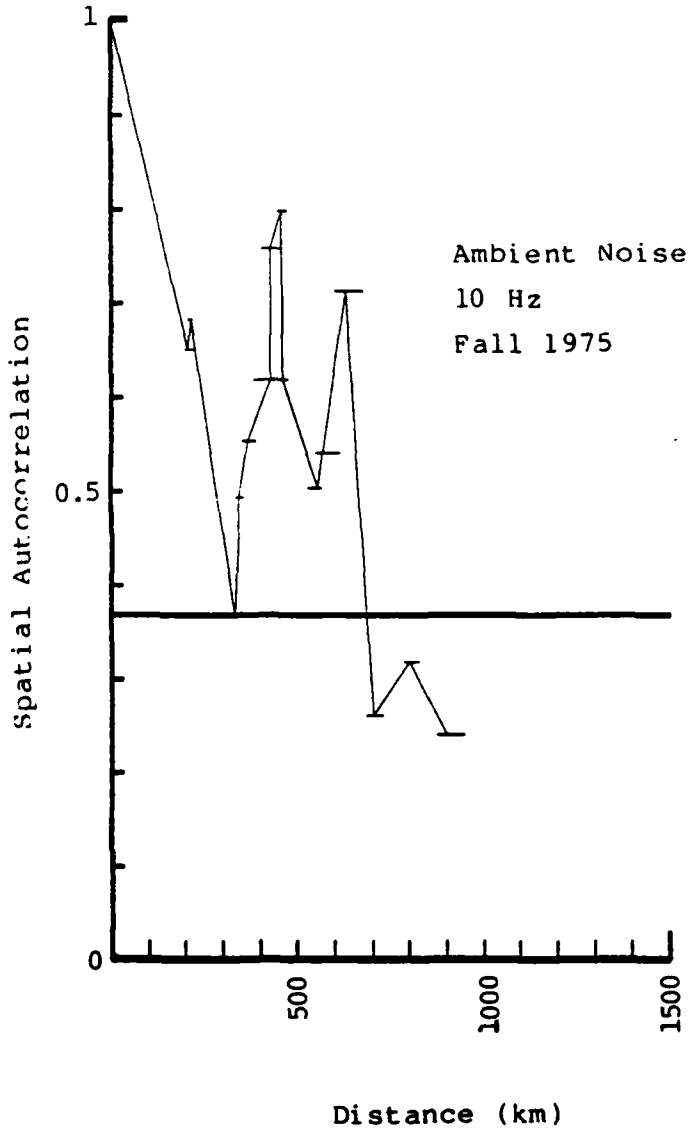

Fig. H.7. Spatial autocorrelations, 10 Hz (dB), based on the AIDJEX noise data.

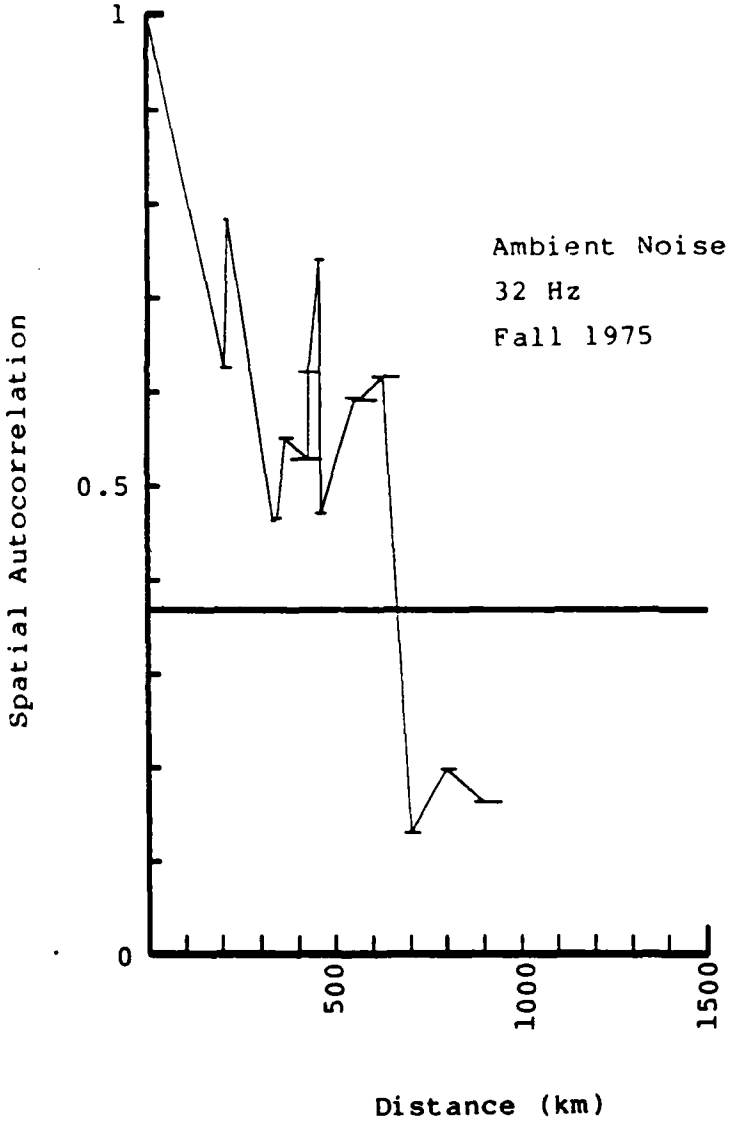

Fig. H.8. Spatial autocorrelations, 32 Hz (dB), based on the AIDJEX noise data.

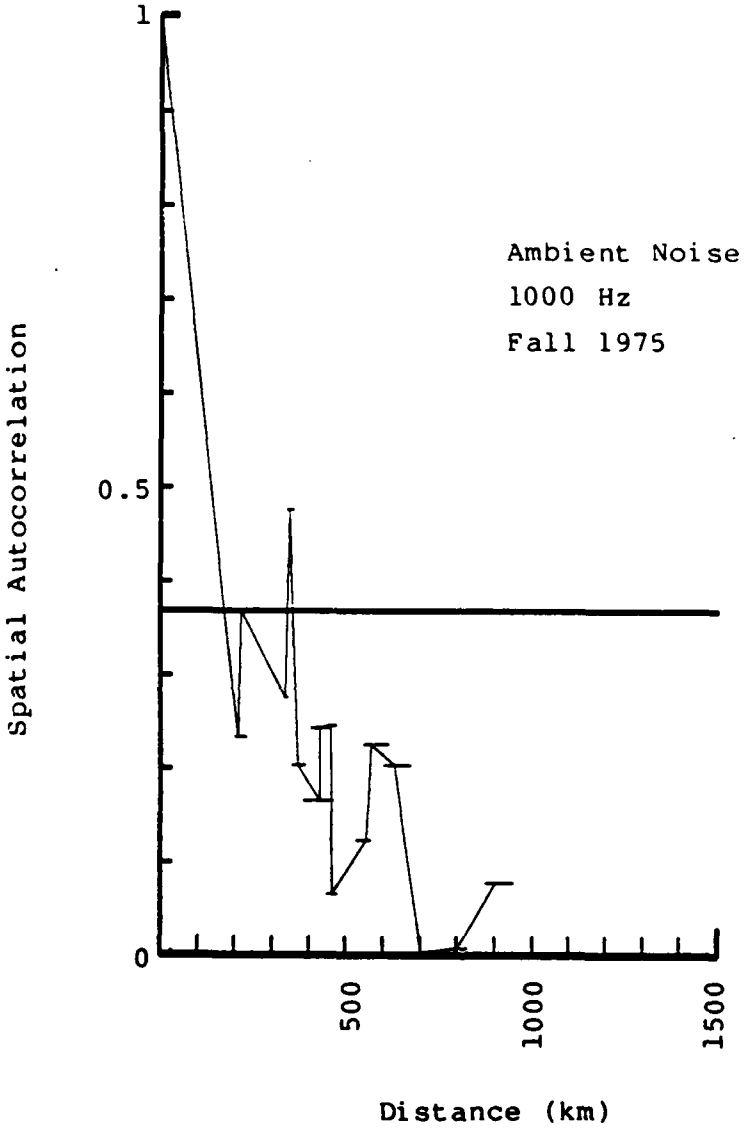

Fig. H.9. Spatial autocorrelations, 1000 Hz (dB), based on the AIDJEX noise data.

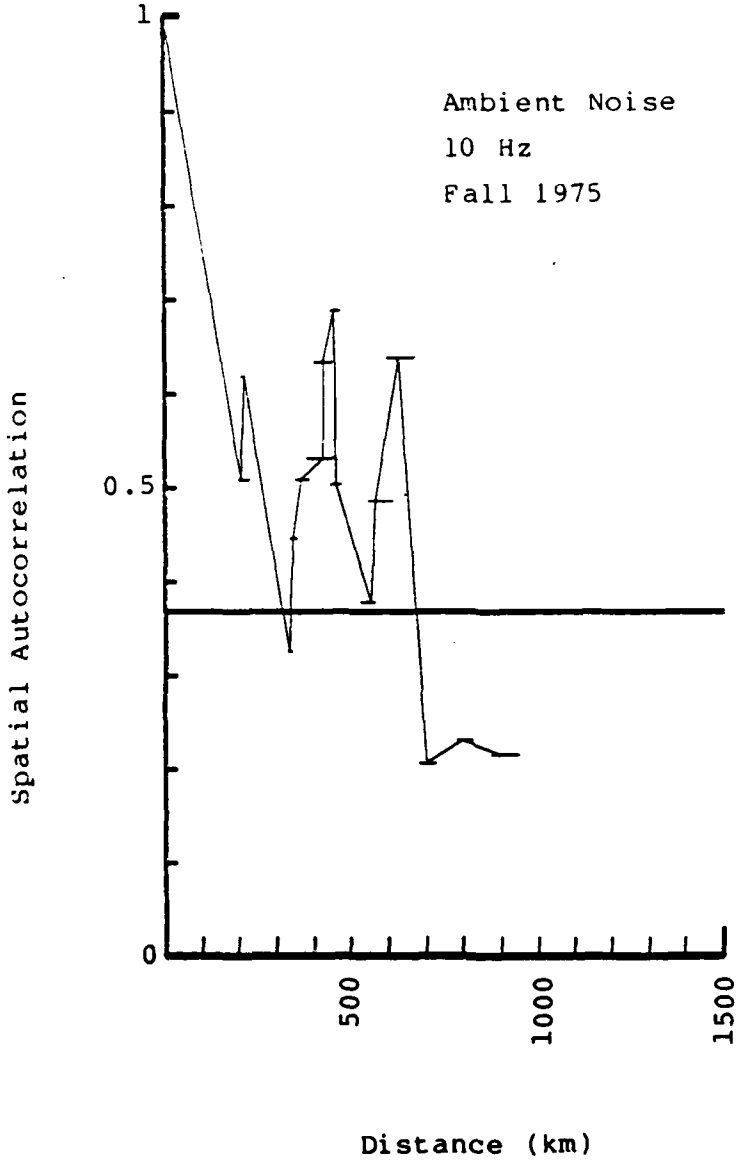

Fig. H.10. Spatial autocorrelations, 10 Hz (pressure amplitude), based on the AIDJEX noise data.

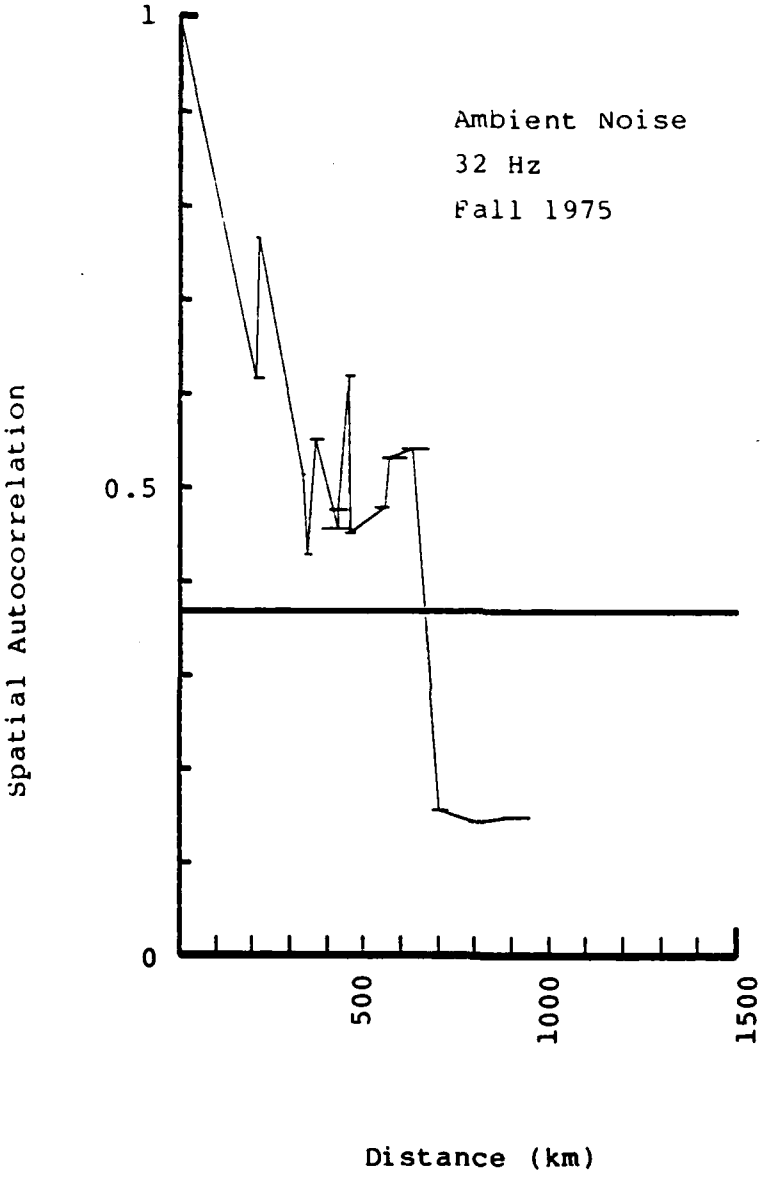

Fig. H.11. Spatial autocorrelations, 32 Hz (pressure amplitude), based on the AIDJEX noise data.

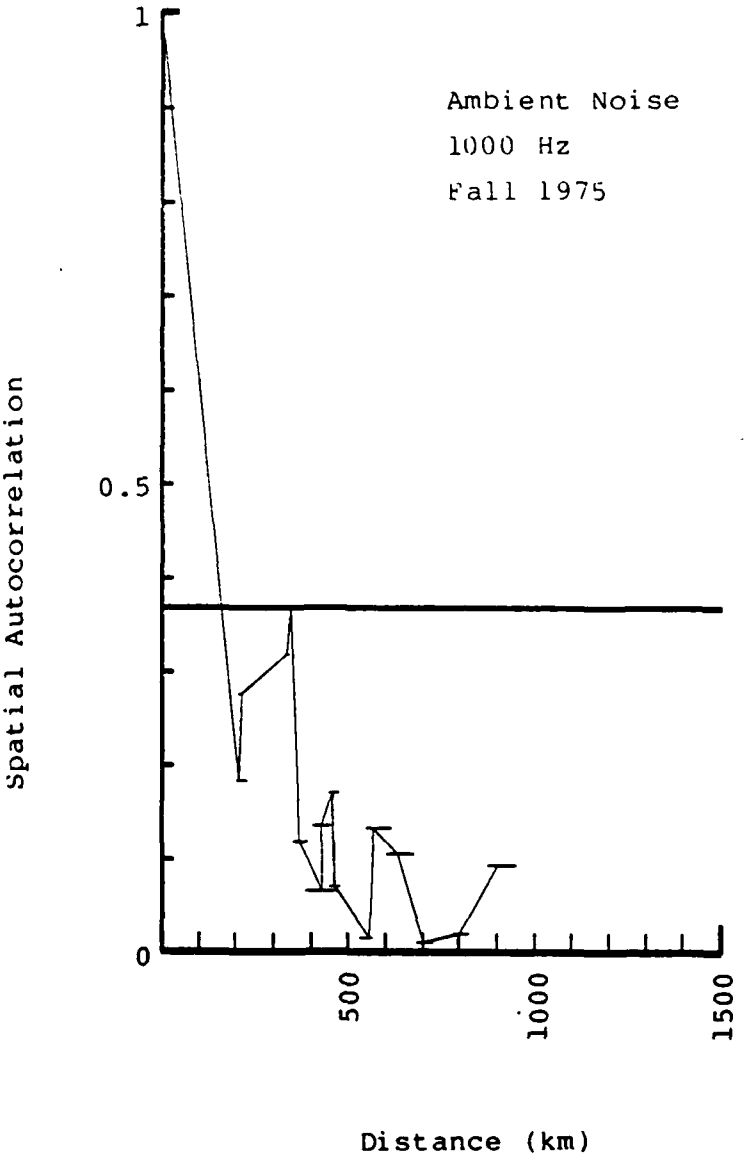

Fig. H.12. Spatial autocorrelations, 1000 Hz (pressure amplitude), based on the AIDJEX noise data.

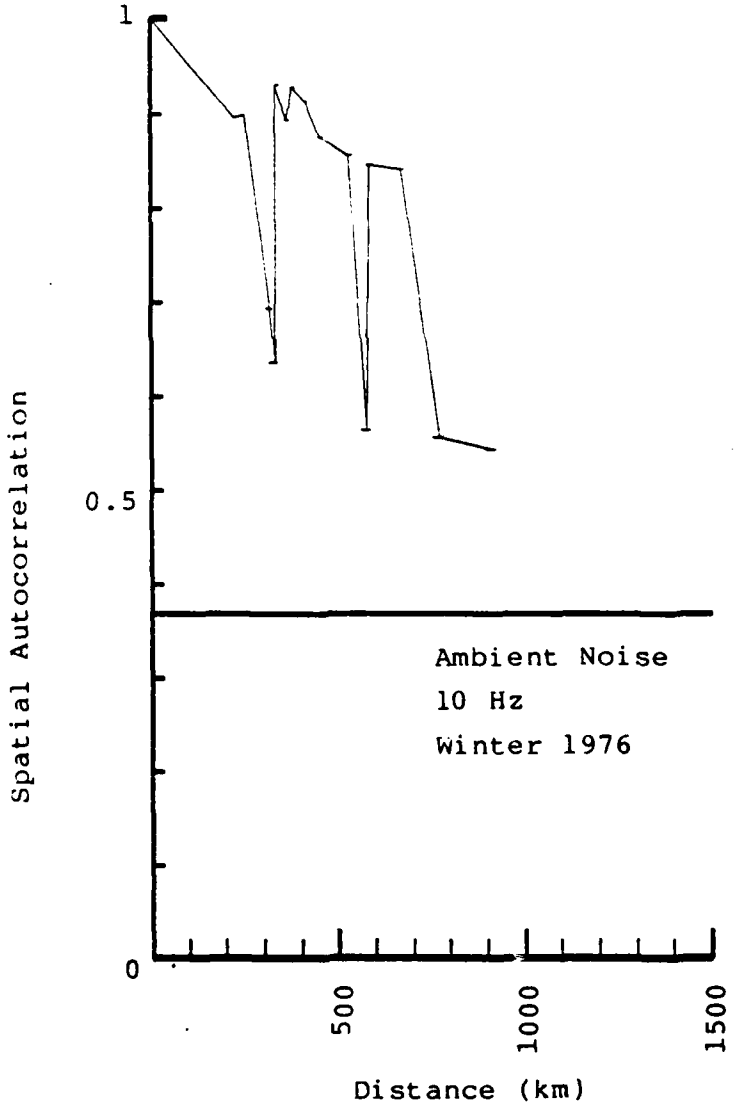

Fig. H.13. Spatial autocorrelations, 10 Hz (dB), based on the AIDJEX noise data.

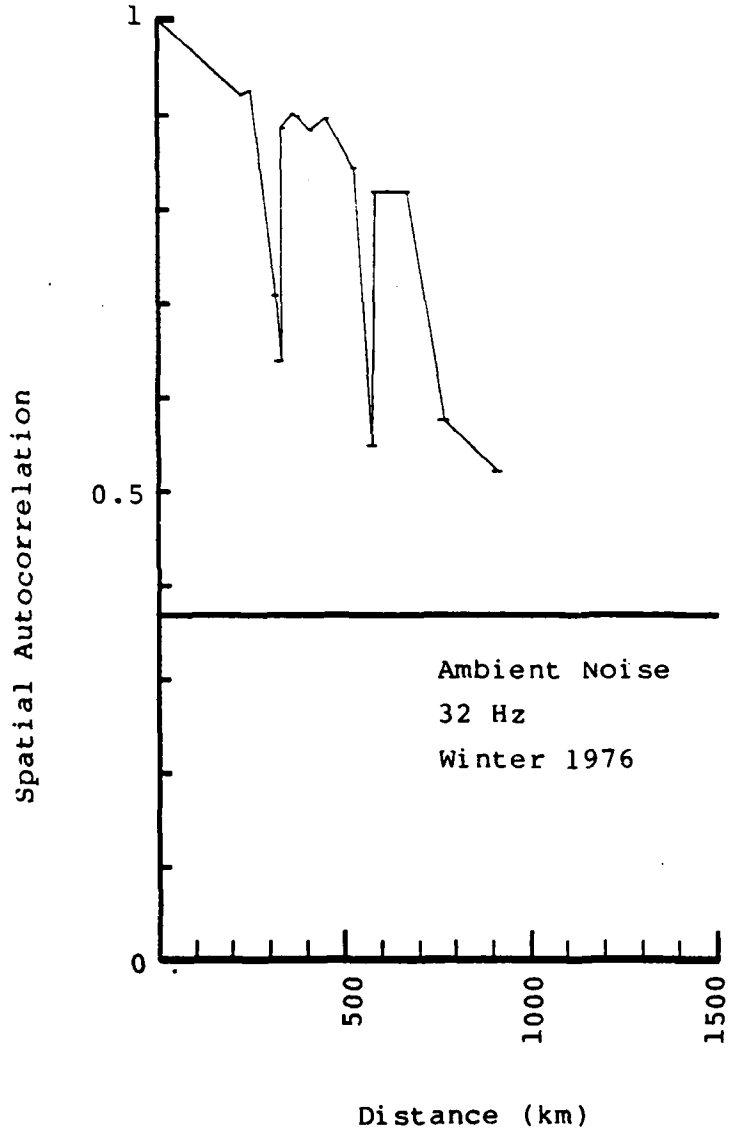

Fig. H.14. Spatial autocorrelations, 32 Hz (dB), based on the AIDJEX noise data.

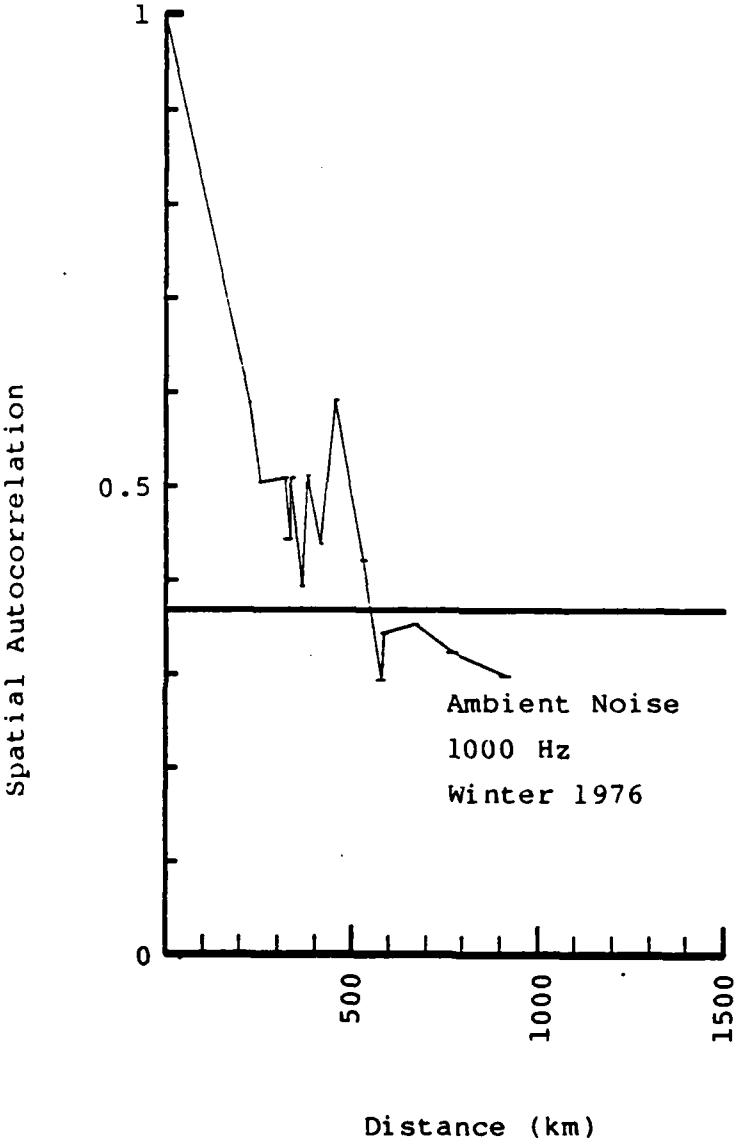

Fig. H.15. Spatial autocorrelations, 1000 Hz (dB), based on the AIDJEX noise data.

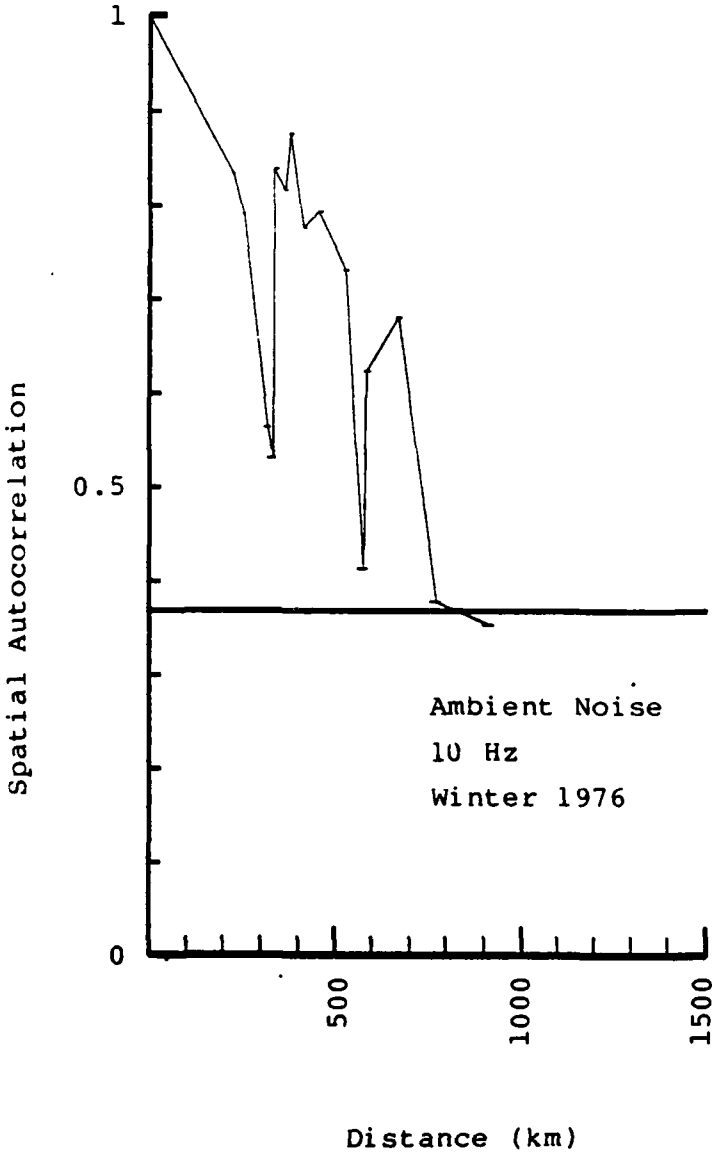

Fig. H.16. Spatial autocorrelations, 10 Hz (pressure amplitude), based on the AIDJEX noise data.

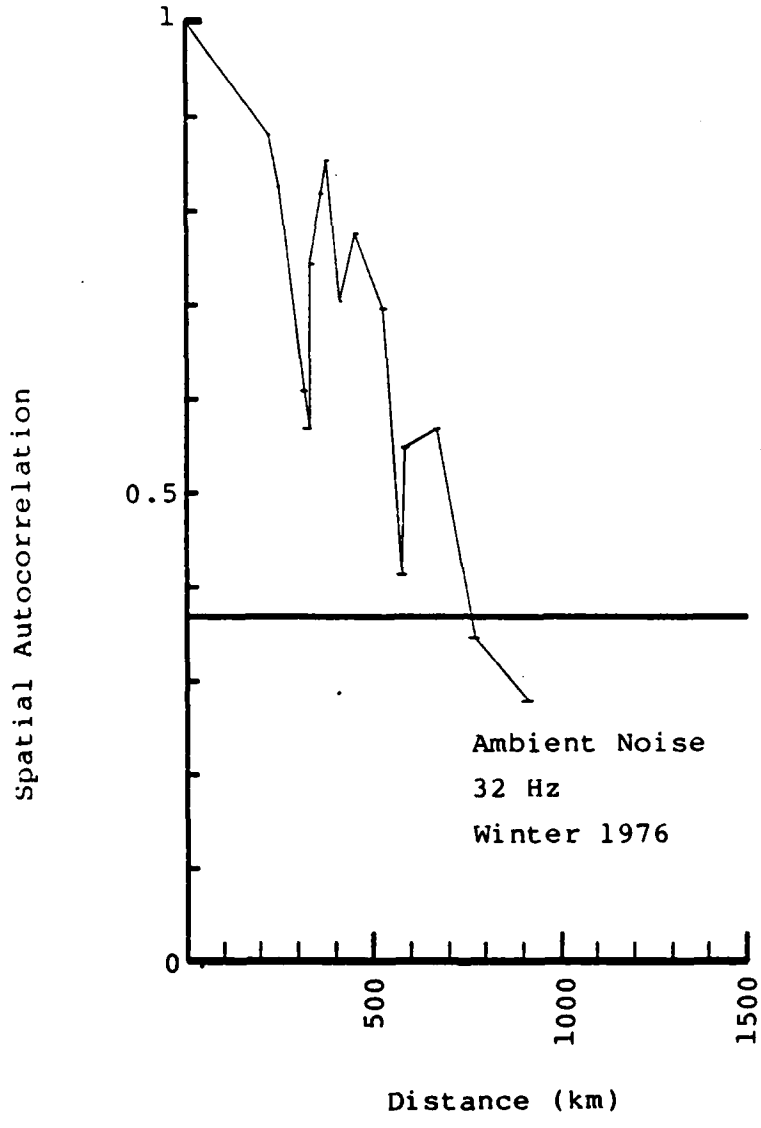

Fig. H.17. Spatial autocorrelations, 32 Hz (pressure amplitude), based on the AIDJEX noise data.

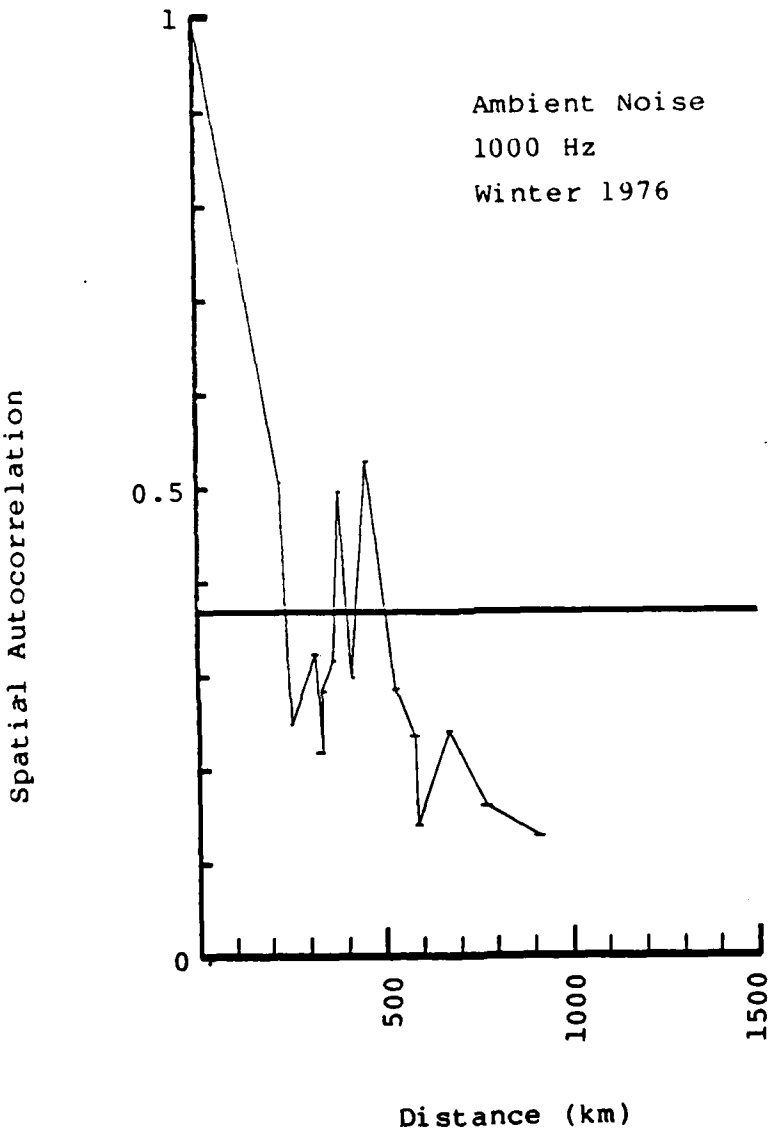

Fig. H.18. Spatial autocorrelations, 1000 Hz (pressure amplitude), based on the AIDJEX noise data.

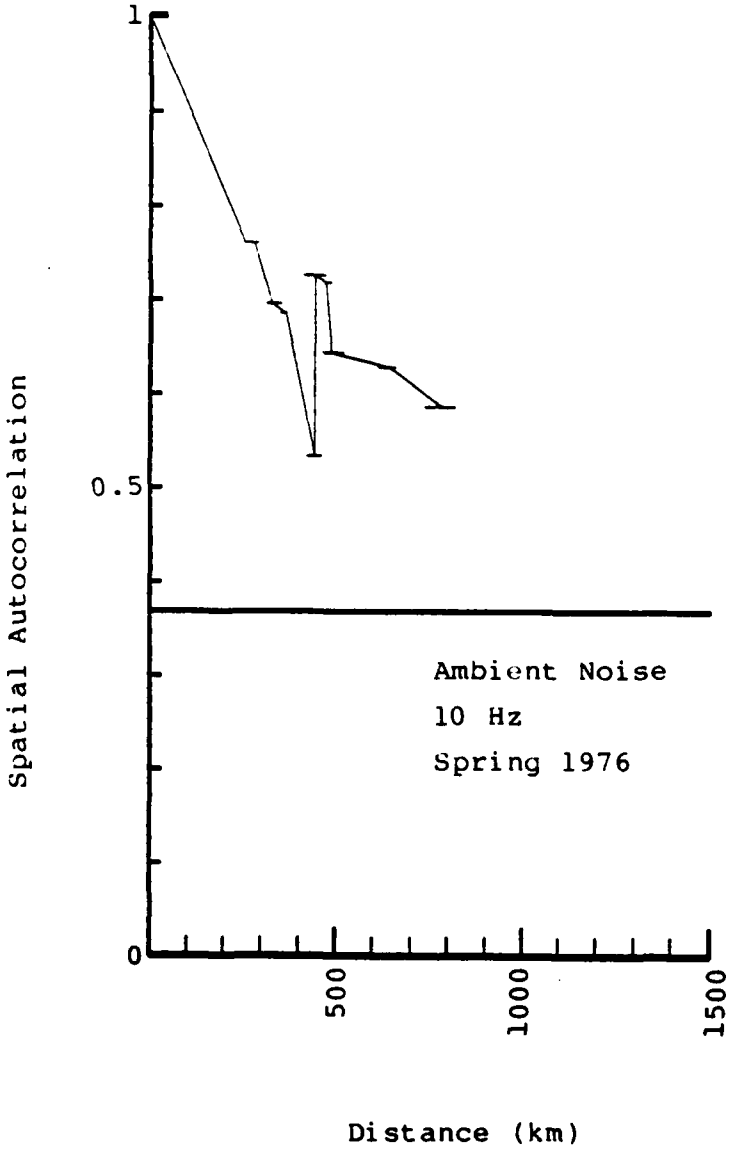

Fig. H.19. Spatial autocorrelations, 10 Hz (dB), based on the AIDJEX noise data.

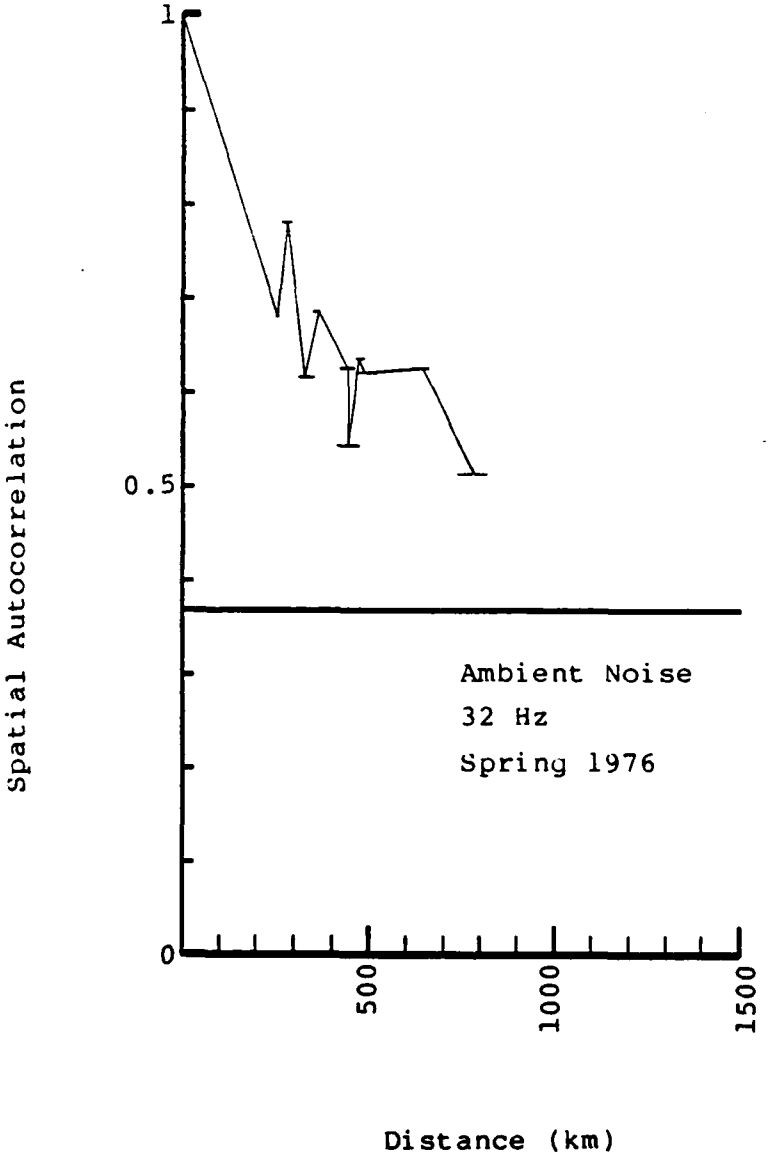

Fig. H.20. Spatial autocorrelations, 32 Hz (dB), based on the AIDJEX noise data.

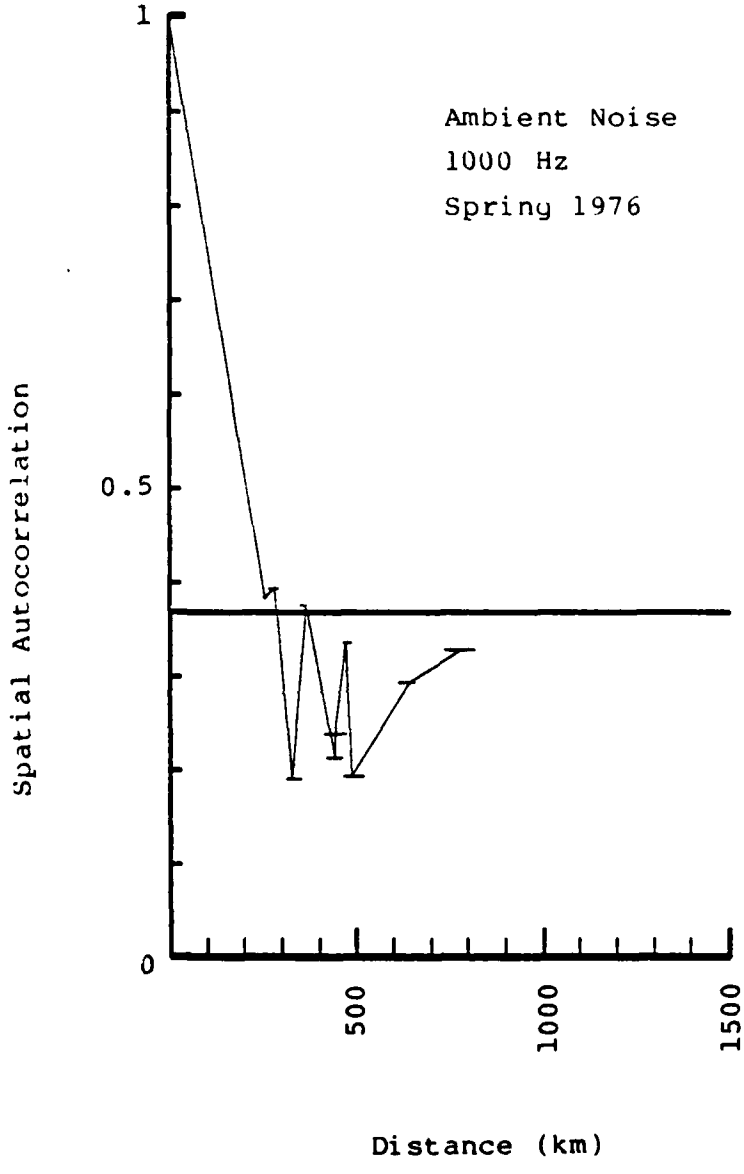

Fig. H.21. Spatial autocorrelations, 1000 Hz (dB), based on the AIDJEX noise data.

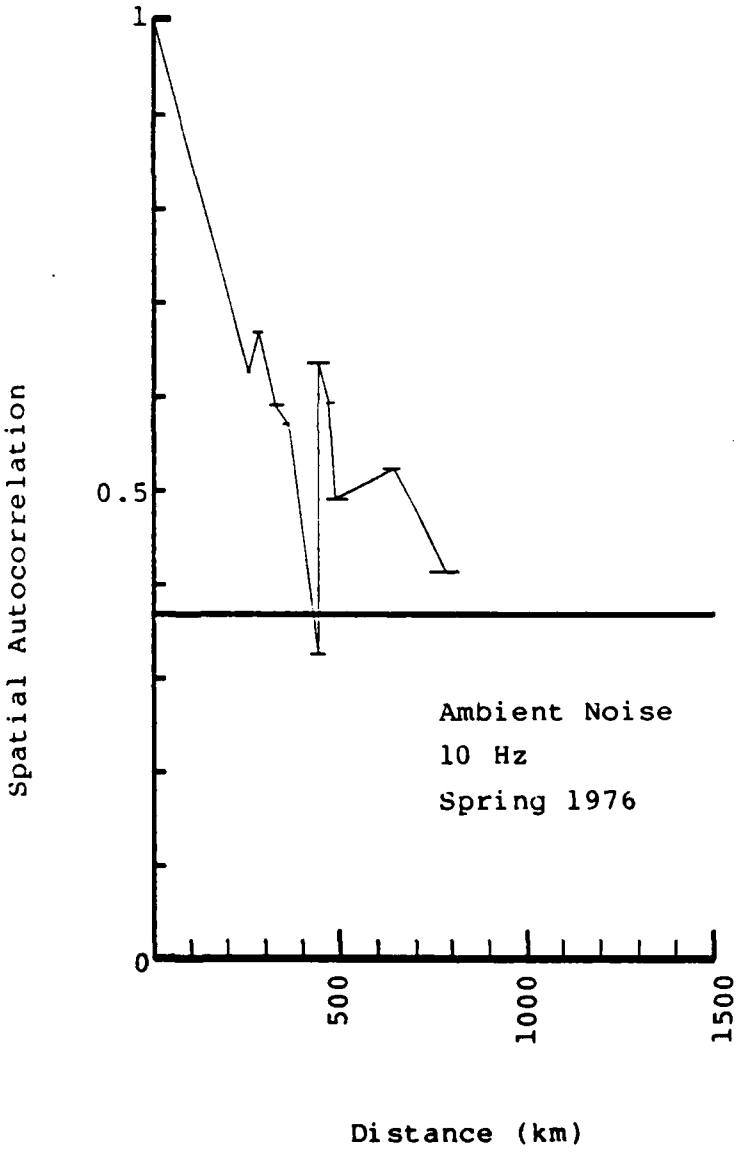

Fig. H.22. Spatial autocorrelations, 10 Hz (pressure amplitude), based on the AIDJEX noise data.

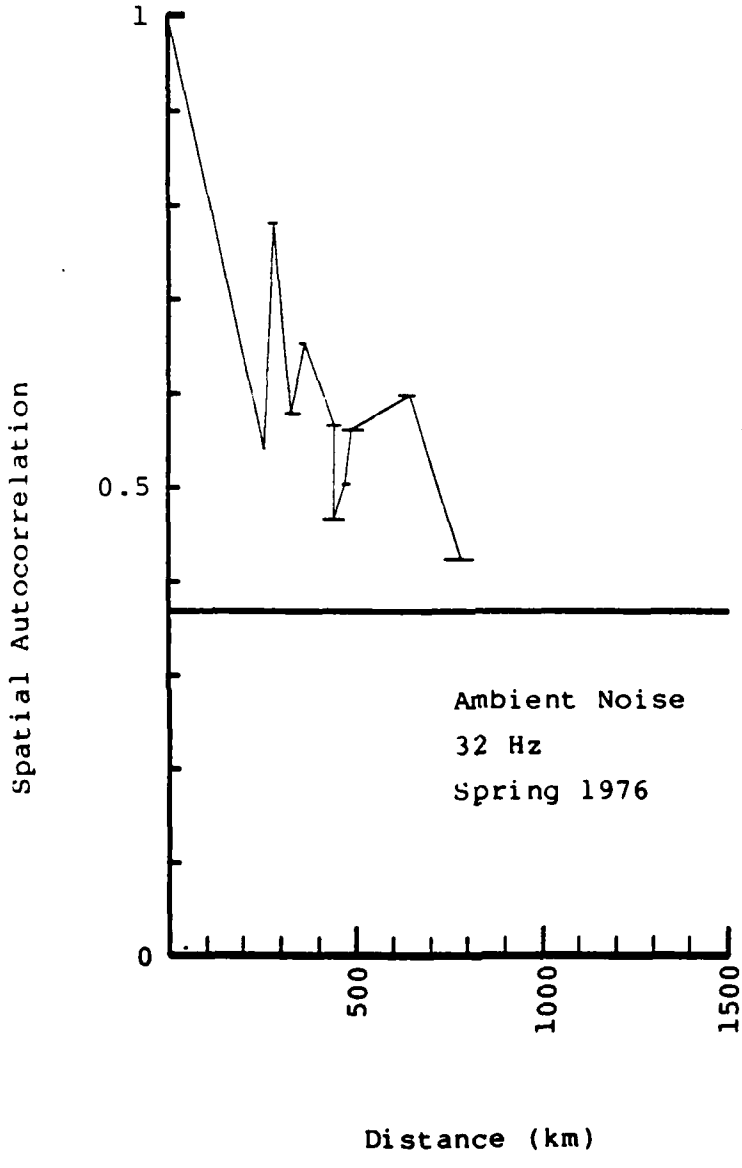

Fig. H.23. Spatial autocorrelations, 32 Hz (pressure amplitude), based on the AIDJEX noise data.

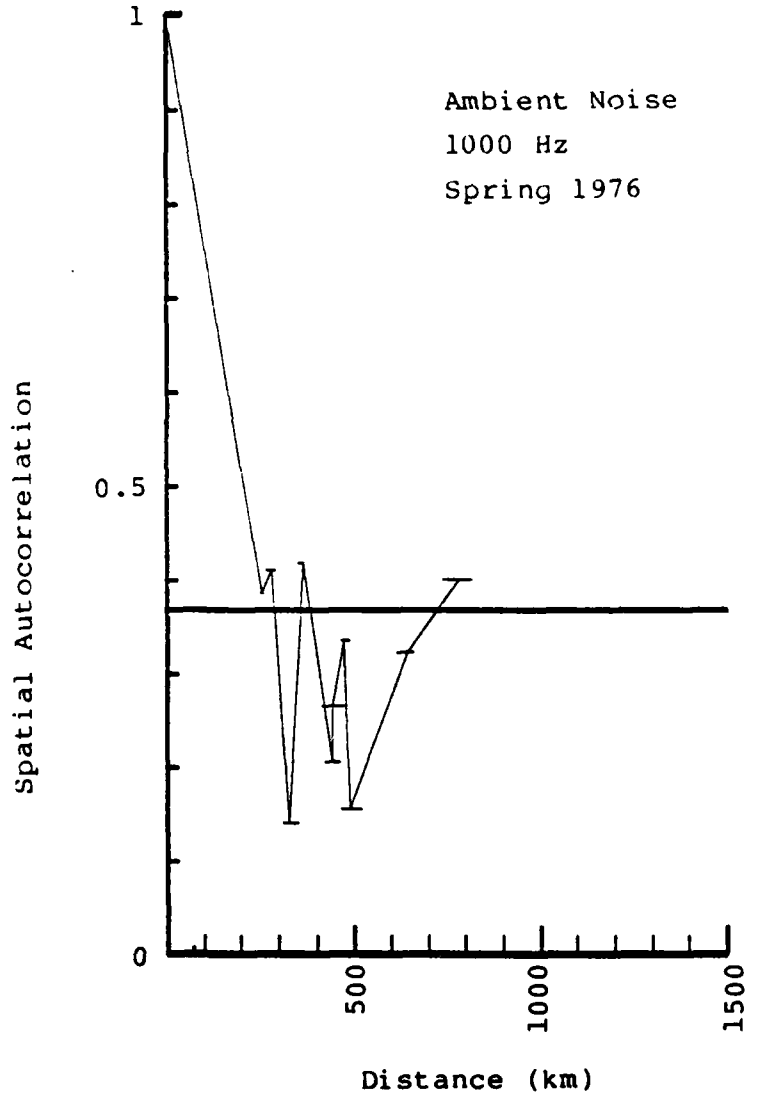

Fig. H.24. Spatial autocorrelations, 1000 Hz (pressure amplitude), based on the AIDJEX noise data.

Appendix I

Seasonal Arctic Ambient Noise Power Spectra, Beaufort Sea, 1975-1976

This appendix shows the power spectra plots of the AIDJEX 10 Hz, 32 Hz, and 1000 Hz ambient noise signals collected at Station 10 (southern part of the Beaufort Sea). We present only the Station 10 results due to the close proximity of that station to the AIDJEX manned camp array throughout the experiment and since much of the spectral information for the other stations is contained in the temporal autocorrelation calculations (Appendix G).

One month of data was used in the spectral density calculations, and each season is represented:

Summer - noise data from August 1975,
Fall - noise data from November 1975,
Winter - noise data from February 1976, and
Spring - noise data from May 1976.

The power spectra were calculated for both pressure amplitude (relative to 1 Pa) and decibell units.

List of Figures
Appendix I

Page

Summer (dB)

Fig. I.1. Spectral density of the 10 Hz ambient noise sign l 3.3-79

Fig. I.2. Spectral density of the 32 Hz ambient noise signal 3.3-80

Fig. I.3. Spectral density of the 1000 Hz ambient noise signal 3.3-81

Summer (Pressure Amplitude)

Fig. I.4. Spectral density of the 10 Hz ambient noise signal 3.3-82

Fig. I.5. Spectral density of the 32 Hz ambient noise signal 3.3-83

Fig. I.6. Spectral density of the 1000 Hz ambient noise signal 3.3-84

Fall (dB)

Fig. I.7. Spectral density of the 10 Hz ambient noise signal 3.3-85

Fig. I.8. Spectral density of the 32 Hz ambient noise signal 3.3-86

Fig. I.9. Spectral density of the 1000 Hz ambient noise signal 3.3-87

Fall (Pressure Amplitude)

Fig. I.10. Spectral density of the 10 Hz ambient noise signal 3.3-88

Fig. I.11. Spectral density of the 32 Hz ambient noise signal 3.3-89

Fig. I.12. Spectral density of the 1000 Hz ambient noise signal 3.3-90

Page

inter (dB)

Fig. I.13. Spectral density of the 10 Hz ambient noise signal 3.3-91

Fig. I.14. Spectral density of the 32 Hz ambient noise signal 3.3-92

Fig. I.15. Spectral density of the 1000 Hz ambient noise signal 3.3-93

Winter (Pressure Amplitude)

Fig. I.16. Spectral density of the 10 Hz ambient noise signal 3.3-94

Fig. I.17. Spectral density of the 32 Hz ambient noise signal 3.3-95

Fig. I.18. Spectral density of the 1000 Hz ambient noise signal 3.3-96

Spring (dB)

Fig. I.19. Spectral density of the 10 Hz ambient noise signal 3.3-97

Fig. I.20. Spectral density of the 32 Hz ambient noise signal 3.3-98

Fig. I.21. Spectral density of the 1000 Hz ambient noise signal 3.3-99

Spring (Pressure Amplitude)

Fig. I.22. Spectral density of the 10 Hz ambient noise signal 3.3-100

Fig. I.23. Spectral density of the 32 Hz ambient noise signal 3.3-101

Fig. I.24. Spectral density of the 1000 Hz ambient noise signal 3.3-102

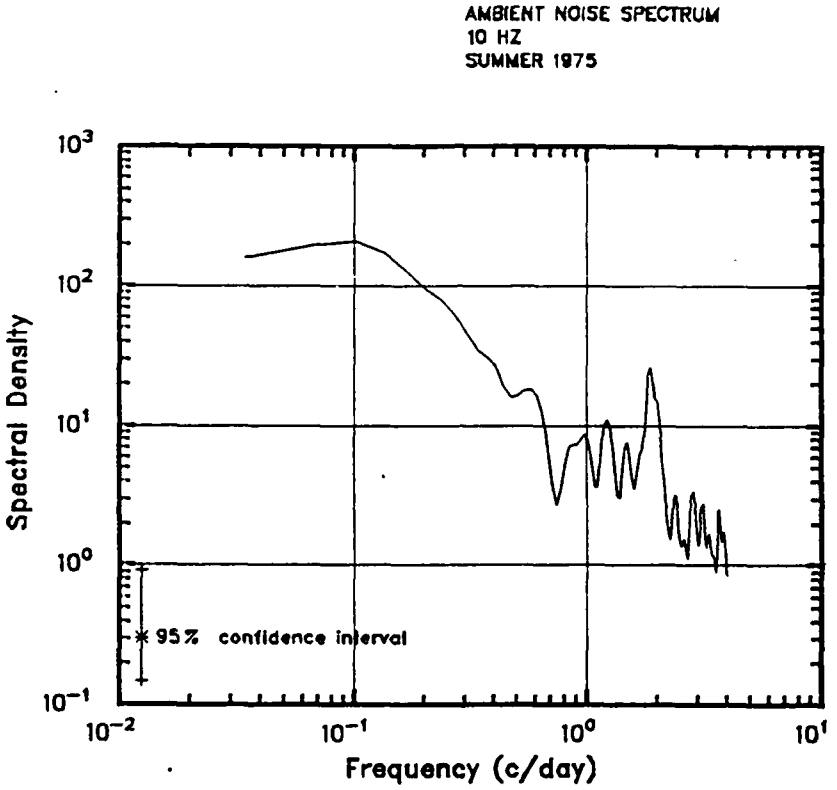

Fig. I.1. Spectral density of the 10 Hz ambient noise signal based on the AIDJEX noise data (dB) from Station 10, August 1975.

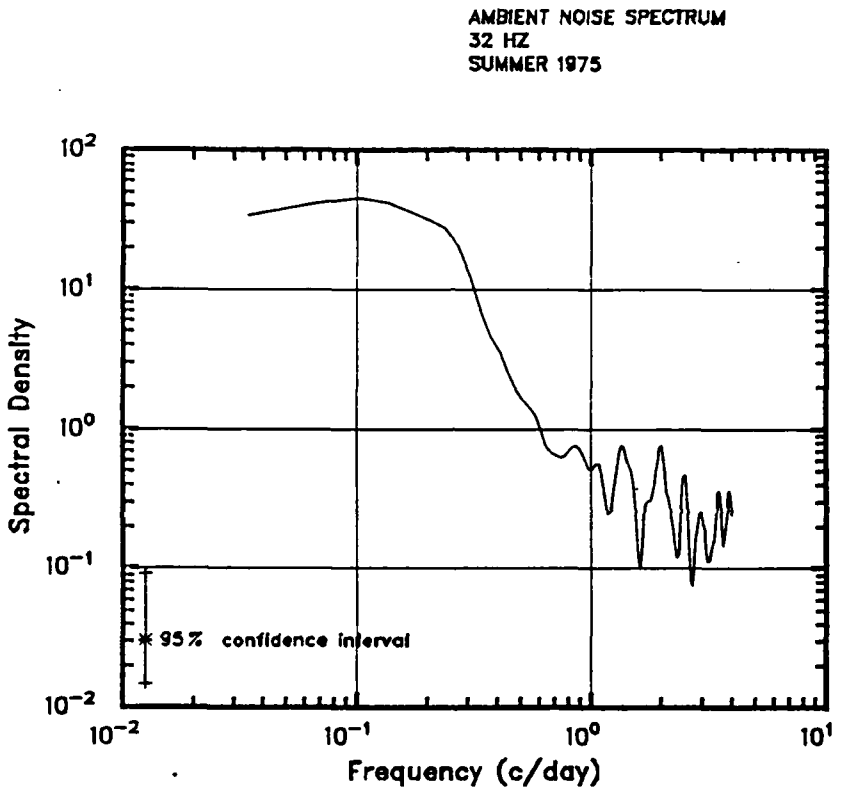

Fig. I.2. Spectral density of the 32 Hz ambient noise signal based on the AIDJEX noise data (dB) from Station 10, August 1975.

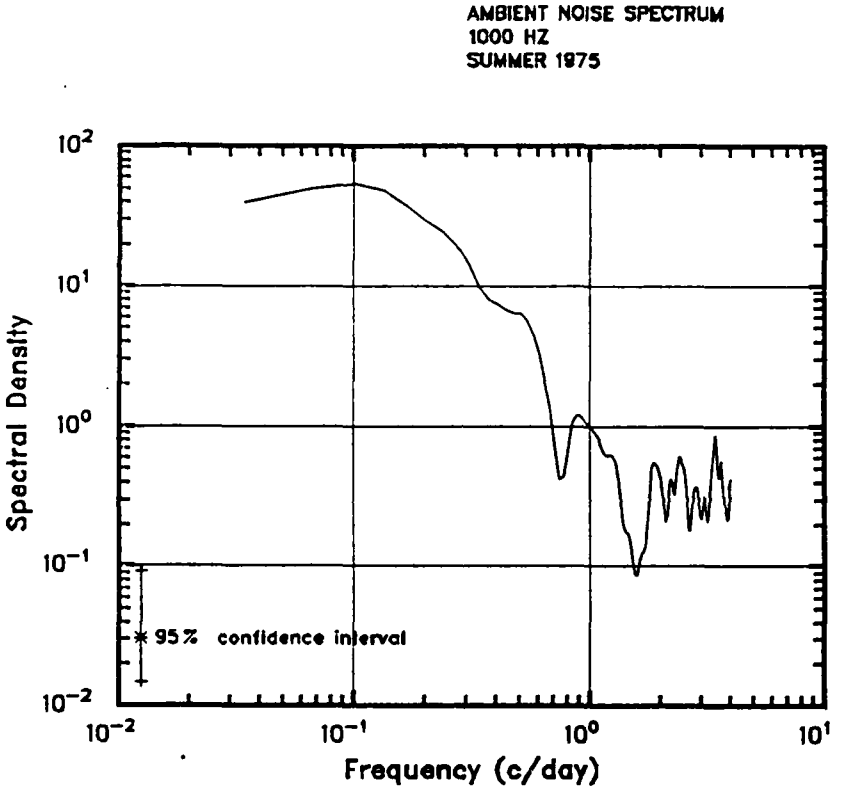

Fig. I.3. Spectral density of the 1000 Hz ambient noise signal based on the AIDJEX noise data (dB) from Station 10, August 1975.

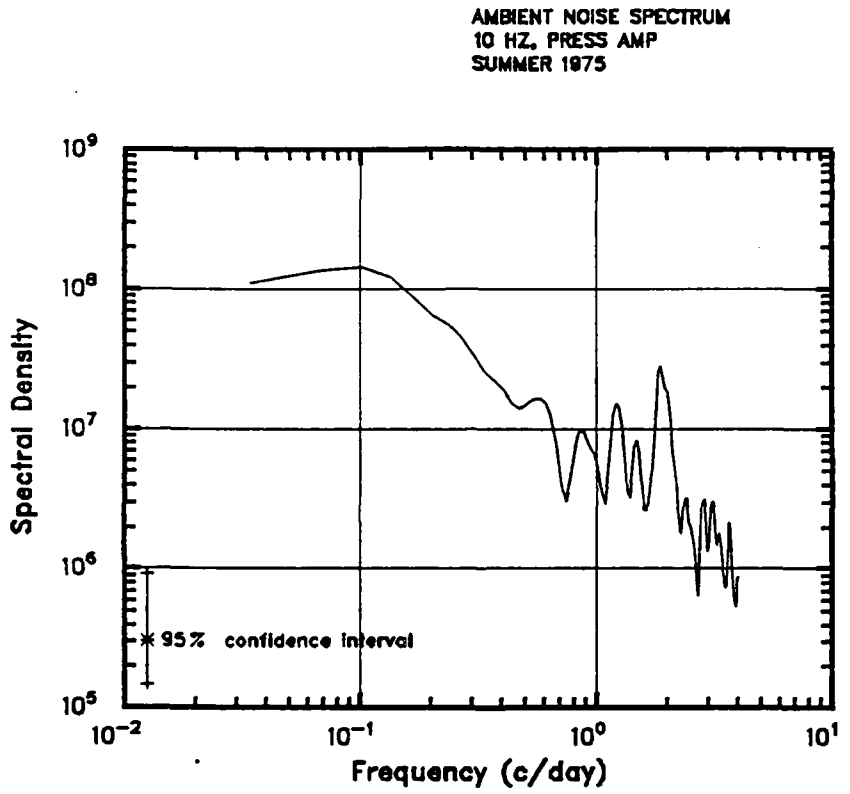

Fig. I.4. Spectral density of the 10 Hz ambient noise data (pressure amplitude) from Station 10, August 1975.

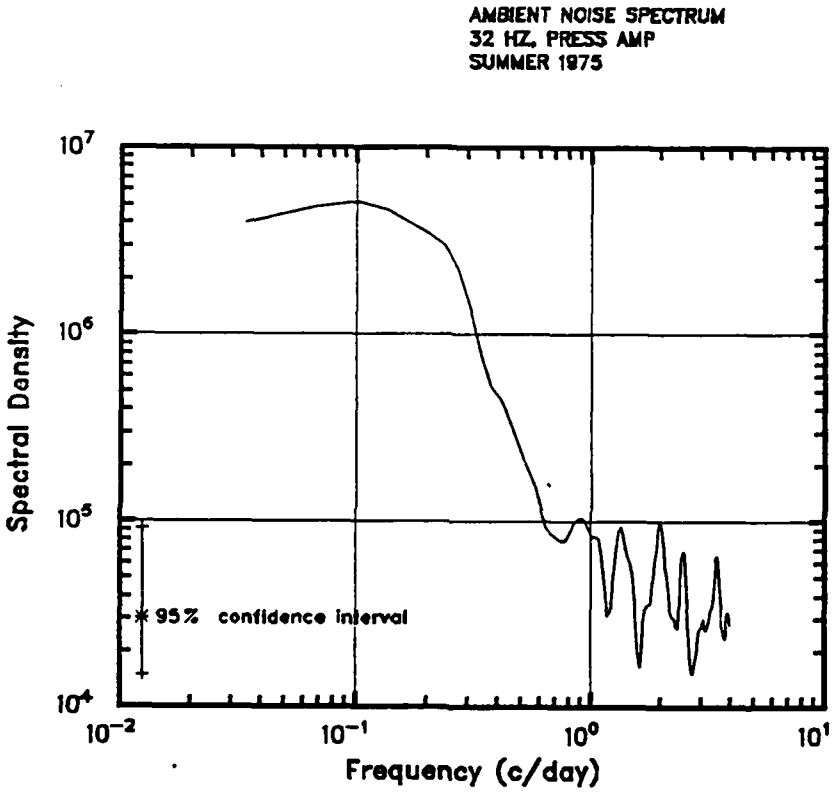

Fig. I.5. Spectral density of the 32 Hz ambient noise data (pressure amplitude) from Station 10, August 1975.

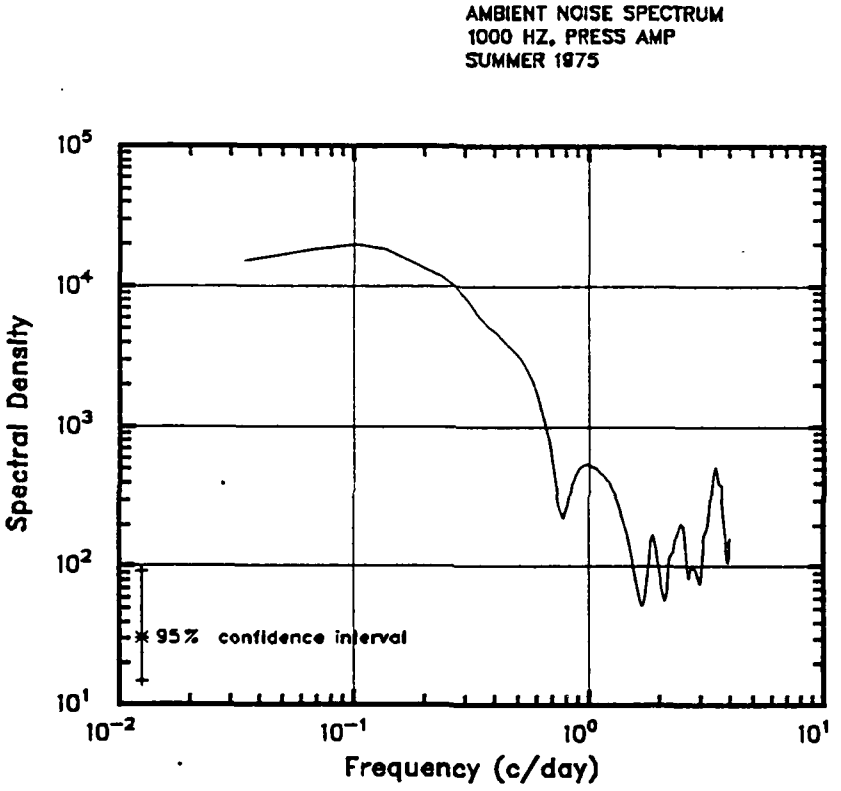

Fig. I.6. Spectral density of the 1000 Hz ambient noise data (pressure amplitude) from Station 10, August 1975.

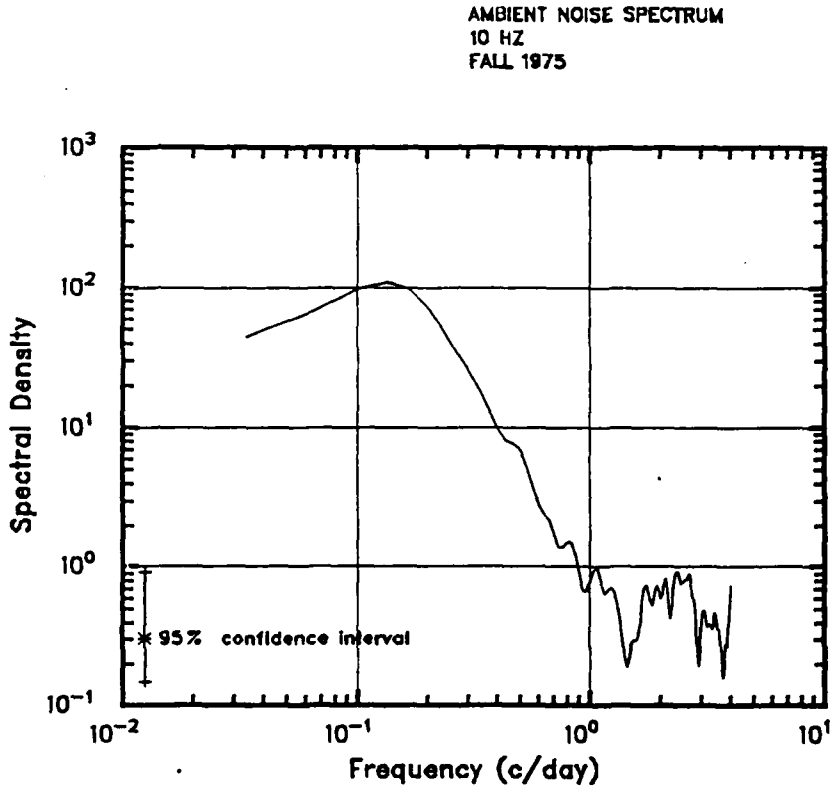

Fig. I.7. Spectral density of the 10 Hz ambient noise data (dB) from Station 10, November 1975.

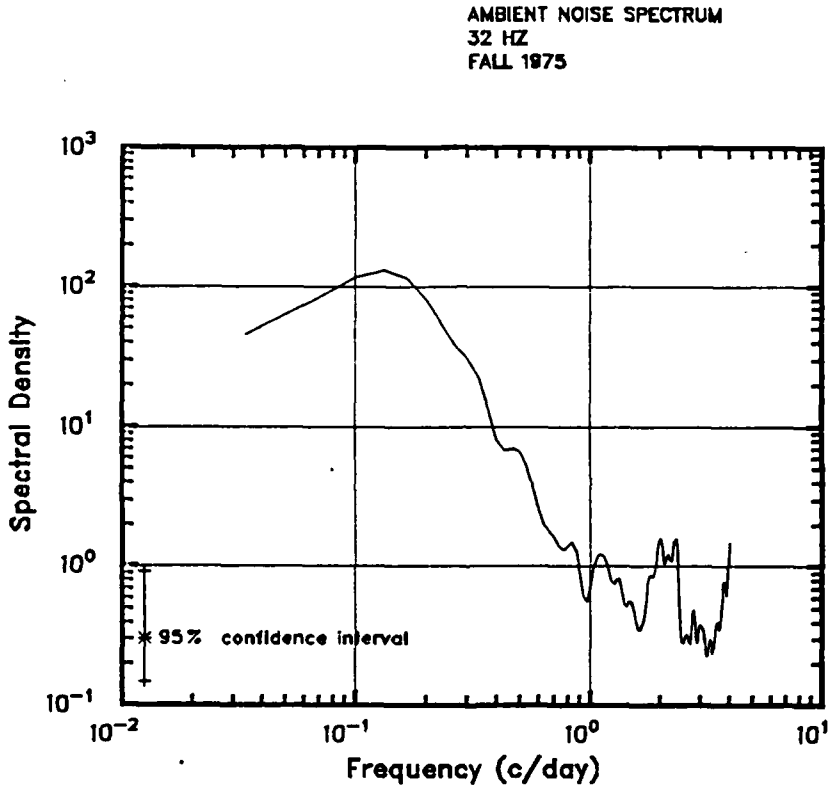

Fig. I.8. Spectral density of the 32 Hz ambient noise data (dB) from Station 10, November 1975.

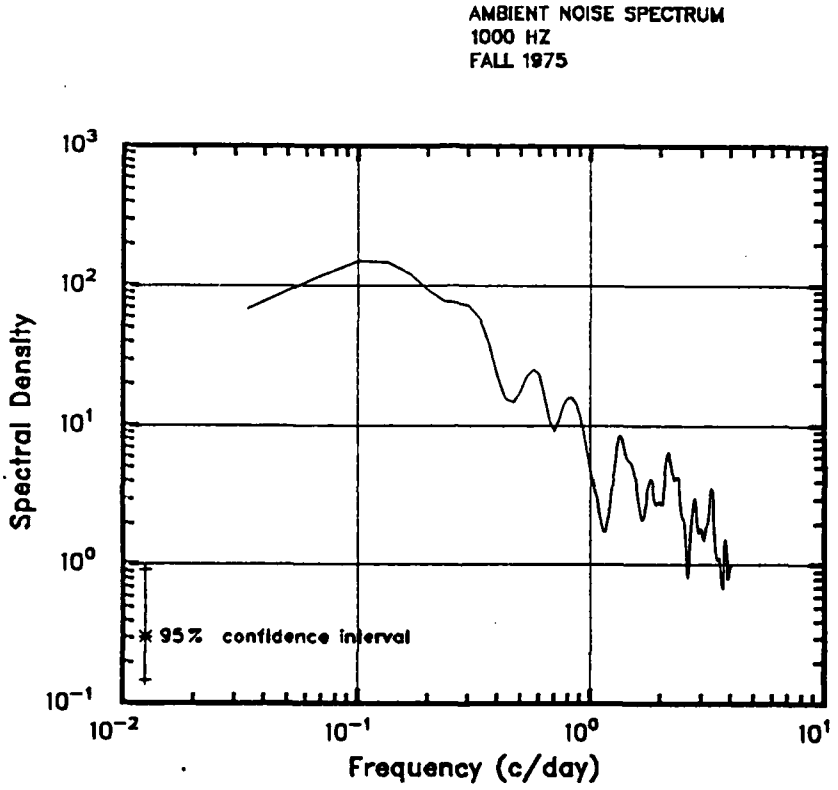

Fig. I.9. Spectral density of the 1000 Hz ambient noise data (dB) from Station 10, November 1975.

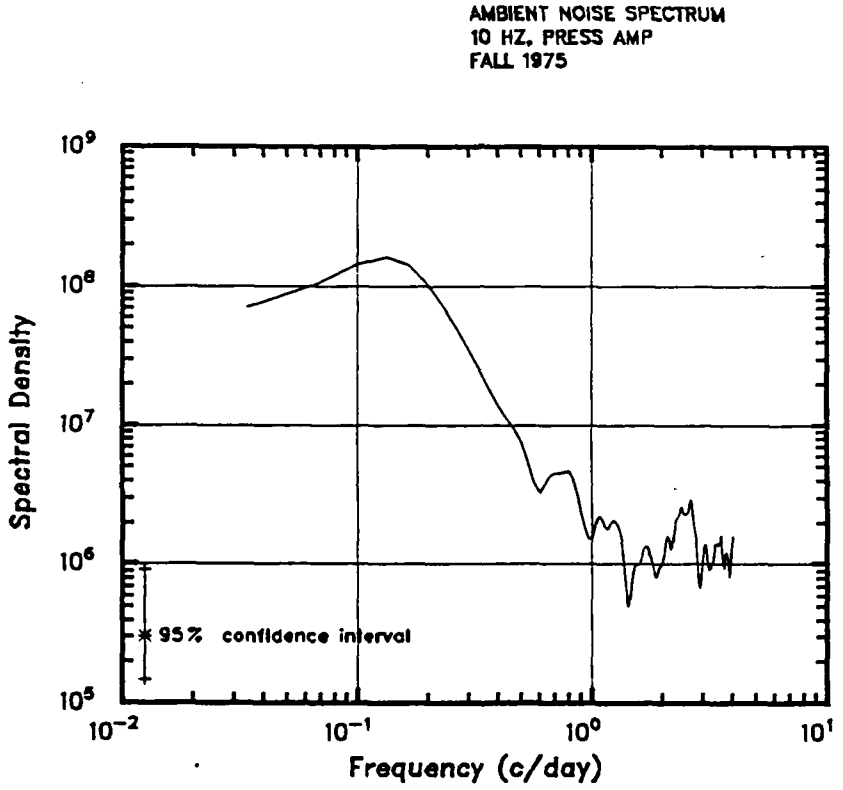

Fig. I.10. Spectral density of the 10 Hz ambient noise data (pressure amplitude) from Station 10, November 1975.

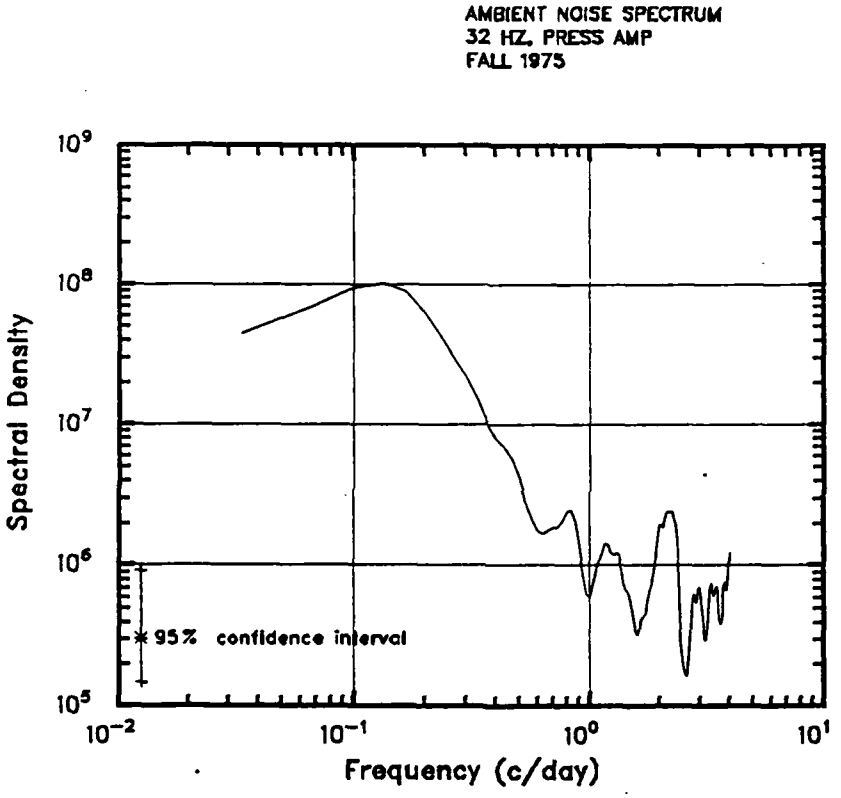

Fig. I.11. Spectral density of the 32 Hz ambient noise data (pressure amplitude) from Station 10, November 1975.

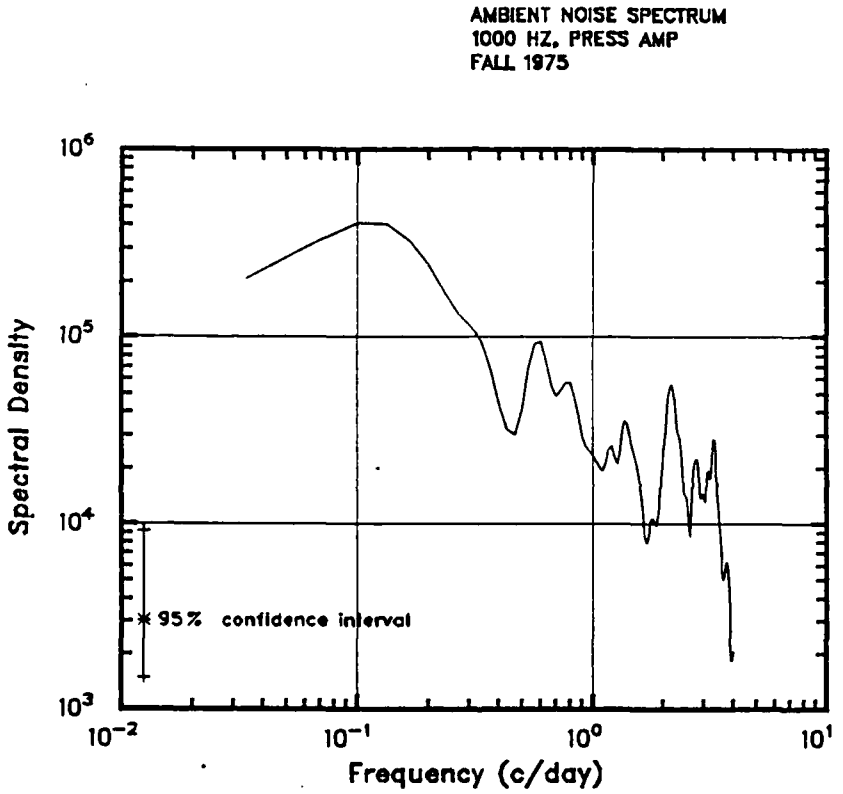

Fig. I.12. Spectral density of the 1000 Hz ambient noise data (pressure amplitude) from Station 10, November 1975.

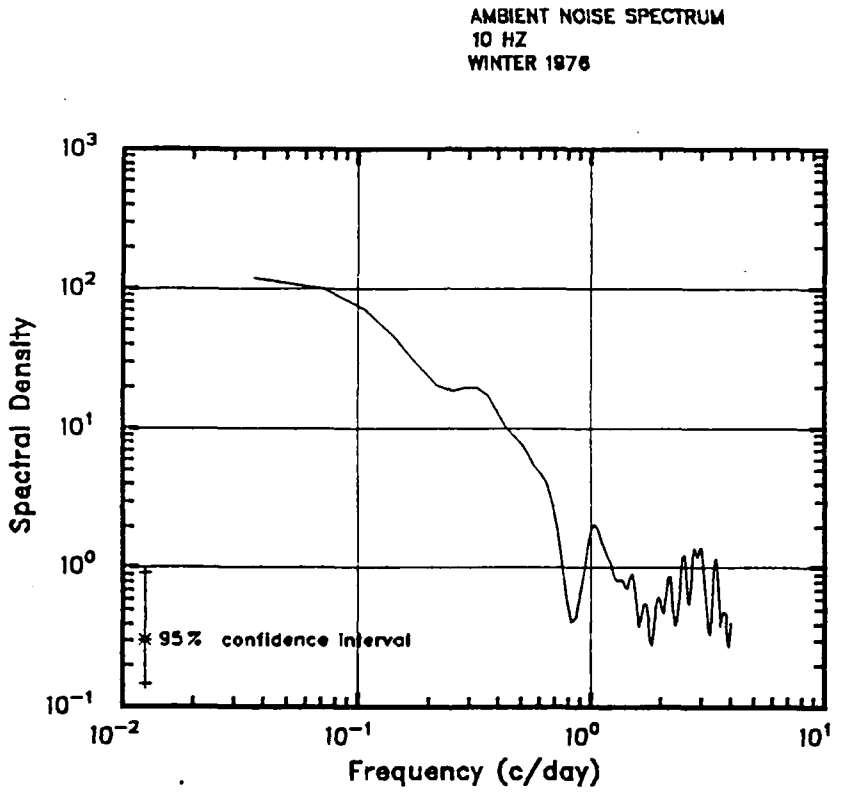

Fig. I.13. Spectral density of the 10 Hz ambient noise data (dB) from Station 10, February 1976.

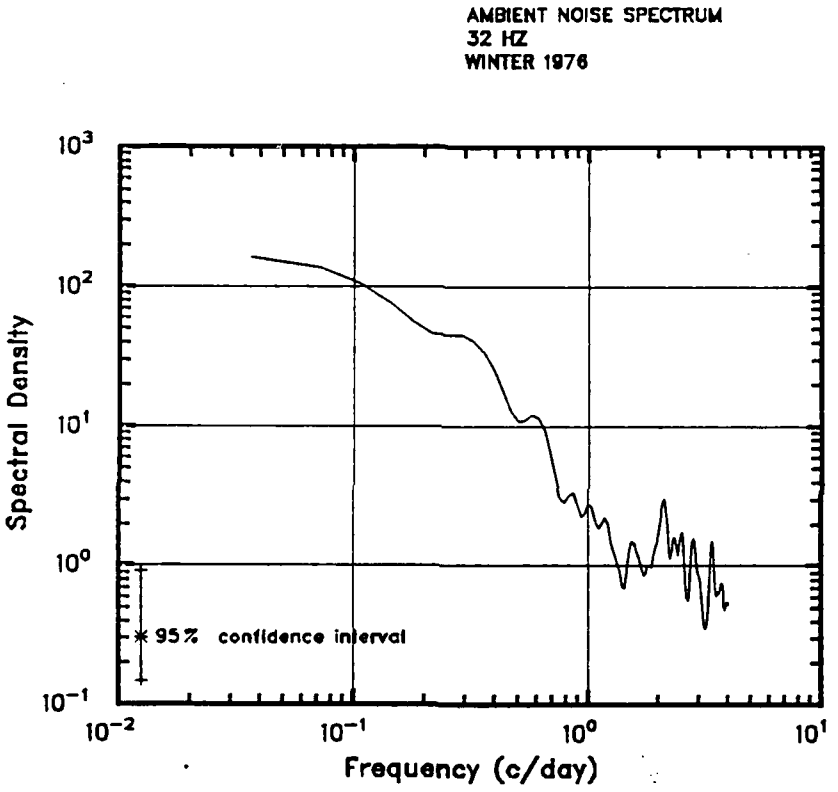

Fig. I.14. Spectral density of the 32 Hz ambient noise data (dB) from Station 10, February 1976.

AD-A165 305 A STUDY OF SEA ICE KINEMATICS AND THEIR RELATIONSHIP TO ARCTIC AMBIENT NO..(U) HONEYWELL INC DUARTE CA ORDNANCE DIV J K LEWIS ET AL. FEB 86 SAIC-85/1950-PT-3-SEC-3 2/2

UNCLASSIFIED N00014-85-C-0531 F/G 8/12 NL

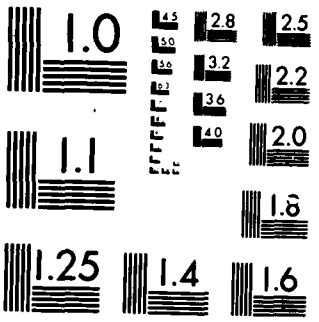

MICROCOPY RESOLUTION TEST CHART
NATIONAL BUREAU OF STANDARDS-1963-A

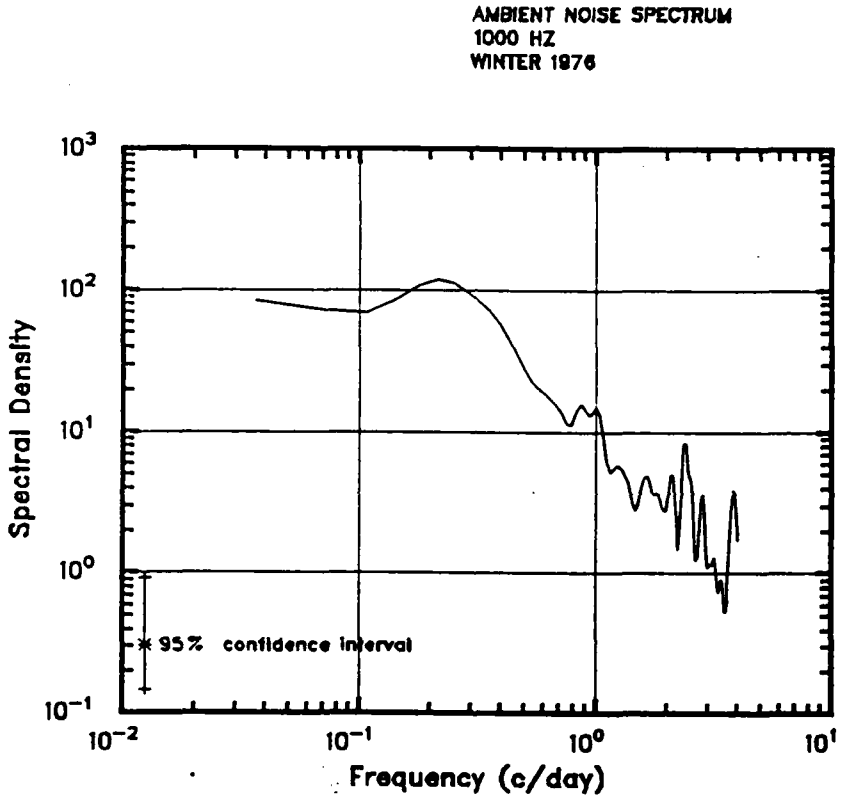

Fig. I.15. Spectral density of the 1000 Hz ambient noise data (dB) from Station 10, February 1976.

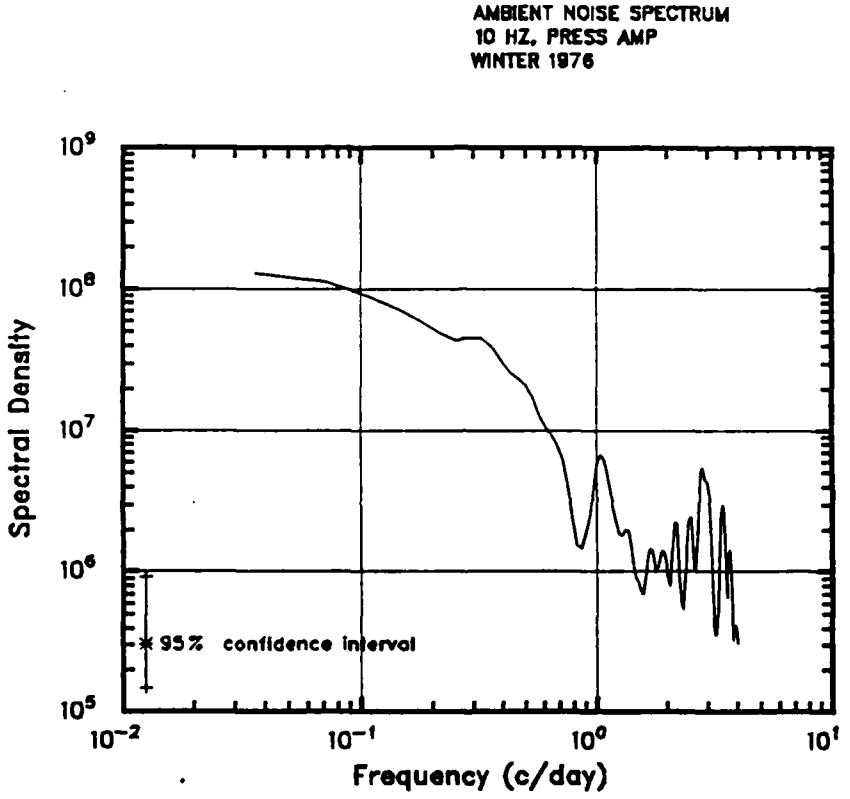

Fig. I.16. Spectral density of the 10 Hz ambient noise data (pressure amplitude) from Station 10, February 1976.

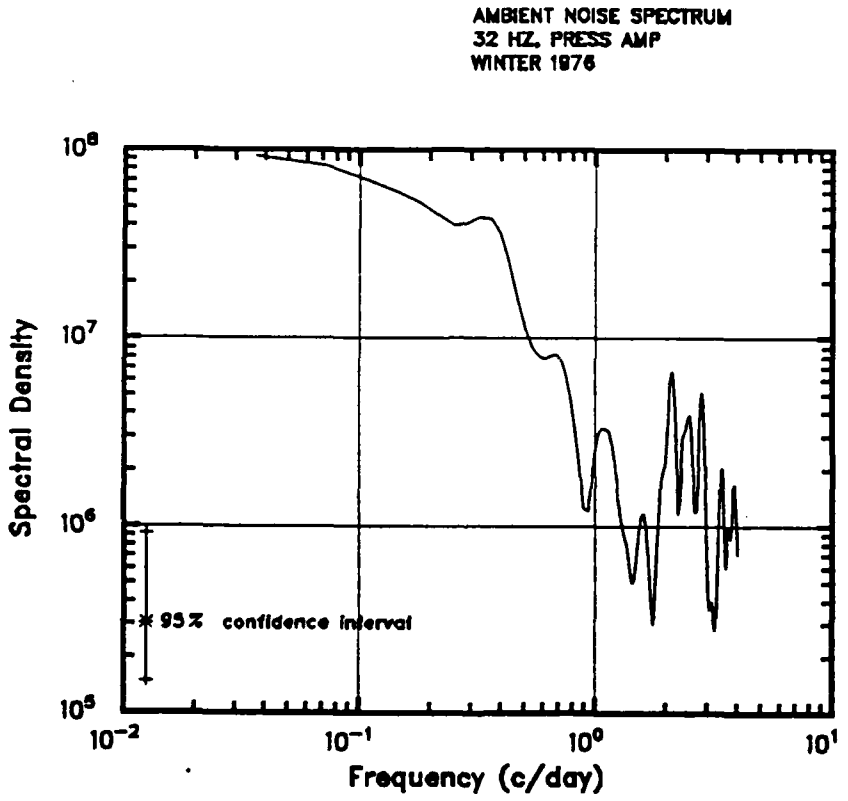

Fig. I.17. Spectral density of the 32 Hz ambient noise data (pressure amplitude) from Station 10, February 1976.

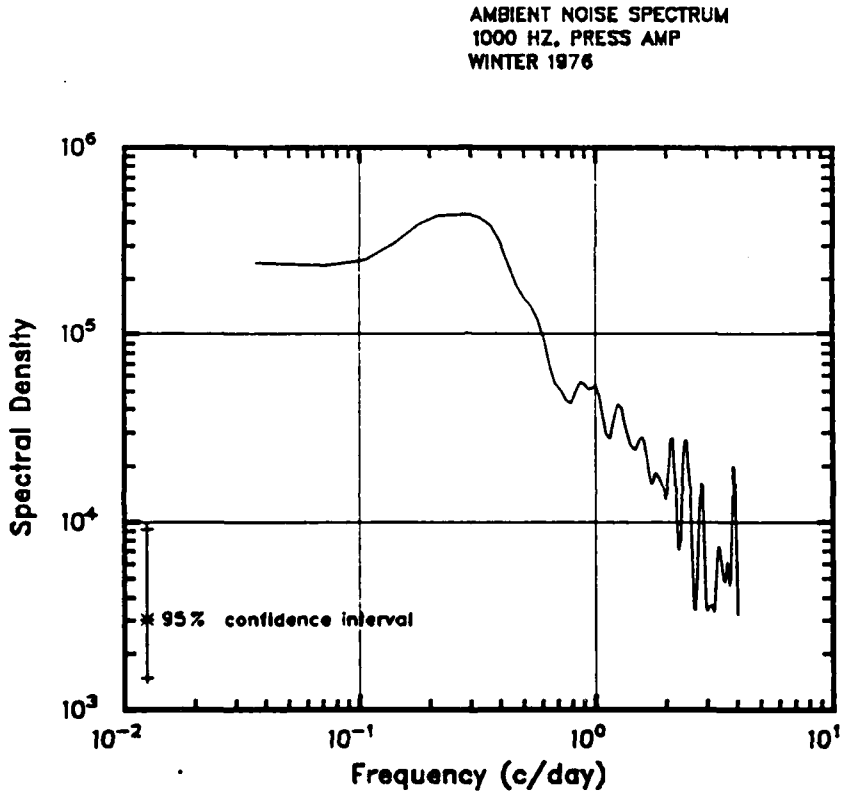

Fig. I.18. Spectral density of the 1000 Hz ambient noise data (pressure amplitude) from Station 10, February 1976.

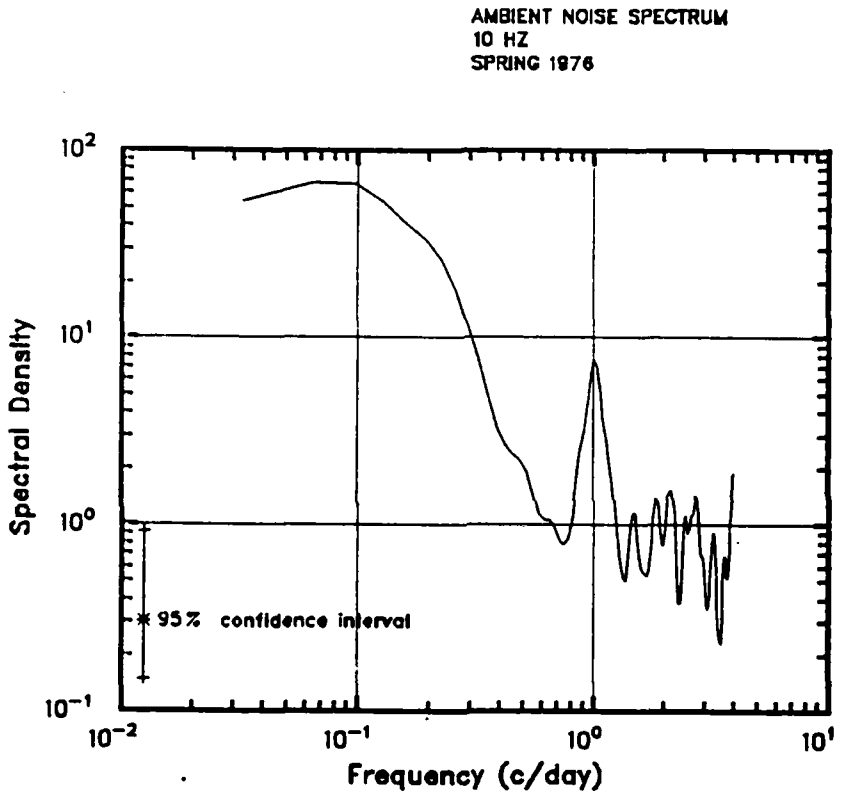

Fig. I.19. Spectral density of the 10 Hz ambient noise data (dB) from Station 10, May 1976.

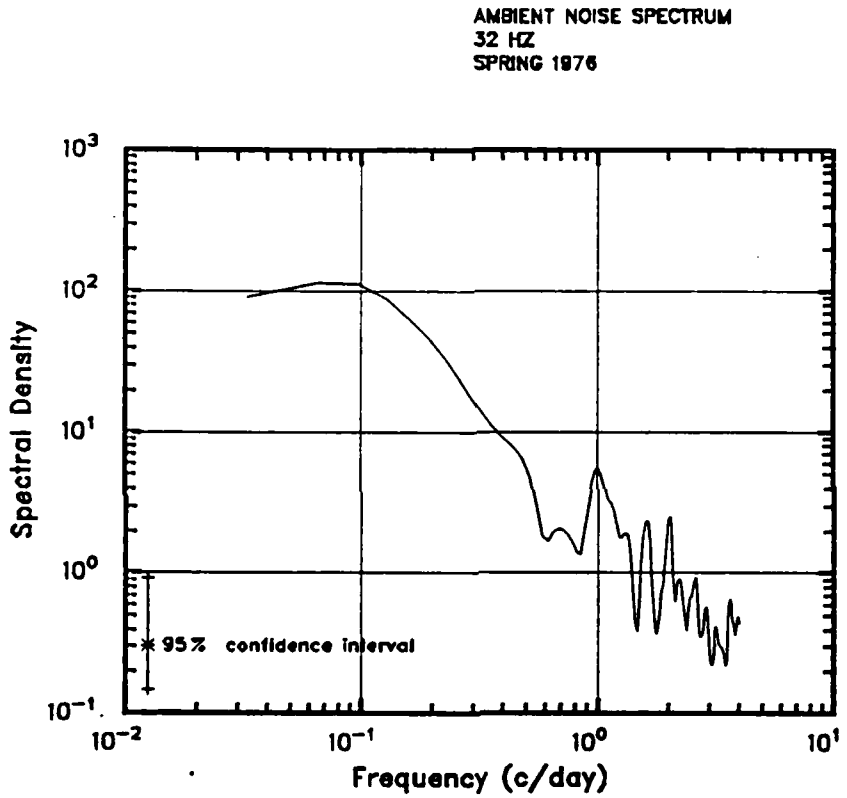

Fig. I.20. Spectral density of the 32 Hz ambient noise data (dB) from Station 10, May 1976.

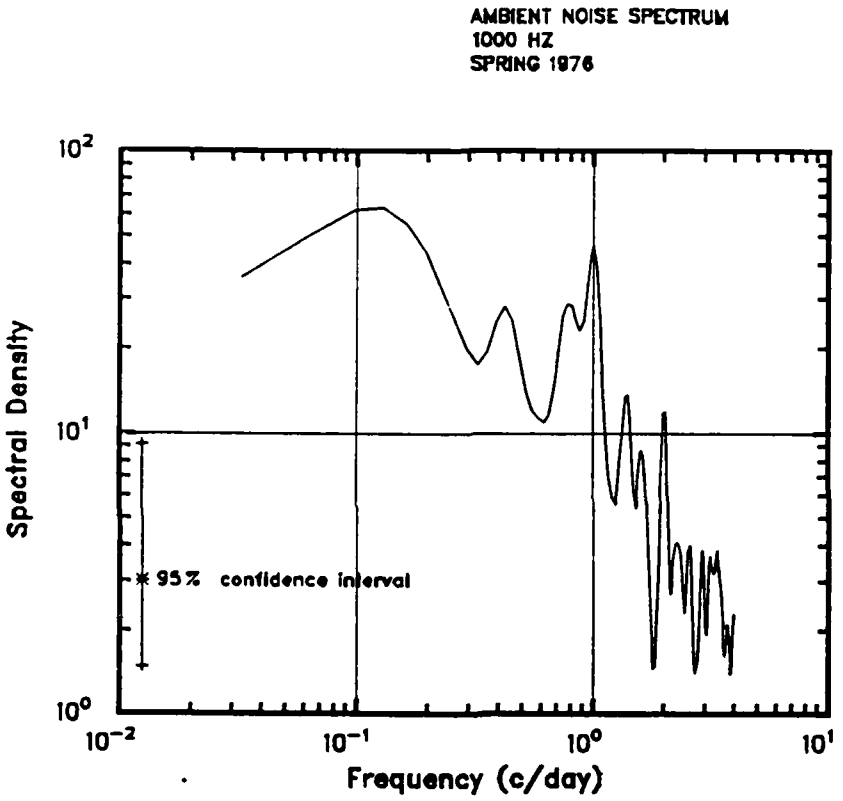

Fig. I.21. Spectral density of the 1000 Hz ambient noise data (dB) from Station 10, May 1976.

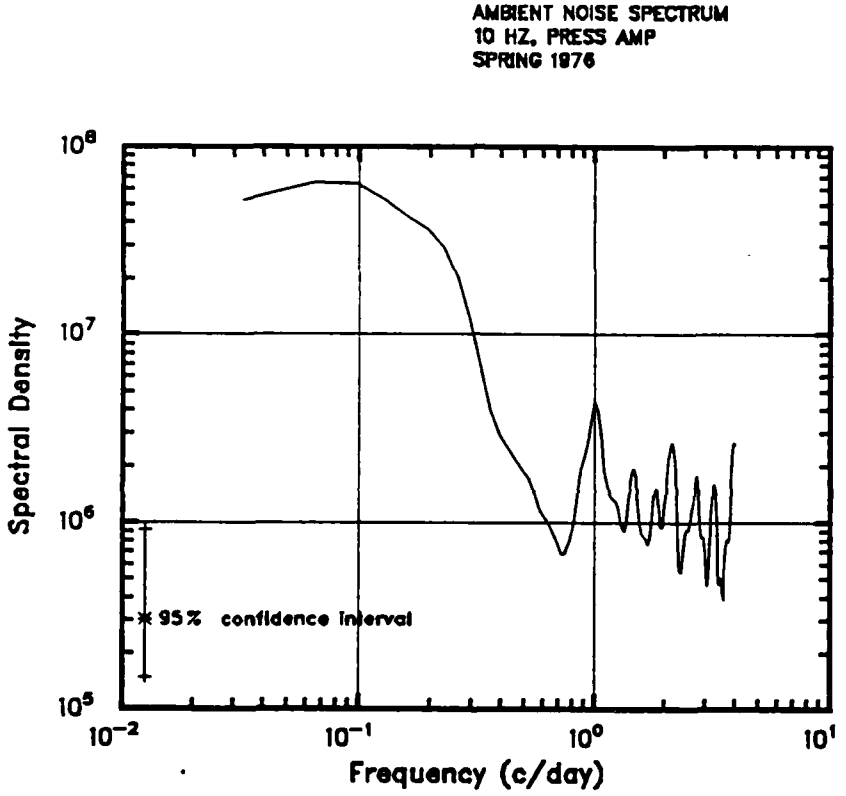

Fig. I.22. Spectral density of the 10 Hz ambient noise data (pressure amplitude) from Station 10, May 1976.

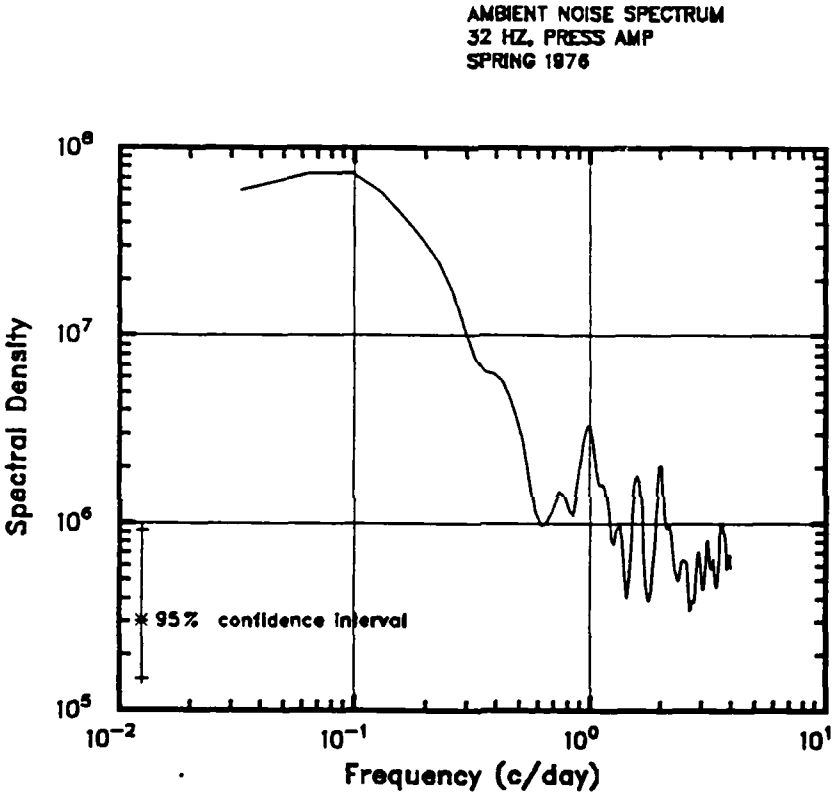

Fig. I.23. Spectral density of the 32 Hz ambient noise data (pressure amplitude) from Station 10, May 1976.

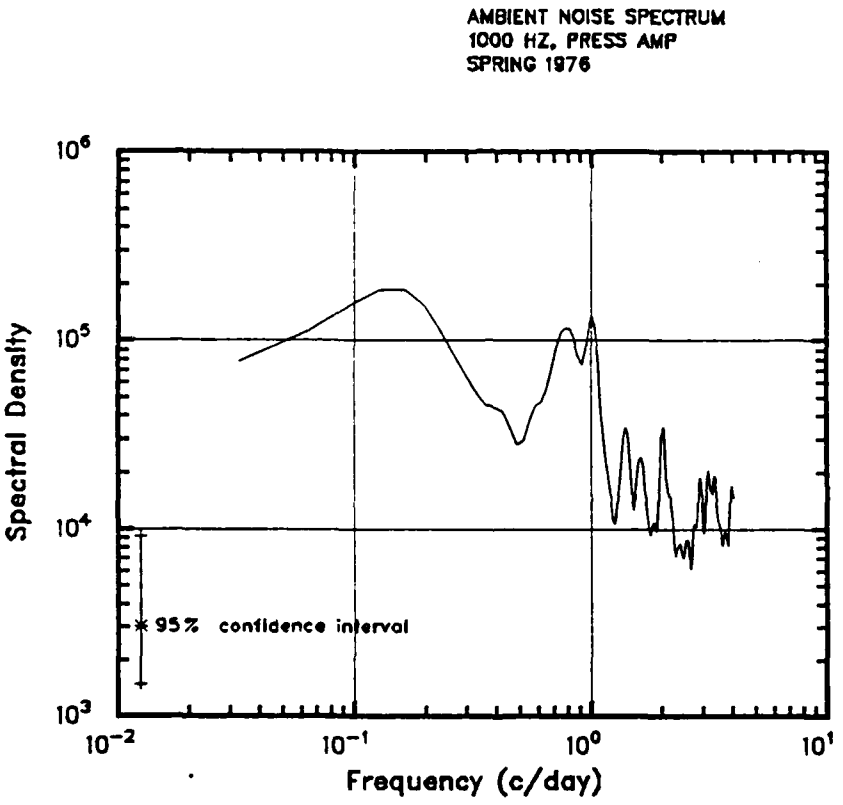

Fig. I.24. Spectral density of the 1000 Hz ambient noise data (pressure amplitude) from Station 10, May 1976.

END

FILMED

4-86

DTIC